Durham E-Theses

The Effective Potential in Kohn-Sham Theory

THOMAS PITTS

How to cite:

Use policy

The Effective Potential in Kohn-Sham Theory

Thomas C. Pitts

A Thesis presented for the degree of
Doctor of Philosophy

Department of Physics
University of Durham

May, 2021

The Effective Potential in Kohn-Sham Theory

Thomas C. Pitts

Abstract

Density functional theory (DFT) is a widely used technique for electronic structure calculations. It allows a first principles solution of the many-electron Schrödinger equation by relating the electron density of the systems ground state to that of a fictitious non-interacting system. The success of DFT methods comes from the use of approximations to the exact total energy functional that, with an appropriate functional, accurately determine the ground state properties of a system. The work presented in this thesis uses properties of the Kohn-Sham effective potential to correct errors in DFT approximations, particularly those associated with self-interactions. Applying a constraint to the effective potential enforcing the correct, self-interaction free asymptotic behaviour significantly improves the calculation of ionisation energies for the LDA, PBE, and B3LYP functionals. For LDA this error is reduced from 4.08 eV to 1.61 eV, with a similar reduction in error found for PBE and B3LYP. Additional methods to improve this self-interaction correction are presented and expanded upon, including a self-interaction free hybrid scheme for the constrained minimisation method. This hybrid further improves ionisation energies over the constrained method. Average errors of PBE ionisation energies are reduced from 4.41 eV to 0.34 eV. These improvements are also found to extend to the ionisation energies of all occupied orbitals and electron affinities. A post-scf correction that corrects ionisation energies from the Kohn-Sham eigenvalue to those from a Δ_{scf} calculation is also developed. Ionisation energies for the LDA approximation are improved from an average error of 3.99 eV to 0.93 eV, with similar improvements seen for lower lying ionisation energies and electron affinities. The final work of this thesis shows that, unlike conventional band theory, spin-DFT (SDFT) can predict insulating behaviours in periodic systems from a unit cell containing an odd number of electrons. Additionally, this result is shown for a novel method for implementing DFT; combining SDFT XC energy functionals with a spin-independent effective potential, through the use of the optimised effective potential method.

Declaration

The work in this thesis is based on research carried out at the Department of Physics of the University of Durham between September 2016 and May, 2021. I confirm that no part of this thesis has been submitted elsewhere for any other degree or qualification and it is all my own work unless referenced to the contrary in the text.

Thomas C. Pitts

May, 2021

Acknowledgements

I would like to thank my supervisors Nikitas Gidopoulos and Stewart Clark for their help and support throughout the past four years. Nikitas for the long discussions we had on the theories of DFT and for his guidance and insight throughout my research, along with his constant efforts to help improve me as both a student and researcher. And Stewart for teaching me how best to use and abuse computers, and providing support with the CASTEP code when I inevitably broke it. I would also like to thank Nektarios Lathiotakis for supplying the HIPPO molecular code with which I performed many of the calculations in this thesis. I was also helped by the work of Tim Callow and Ben Pearce who streamlined and updated the HIPPO code, greatly improving its usability. I would also like to thank all the members of the office: Tim C., Ben H., Ben P., Zack H., Matt H., Matjaz G., and Faten A. for their various inputs, useful discussions, and for the introduction of Wine Friday.

Outside of work I would like to thank all the members of the Ustinov College, and beyond, who have helped me greatly enjoy my time at Durham. Specifically I would like to thank Alastair, Alex, Diane, and Ed for being a source of much entertainment, camaraderie, and the occasional nugget of wisdom.

Finally, my family has been a great source of inspiration, with my brothers Michael and Steve and sister Annabel motivating me to keep pushing myself, and my parents Cath and Paul for the unbelievable amount of support and guidance they have offered, without whom non of this would have been possible.

Contents

List of Figures

List of Tables

Chapter 1

Introduction

1.1 Introduction

A popular method for the accurate simulation of quantum mechanical systems is density functional theory (DFT). Since its inception, the techniques and functional approximations used in DFT methods have been refined and improved with the aim of approaching the exact DFT functional. As these methods improve, along with ever increasing access to computational resources, the applicability of DFT continues to expand into larger or more physically challenging systems. Despite the success of DFT for a wide variety of systems and properties, there are some significant shortcomings related to particular aspects of the Kohn-Sham formulation. Self-interactions are a well known source of error in DFT calculations, and can significantly impact the accuracy of one-electron properties such as the ionisation energy. In this thesis methods that correct for this self-interaction error will be introduced and developed. The aim is to provide simple methods that can be applied within the framework of DFT to reduce the effect of self-interaction error. Two main correction methods will be demonstrated: a self-consistent method where the solution is constrained to obey exact self-interaction free properties, and a post-scf method of correcting the results of a DFT calculation and reducing the significant self-interaction errors found in DFT methods. Several extensions to the self-consistent constrained correction will be demonstrated that improve its applicability, along with a simple hybrid scheme offering further improvements when

calculating ionisation energies, improving even valence and core ionisation energies.

This thesis will also consider DFT and spin-DFT for magnetic systems. Contrary to the expected results from conventional band theory, it will be demonstrated that insulating behaviour can be predicted in periodic systems containing an odd number of electrons per unit cell. Key features of the conducting behaviour of a system can be found by only considering a single primitive unit cell. For unit cells with an odd number of electrons, the inclusion of magnetic ground states allow a metal-insulator transition as interatomic distances are increased. An alternative method for treating spin-dependent systems will also be introduced. In this method the spin-up and spin-down electrons are treated using a common effective potential in a DFT manner. This will provide a simplified method for performing restricted Kohn-Sham calculations with SDFT accuracy; showing that, even in this restricted case, a metal-insulator transition can be reproduced for unit cells containing an odd number of electrons.

1.2 Outline of Thesis

1.2.1 Chapter 2

The many body problem is introduced and the basic principles of DFT are covered, along with the Hartree-Fock and optimised effective potential methods. These methods allow the many body problem to be solved under various approximations. Computational methods utilised when solving electronic structure calculations are also shown along with a description of the codes used to perform calculations in this thesis.

1.2.2 Chapter 3

This chapter reviews properties of the Kohn-Sham system including the relation between the Kohn-Sham eigenvalues and the ionisation energy of the interacting system. These properties of the Kohn-Sham potential are affected by several errors

in DFT methods, particularly the self-interaction error.

1.2.3 Chapter 4

The constrained self-interaction correction method of Gidopoulos and Lathiotakis is introduced. This method uses asymptotic properties of the exact Kohn-Sham potential to correct for self-interactions in DFT approximations. I will apply this method to several DFT functionals and to a variety of molecular systems, demonstrating its applicability.

1.2.4 Chapter 5

Several extensions to the constrained self-interaction correction are introduced dealing with: the effects of finite basis sets, the removal of the positivity constraint, the separation of the exchange and correlation potentials, and an alternative method for imposing the positivity constraint on the auxiliary density. A new, fully self-interaction free hybrid method, combining the constrained method and Hartree-Fock exact exchange, is introduced. The results when using this hybrid method to calculate ionisation energies are presented and the method is seen to provide accurate ionisation energies for a range of systems. Additionally, this hybrid method improves the calculation of ionisation energies for all occupied orbitals and the electron affinity. This method proves to be particularly accurate when calculating core electron ionisation energies.

1.2.5 Chapter 6

The discrepancy between the ionisation energy, as calculated using a difference of total energies, and the negative of the Kohn-Sham eigenvalue are investigated for approximate functionals. This difference is used to construct an orgional zero- and first-order correction to the Kohn-Sham eigenvalues. These terms form a correction that can be applied to correct ionisation energies of all occupied electron orbitals, and the electron affinity. Significant improvements when using this correction will be demonstrated. Additionally, the magnitude of this correction for the ionisation

energy of the highest occupied orbital is a measure of an approximate functionals agreement with the exact DFT functional.

1.2.6 Chapter 7

Spin DFT methods are shown to be able to demonstrate a metal-insulator transition in systems containing an odd number of electrons per unit cell, contrary to results in conventional band theory. This result is found by allowing magnetic ground states in the spin-DFT calculation. A novel DFT method for spin-polarised states will be introduced. In this method spin-DFT energy functionals are combined with a common Kohn-Sham potential for both up and down spin electrons. This method is shown to be able to reproduce the metal-insulator transition shown for unrestricted spin-DFT.

1.2.7 Chapter 8

A summary and a conclusion to the work undertaken in this thesis along with possible future avenues for further investigation.

Chapter 2

An Overview of Density Functional Theory

2.1 The Many Body Problem

In the first half of the 20th century the framework of quantum mechanics was put in place providing great insight into the physics of interacting quantum mechanical systems. Such systems are of great value for studies in the fields of physics, chemistry, biology, and materials science. In principle, a solution of the time independent Schrödinger equation for any stationary quantum mechanical system will allow for the calculation of real world properties of the system without the need for experiment.

For a quantum mechanical system described by a wave function Ψ all the information about the system is contained within the wave function Ψ which satisfies the equation

$$\hat{\mathcal{H}}\Psi = E\Psi, \tag{2.1.1}$$

where $\hat{\mathcal{H}}$ is the Hamiltonian operator, which for a time independent non-relativistic system with no magnetic field is

$$\hat{\mathcal{H}} = \hat{T} + \hat{V} \tag{2.1.2}$$

where $\hat{T}$ is the kinetic energy operator and $\hat{V}$ is the potential energy operator. The behaviour of atoms, molecules, and crystals can be simply be represented as an interacting system of electrons and atomic nuclei with a combined wave function

$$\Psi(\mathbf{R}_1, \mathbf{R}_2, \ldots, \mathbf{R}_M : \mathbf{r}_1, \mathbf{r}_2, \ldots, \mathbf{r}_N) \tag{2.1.3}$$

where $\mathbf{R}$ are the positions of M nuclei, and $\mathbf{r}$ are the positions of N electrons. The Kinetic energy operator of this system is

$$\hat{T} = -\frac{1}{2} \left[\sum_I^M \frac{\nabla_I^2}{M_I} + \sum_i^N \nabla_i^2 \right] \tag{2.1.4}$$

with M_I the atomic masses of the nuclei. The potential energy operator is

$$\hat{V} = -\sum_I^M \sum_i^N \frac{Z_I}{|\mathbf{R}_I - \mathbf{r}_i|} + \frac{1}{2} \left[\sum_I^M \sum_{J \neq I} \frac{Z_I Z_J}{|\mathbf{R}_I - \mathbf{R}_J|} + \sum_i^N \sum_{j \neq i} \frac{1}{|\mathbf{r}_i - \mathbf{r}_j|} \right] \tag{2.1.5}$$

where Z_I are the charges of the nuclei. These expressions are represented in dimensionless atomic units which will be used throughout this thesis.

Equation (2.1.4) treats both the nuclei and electrons as quantum mechanical objects, however often it is the case that the nuclei are well described through classical equations and a full quantum mechanical treatment is unnecessary. The Born-Oppenheimer (BO) approximation [3] is a commonly used simplification, where the wave function of the more massive nuclei is treated as separable from the wave function of the electrons. A justification for this is that the nuclei are moving much slower than the surrounding electrons and the electrons can be considered to exist in the ground state of a "background" potential provided by the instantaneous positions of the nuclei.

Under the BO approximation the full wave function may be expressed as a product of a nuclear and electronic wave functions

$$\boldsymbol{\Psi}(\mathbf{R}_1, \mathbf{R}_2, \ldots, \mathbf{R}_M, \mathbf{r}_1, \mathbf{r}_2, \ldots, \mathbf{r}_N)$$
$$= \theta(\mathbf{R}_1, \mathbf{R}_2, \ldots, \mathbf{R}_M)\boldsymbol{\Phi}(\mathbf{r}_1, \mathbf{r}_2, \ldots, \mathbf{r}_N; \mathbf{R}_1, \mathbf{R}_2, \ldots, \mathbf{R}_M) \quad (2.1.6)$$

where θ is the wave function of the nuclei and $\boldsymbol{\Phi}$ is the wave function of the electrons. These product wave functions are normalised such that

$$\int d\mathbf{R}_1 \int d\mathbf{R}_2 \cdots \int d\mathbf{R}_M \left|\theta(\mathbf{R}_1, \mathbf{R}_2, \ldots, \mathbf{R}_M)\right|^2 = 1, \quad (2.1.7)$$

$$\int d\mathbf{r}_1 \int d\mathbf{r}_2 \cdots \int d\mathbf{r}_N \left|\boldsymbol{\Phi}(\mathbf{r}_1, \mathbf{r}_2, \ldots, \mathbf{r}_N; \mathbf{R}_1, \mathbf{R}_2, \ldots, \mathbf{R}_M)\right|^2 = 1. \quad (2.1.8)$$

The nuclear wave function is independent of the electron positions and the electronic wave function does not depend on the motion of the nuclei. The electron wave function does, however, depend parametrically upon the positions of the nuclei. The many body problem for a specific set of nuclear positions can be solved by finding the electronic ground state with an electron wave function $\boldsymbol{\Phi}$. The governing BO electronic Hamiltonian becomes

$$\hat{H}_{\mathrm{e}} = -\sum_i^N \frac{\nabla_i^2}{2} + \hat{V}_{\mathrm{ext}} + \frac{1}{2}\sum_i^N \sum_{j \neq i} \frac{1}{|\mathbf{r}_i - \mathbf{r}_j|}, \quad (2.1.9)$$

with, the positions of the atomic nuclei only entering the equation through an external potential

$$\hat{V}_{\mathrm{ext}} = \sum_i^N V_{\mathrm{ext}}(\mathbf{r}_i), \qquad V_{\mathrm{ext}}(\mathbf{r}_i) = -\sum_I^M \frac{Z_I}{|\mathbf{R}_I - \mathbf{r}_i|}. \quad (2.1.10)$$

The Hamiltonian in Eq. (2.1.9) can be solved for any nuclear positions to obtain an electronic wave function thus allowing a solution to be found for a particular nuclear configuration.

While the equations governing these systems are simple to obtain, solving them proves to become impractical for systems more complicated than small isolated atoms or simple highly-symmetric molecules. This difficulty is due to the scaling of the coordinate space of the wave function. For N electrons represented on a

grid with G points in each dimension the coordinate space scales as G^{3N}. As grid size increases, calculations quickly become unmanageable even for relatively coarse coordinate grids. In order to obtain solutions for systems more complicated than simple atoms and molecules, further approximations are necessary.

2.2 The Hartree-Fock Method

One method to reduce the size of the coordinate space of the wave function, $\mathbf{\Phi}$, is the Hartree-Fock method [4]. In the Hartree-Fock method, the electron wave function is constructed as a product of orbitals. As electrons obey fermion statistics, the product wave function must also satisfy the correct antisymmetry relations. This is achieved by constructing the product wave function as a Slater determinant [5]

$$\mathbf{\Phi}(\mathbf{r}_1, \mathbf{r}_2, \ldots, \mathbf{r}_N) = \frac{1}{\sqrt{N!}} \begin{vmatrix} \phi_1(\mathbf{r}_1) & \phi_2(\mathbf{r}_1) & \cdots & \phi_N(\mathbf{r}_1) \\ \phi_1(\mathbf{r}_2) & \phi_2(\mathbf{r}_2) & \cdots & \phi_N(\mathbf{r}_2) \\ \vdots & \vdots & \ddots & \vdots \\ \phi_1(\mathbf{r}_N) & \phi_2(\mathbf{r}_N) & \cdots & \phi_N(\mathbf{r}_N) \end{vmatrix} \tag{2.2.11}$$

where each ϕ_n is an orthonormal orbital. By the BO approximation the wave functions Φ and orbitals ϕ_i are all parametrically dependent on the nuclear positions, for brevity this dependence will not be explicitly stated.

The Hartree-Fock energy is the energy of this wave function calculated using the electronic Hamiltonian $\hat{H}_\mathrm{e}$ by evaluating

$$E_\mathrm{HF} = \langle \mathbf{\Phi} | \hat{H}_\mathrm{e} | \mathbf{\Phi} \rangle. \tag{2.2.12}$$

This total energy can be broken down into the evaluation of

$$E_\mathrm{HF} = E_\mathrm{kin} + E_\mathrm{ext} + E_\mathrm{ee} \tag{2.2.13}$$

where

$$E_{\text{kin}} = -\sum_i \langle \mathbf{\Phi} | \frac{\nabla_i^2}{2} | \mathbf{\Phi} \rangle, \tag{2.2.14}$$

$$E_{\text{ext}} = \langle \mathbf{\Phi} | V_{\text{ext}} | \mathbf{\Phi} \rangle, \tag{2.2.15}$$

$$E_{\text{ee}} = \frac{1}{2} \sum_i \sum_{j\neq i} \langle \mathbf{\Phi} | \frac{1}{|\mathbf{r}_i - \mathbf{r}_j|} | \mathbf{\Phi} \rangle \tag{2.2.16}$$

correspond to the kinetic, external potential, and the electron-electron energies respectively. When $\mathbf{\Phi}(\mathbf{r}_1, \mathbf{r}_2, \ldots, \mathbf{r}_N)$ is given as a Slater determinant of orthonormal orbitals, these energies are found, following the Slater-Condon [5, 6] rules, to be

$$E_{\text{kin}} = -\sum_\sigma \sum_i^{N^\sigma} \int d\mathbf{r} \, [\phi_i^\sigma(\mathbf{r})]^* \frac{\nabla^2}{2} \phi_i^\sigma(\mathbf{r}) \tag{2.2.17}$$

$$E_{\text{ext}} = \sum_\sigma \sum_i^{N^\sigma} \int d\mathbf{r} \, [\phi_i^\sigma(\mathbf{r})]^* V_{\text{ext}}(\mathbf{r}) \phi_i^\sigma(\mathbf{r}) \tag{2.2.18}$$

$$E_{\text{ee}} = \frac{1}{2} \sum_{(i,\sigma)\neq(j,\sigma')} \int d\mathbf{r} d\mathbf{r}' \frac{[\phi_i^\sigma(\mathbf{r})]^* \phi_i^\sigma(\mathbf{r}) [\phi_j^{\sigma'}(\mathbf{r}')]^* \phi_j^{\sigma'}(\mathbf{r}')}{|\mathbf{r} - \mathbf{r}'|}$$
$$- \frac{1}{2} \sum_\sigma \sum_{i\neq j} \int d\mathbf{r} d\mathbf{r}' \frac{[\phi_i^\sigma(\mathbf{r})]^* \phi_i^\sigma(\mathbf{r}') \phi_j^\sigma(\mathbf{r}) [\phi_j^\sigma(\mathbf{r}')]^*}{|\mathbf{r} - \mathbf{r}'|} \tag{2.2.19}$$

where a spin component to each electron state has been introduced. The electron spin is either $\sigma = \uparrow, \downarrow$ with N^σ electrons in each spin state. The two terms of E_{ee} can be further separated into the Hartree energy

$$E_{\text{H}} = \frac{1}{2} \sum_{\sigma,\sigma'} \sum_i^{N^\sigma} \sum_j^{N^{\sigma'}} \int d\mathbf{r} d\mathbf{r}' \frac{[\phi_i^\sigma(\mathbf{r})]^* \phi_i^\sigma(\mathbf{r}) [\phi_j^{\sigma'}(\mathbf{r}')]^* \phi_j^{\sigma'}(\mathbf{r}')}{|\mathbf{r} - \mathbf{r}'|} \tag{2.2.20}$$

and the Fock exchange energy

$$E_{\text{X}} = -\frac{1}{2} \sum_\sigma \sum_{i,j}^{N^\sigma} \int d\mathbf{r} d\mathbf{r}' \frac{[\phi_i^\sigma(\mathbf{r})]^* \phi_i^\sigma(\mathbf{r}') \phi_j^\sigma(\mathbf{r}) [\phi_j^\sigma(\mathbf{r}')]^*}{|\mathbf{r} - \mathbf{r}'|}. \tag{2.2.21}$$

In these equations the sum over both the Hartree and Fock-exchange energies both include a $i = j, \sigma = \sigma'$ term. This term is common in both E_{H} and E_{X} and cancels when the two expressions are added. Minimising the total Hartree-Fock energy

with respect to the orbitals ϕ_i will find the ground state energy of the system. This minimisation cannot be unconstrained as the orthonormality of ϕ_i must be maintained; therefore, a minimisation using the method of Lagrange multipliers is used to ensure $\langle \phi_i^\sigma | \phi_j^\sigma \rangle = \delta_{ij}$. The resulting objective functional to be minimised is

$$\mathcal{L} = E_{\text{HF}} - \sum_{\sigma,\sigma'} \sum_{i,j} \epsilon_{ij}^\sigma \langle \phi_i^\sigma | \phi_j^\sigma \rangle \tag{2.2.22}$$

where, at the minimum,

$$\frac{\delta \mathcal{L}}{\delta \left[\phi_i^\sigma(\mathbf{r}) \right]^*} = 0. \tag{2.2.23}$$

Performing this derivative on the total energy expression gives

$$\left[-\frac{\nabla^2}{2} + V_{\text{ext}}(\mathbf{r}) + \sum_{\sigma'} \sum_j^{N^{\sigma'}} \int d\mathbf{r}' \frac{\left[\phi_j^{\sigma'}(\mathbf{r}') \right]^* \phi_j^{\sigma'}(\mathbf{r}')}{|\mathbf{r} - \mathbf{r}'|} \right] \phi_i^\sigma(\mathbf{r})$$
$$- \sum_j^{N^\sigma} \int d\mathbf{r}' \frac{\phi_i^\sigma(\mathbf{r}')\phi_j^\sigma(\mathbf{r}) \left[\phi_j^\sigma(\mathbf{r}') \right]^*}{|\mathbf{r} - \mathbf{r}'|} = \sum_j^{N^\sigma} \epsilon_{ij}^\sigma \phi_j^\sigma(\mathbf{r}). \tag{2.2.24}$$

The total energy of this expression is unchanged if a unitary transformation is applied to the orbitals, allowing for a choice of orbitals that diagonalise ϵ_{ij}^σ, resulting in

$$\left[-\frac{\nabla^2}{2} + V_{\text{ext}}(\mathbf{r}) + \sum_{\sigma'} \sum_j^{N^{\sigma'}} \int d\mathbf{r}' \frac{\left| \tilde{\phi}_j^{\sigma'}(\mathbf{r}') \right|^2}{|\mathbf{r} - \mathbf{r}'|} \right] \tilde{\phi}_i^\sigma(\mathbf{r})$$
$$- \sum_j^{N^\sigma} \int d\mathbf{r}' \frac{\tilde{\phi}_i^\sigma(\mathbf{r}')\tilde{\phi}_j^\sigma(\mathbf{r}) \left[\tilde{\phi}_j^\sigma(\mathbf{r}') \right]^*}{|\mathbf{r} - \mathbf{r}'|} = \epsilon_i^\sigma \tilde{\phi}_i^\sigma(\mathbf{r}) \tag{2.2.25}$$

where $\tilde{\phi}$ are the canonical orbitals that diagonalise ϵ_i^σ.

This set of N eigenvalue equations allow the ground state orbitals to be determined. In general there is not an analytical solution and these equations must be solved iteratively. This iterative solution starts from a trial set of orbitals and re-calculates new orbitals until the energy converges to a self-consistent solution. Calculating the Hartree-Fock total energy has a computational cost proportional to N^4 where N is

the number of basis set elements used in the expansion of the orbitals ϕ_i. Although this is a significant improvement over solving the fully interacting Hamiltonian, this scaling can still be prohibitive of application to large systems.

The Hartree-Fock method allows a wide variety of systems to be treated quantum mechanically; allowing the treatment of many-body systems from atoms to molecules and crystals. However, total energies calculated using the Hartree-Fock method do not offer good agreement with experimental results. This is due to the key approximation of the Hartree-Fock method; that the full electronic wave function has the form of a Slater determinant. A Slater determinant is only an exact solution for a system of non-interacting electrons. In a fully interacting system the true electronic wave function will include additional effects related to correlation between the electrons. These missing correlation effects can be accounted for with various further developments in beyond Hartree Fock theories such as MP2 [7], multiconfiguration self-consistent field methods [8], and the coupled cluster method [9–11]. These methods usually involve additional Slater determinants in order to more accurately describe the true wave function. The exact interacting wave function can only be described with an infinite number of these determinants. However, accurate calculations can be performed by using a large numbers of Slater determinants. These further developments can offer very accurate descriptions of electronic behaviour, however the additional computational cost of these methods limits their use to smaller systems.

2.2.1 Koopmans' Theorem

As well as allowing the total energies to be calculated, the Hartree-Fock method also provides a way to approximate the ionisation energies of electron orbitals through Koopmans' theorem [12]. The ionisation energy of a system is the energy required to remove an electron and is defined as

$$I = E_{N-1} - E_N \tag{2.2.26}$$

where E_N is the energy of a system of N electrons and E_{N-1} is the energy of an

$N-1$ electron system. Koopmans' theorem approximates the ionisation energy by making the frozen orbital approximation where the removal of the electron is assumed to be instantaneous and the single particle electron orbitals of the $N-1$ electron system are the same as for the N electron system. Assuming the orbitals are frozen the total energy of the $N-1$ electron system when the mth electron has been removed is

$$E_{N-1} = E_N - \epsilon_m, \tag{2.2.27}$$

where ϵ_m is the eigenvalue associated with the mth orbital. The ionisation of the mth electron is given by

$$I_m = E_{N-1} - E_N = -\epsilon_m \tag{2.2.28}$$

and the mth eigenvalue is an approximation to the mth ionisation energy.

These eigenvalues are good approximations of the electron ionisation energies [13], although the results, in general, overestimate experimental ionisation energies. These generally good approximations of ionisation energies are the result of a cancellation errors between correlation and orbital relaxation effects. Relaxation effects arise when the frozen orbital approximation neglects the change in the electron orbitals when an electron is removed from a system. The true ground state energy of the $N-1$ electron system is lower than the energy of the $N-1$ electron system under the frozen orbital approximation. This brings the total energies of the N and $N-1$ electron systems closer together, thereby reducing the predicted ionisation energy. Correlation errors are present in Hartree-Fock due the the method neglecting the effects of correlation between electrons. These errors increase the total energy over that of the exact interacting system. This increase is proportional to the number of electrons in the system, and as such the $N-1$ electron system has a smaller correlation error than the N electron system. This has the effect of widening the energy gap between the N and $N-1$ electron systems, increasing the predicted ionisation energy. Generally the increase in energy from correlation error is slightly larger than the reduction from relaxation effects, leading to a systematic overestimation of ionisation energies in Koopmans' theorem.

2.3   Density Functional Theory

2.3.1   The Thomas-Fermi Method

Before the development of the Hartree-Fock method, the Thomas-Fermi method [14, 15] was used as a simple approximation for electronic systems. In the Thomas Fermi method the controlling quantity is not the individual orbitals, but instead the electron density. As opposed to having to calculate many orbitals, using the electron density requires evaluation of only a single function, making calculation simpler and more efficient. However, the kinetic energy of an interacting electron density is not known and must be approximated. The interacting kinetic energy is difficult to approximate and this introduces large errors in the Thomas-Fermi method resulting in inaccurate total energies. Despite these failings this method introduced the electron density as a key quantity, which would go on to be further developed into DFT.

2.3.2   Hohenberg-Kohn Theorems

The electron density had been identified as an important quantity in in the Thomas-Fermi method for the calculation of a system's total energy. But it was unknown whether the electron density alone could provide a full description of a fully interacting system of electrons. The dependence of the total energy of a system on its electron density was proved through the Hohenberg-Kohn theorems [16] in 1964. These two theorems establish the relationship between the electron density and total energy for a ground-state system:

Theorem 2.3.1 The external potential $\hat{V}_{\text{ext}}$ and hence the total energy, is a unique functional of the electron density.

Proof: This theorem can be proved through *reductio ad absurdum* by assuming that there are systems with potentials $\hat{V}_1, \hat{V}_2$ which differ by more than a constant and have the same electron density $\rho(\mathbf{r})$. If the two potentials differ only by a constant the ground state wave functions are automatically the same with the same electron density, while the constant difference only serves to shift the total energy of the

system. The Hamiltonians with potentials $\hat{V}_1, \hat{V}_2$ are then

$$H_1 = \hat{T} + \hat{V}_{\text{ee}} + \hat{V}_1 \tag{2.3.29}$$

$$H_2 = \hat{T} + \hat{V}_{\text{ee}} + \hat{V}_2 \tag{2.3.30}$$

where the kinetic energy and the electron-electron interaction operators are the same in both Hamiltonians. We assume the ground state wave functions $\Psi_1 \neq \Psi_2$ are both different and have the same electron density $\rho(\mathbf{r})$. Because the total energy of the Hamiltonian H_i is uniquely minimised by the wave function Ψ_i this gives the inequalities

$$E_1 = \langle \Psi_1 | \hat{H}_1 | \Psi_1 \rangle < \langle \Psi_2 | \hat{H}_1 | \Psi_2 \rangle = \langle \Psi_2 | \hat{H}_2 | \Psi_2 \rangle - \langle \Psi_2 | \hat{H}_2 - \hat{H}_1 | \Psi_2 \rangle \tag{2.3.31}$$

$$E_2 = \langle \Psi_2 | \hat{H}_2 | \Psi_2 \rangle < \langle \Psi_1 | \hat{H}_2 | \Psi_1 \rangle = \langle \Psi_1 | \hat{H}_1 | \Psi_1 \rangle - \langle \Psi_1 | \hat{H}_1 - \hat{H}_2 | \Psi_1 \rangle \tag{2.3.32}$$

as the Hamiltonians only differ in the choice of $\hat{V}_{\text{ext}}$ this gives

$$E_1 < E_2 - \langle \Psi_2 | \hat{V}_2 - \hat{V}_1 | \Psi_2 \rangle = E_2 - \int d\mathbf{r} \left[V_2(\mathbf{r}) - V_1(\mathbf{r}) \right] \rho(\mathbf{r}) \tag{2.3.33}$$

$$E_2 < E_1 - \langle \Psi_1 | \hat{V}_1 - \hat{V}_2 | \Psi_1 \rangle = E_1 + \int d\mathbf{r} \left[V_2(\mathbf{r}) - V_1(\mathbf{r}) \right] \rho(\mathbf{r}) \tag{2.3.34}$$

adding these expressions together leaves the inequality

$$E_1 + E_2 < E_1 + E_2 \tag{2.3.35}$$

which is a contradiction. This contradiction proves that any V_{ext} must lead to a unique electron density in the ground state of the system.

As the electron density uniquely defines a ground state V_{ext} which in turn defines the wave function Ψ, this uniquely determines the kinetic and electron-electron interaction energies. Defining the operator $\hat{F} = \hat{T} + \hat{V}_{\text{ee}}$ allows the electronic energy to be written as a universal energy functional of the electron density:

$$F[\rho] = \langle \Psi | \hat{F} | \Psi \rangle = \langle \Psi | \hat{T} + \hat{V}_{\text{ee}} | \Psi \rangle . \tag{2.3.36}$$

This allows a generic total energy functional for some arbitrary external potential $V(\mathbf{r})$ to be defined as

$$E_{V_{\text{ext}}}[\rho] = F[\rho] + \int d\mathbf{r} V_{\text{ext}}(\mathbf{r})\rho(\mathbf{r}) \tag{2.3.37}$$

where V_{ext} has a ground state ρ_0 that is distinct from, in general, the generic density ρ. The density ρ is itself the ground state density of some potential V, where ground state V-representability has been assumed here for ρ.

Theorem 2.3.2 The electron density which minimises the total energy functional $E_{V_{\text{ext}}}[\rho]$ is the exact ground state density.

Proof:

Consider the ground state energy of a system with an external potential V_{ext}

$$E_0 = \langle \Psi_0 | \hat{H} | \Psi_0 \rangle = \langle \Psi_0 | \hat{F} | \Psi_0 \rangle + \langle \Psi_0 | \hat{V}_{\text{ext}} | \Psi_0 \rangle \tag{2.3.38}$$

where Ψ_0 is the ground state wave function. If now a trial density ρ, defined by an external potential V, with wave function Ψ then the energy of this state is

$$\langle \Psi | \hat{H} | \Psi \rangle = \langle \Psi | \hat{F} | \Psi \rangle + \langle \Psi | \hat{V}_{\text{ext}} | \Psi \rangle = E_{V_{\text{ext}}}[\rho] \geq E_0. \tag{2.3.39}$$

This expression is only an equality if the wave function Ψ is the ground state for the Hamiltonian with potential V_{ext}. Thus the ground state electron density can be found using variational methods by minimising the energy functional $E_{V_{\text{ext}}}[\rho]$.

The first of these theorems makes two key assumptions: that the ground state energy is non-degenerate, and that the densities considered are associated with an external potential (V-representable). The proof was generalised to cover these exceptions by the constrained search approach of Levy and Lieb [17–19], which showed that these theorems hold for any system where the density corresponds to a N electron wave function (N-representable), a weaker constraint than V-representability and one that is satisfied by any finite, non-negative, differentiable function [20].

The Hohenberg-Kohn theorems lay the foundation for a theory where the electron density is the controlling quantity, and show that this density can be obtained by a

minimisation of the ground state energy functional $E_V[\rho]$. Though these theorems themselves offer no way to obtain this density dependent energy expression. Subsequent work by Kohn and Sham in 1965 defined a suitable energy functional allowing meaningful calculations to be performed and establishing the method of DFT.

2.3.3 The Kohn-Sham Method

With the Hohenberg-Kohn theorems it had been shown that the ground state properties of a system can be fully described by considering only the electron density. This leaves the total energy expression that must be minimised to obtain this ground state electron density. While the Thomas-Fermi method provided a density dependent energy expression, large errors in the approximation of the kinetic energy of interacting electrons made the method unsuitable for most applications, except in the high density limit [21, 22], with a notable failing being an inability to describe molecular bonding [21, 23, 24]. A better description of the interacting kinetic energy is needed to improve the results.

The Kohn-Sham formulation of DFT [25] reduces the error in the kinetic energy by relating it to the kinetic energy of a non-interacting system with the same electron density. Beginning from the total energy of the interacting system the minimum energy with respect to varying the electron density is given by

$$\frac{\delta}{\delta\rho(\mathbf{r})}\left[E_{V_{\text{ext}}}[\rho] - \mu \int d\mathbf{r}\rho(\mathbf{r})\right] = 0 \qquad (2.3.40)$$

where the Lagrange multiplier μ is used to constrain the density to integrate to N. By introducing a non-interacting system of electrons with the same electron density as the interacting system the total energy expression of Eq. 2.3.37 can be partitioned into

$$E_{V_{\text{ext}}}[\rho] = T_{\text{s}}[\rho] + E_{\text{H}}[\rho] + E_{\text{XC}}[\rho] + \int d\mathbf{r}\rho(\mathbf{r})V_{\text{ext}}(\mathbf{r}), \qquad (2.3.41)$$

where T_{s} is the kinetic energy of a non-interacting system of electrons. E_{H} is the Hartree energy given by:

$$E_{\mathrm{H}}[\rho] = \frac{1}{2} \int d\mathbf{r} d\mathbf{r}' \frac{\rho(\mathbf{r})\rho(\mathbf{r}')}{|\mathbf{r} - \mathbf{r}'|}. \tag{2.3.42}$$

E_{XC} is the exchange-correlation energy which contains components of the electron-electron interaction not in the Hartree term and also terms from the interacting electron kinetic energy; it is defined as:

$$E_{\mathrm{XC}}[\rho] = F[\rho] - T_{\mathrm{s}}[\rho] - E_{\mathrm{H}}[\rho]. \tag{2.3.43}$$

From the second Hohenberg-Kohn theorem, the ground state density is the density that minimises the energy $E_{V_{\mathrm{ext}}}$. This minimum is found when Eq. (2.3.40) is satisfied. Using the partitioning in Eq. (2.3.41), the minimum energy is found when

$$\mu = \frac{\delta T_{\mathrm{s}}}{\delta \rho(\mathbf{r})} + V_{\mathrm{ext}}(\mathbf{r}) + V_{\mathrm{H}}(\mathbf{r}) + V_{\mathrm{XC}}(\mathbf{r}), \tag{2.3.44}$$

where

$$V_{\mathrm{H}}(\mathbf{r}) = \frac{\delta E_{\mathrm{H}}}{\delta \rho(\mathbf{r})} = \int d\mathbf{r} \frac{\rho(\mathbf{r})}{|\mathbf{r} - \mathbf{r}'|}, \tag{2.3.45}$$

$$V_{\mathrm{XC}}(\mathbf{r}) = \frac{\delta E_{\mathrm{XC}}}{\delta \rho(\mathbf{r})}. \tag{2.3.46}$$

In order to find the derivative $\frac{\delta T_{\mathrm{s}}}{\delta \rho(\mathbf{r})}$, a non-interacting auxiliary system with the same electron density as the fully interacting system is introduced. For this non-interacting system the density $\rho(\mathbf{r})$ is constructed as

$$\rho(\mathbf{r}) = \sum_i^N |\phi_i(\mathbf{r})|^2, \tag{2.3.47}$$

where $\phi_i(\mathbf{r})$ are a set of N orthonormal orbitals. These orbitals are dependent on an external potential $V_{\mathrm{KS}}(\mathbf{r})$, such that they satisfy the Schrödinger equation

$$\left[-\frac{\nabla^2}{2} + V_{\mathrm{KS}}(\mathbf{r}) \right] \phi_i(\mathbf{r}) = \epsilon_i \phi_i(\mathbf{r}) \tag{2.3.48}$$

The Lagrange multiplier ϵ_i ensures orthonormality of the orbitals $\phi_i(\mathbf{r})$. The total energy of this non-interacting system is given by

$$E_{\text{KS}} = T_{\text{s}}[\rho] + \int d\mathbf{r}\rho(\mathbf{r})V_{\text{KS}}(\mathbf{r}) \tag{2.3.49}$$

and this energy can be minimised as for the interacting system in equation (2.3.40). The resulting equation is

$$\mu_s = \frac{\delta T_{\text{s}}}{\delta\rho(\mathbf{r})} + V_{\text{KS}}(\mathbf{r}) \tag{2.3.50}$$

where the Lagrange multiplier μ_s constrains the electron density to integrate to N. Substituting Eq. (2.3.50) into Eq. (2.3.44), the Kohn-Sham potential $V_{\text{KS}}(\mathbf{r})$ is obtained as

$$V_{\text{KS}}(\mathbf{r}) = V_{\text{ext}}(\mathbf{r}) + V_{\text{H}}(\mathbf{r}) + V_{\text{XC}}(\mathbf{r}) + C. \tag{2.3.51}$$

where C is a constant given by $\mu_s - \mu$. This equation allows a link between the interacting and non-interacting systems to be established. Calculating the Kohn-Sham potential from equation (2.3.51) allows the non-interacting electron orbitals to be calculated from equation (2.3.48), from which the electron density for both the fully interacting and non-interacting electron system can be calculated. The density of the fully interacting system can be exactly determined from the Kohn-Sham potential V_{KS} by solving N one-electron equations, greatly simplifying the fully interacting problem. The ground state density cannot, in general, be calculated analytically and in practice must be determined numerically. This is achieve by iteratively calculating $V_{\text{KS}}(\mathbf{r})$, updating $\phi_i(\mathbf{r})$, and from the resulting $\rho(\mathbf{r})$ recalculating the Kohn-Sham potential. This is repeated until self consistency between the potential and electron density is obtained.

In principle, the Kohn-Sham formulation is an exact method allowing an exact ground state calculation to be performed. However, in practice, the exact description of E_{XC} is unknown and must be approximated. The error when approximating E_{XC} is much smaller than when approximating the interacting kinetic energy. In this way the Kohn-Sham formulation reduces the dominant error from that of the poorly approximated kinetic energy to the more easily approximated E_{XC}. Finding a good

approximation to E_{XC} is important in order to perform accurate DFT calculations and many functional approximations have been developed.

2.3.4 Functional Approximations

Jacob's Ladder of DFT Methods

In DFT the aim is to accurately approximate the exact exchange and correlation energy functional. Development of DFT over the past half century since the introduction of the Kohn-Sham method has aimed to improve the DFT functionals in order to obtain accurate energies and electronic properties. These improvements have been made by adding additional levels of theory into the approximation of the exchange-correlation energy functional.

Heaven of chemical accuracy

Hartee World
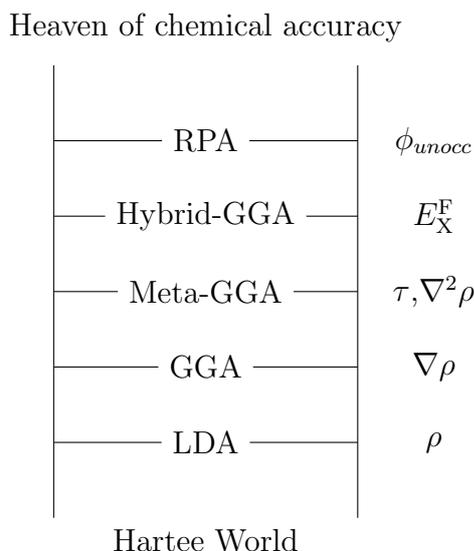
Figure 2.1: Jacob's ladder of approximations to E_{XC}.

The increasingly complex functionals form a "Jacob's Ladder" of increasing complexity and improved accuracy towards the exact functional in the "Heaven of chemical accuracy" [26]. This ladder leads from the Hartree world of non-interacting electron systems to the fully interacting system. Each step in the ladder adds additional interactions between the electrons with increasing complexity. For functionals near the top of the ladder an additional component is the exact non-local Fock exchange energy. A method near the top of the ladder is the random phase approximation

(RPA) which utilises both the occupied and unoccupied Kohn-Sham orbitals [27,28]. Being at a higher "rung" on the ladder generally indicates a higher level of theory and a more accurate approximation of the exact functional, coming at a cost to the computational effort required to implement the functional. There have been many functionals developed at all levels of theory and the most widely used functionals are the local density approximation (LDA) and generalised gradient approximations (GGAs) methods. Despite occupying a lower rung on the ladder, these functionals offer a suitable compromise between accuracy and computational efficiency allowing application to large complex systems.

Local Density Approximation

A simple way to approximate exchange and correlation is the LDA which uses an energy functional that depends only on the density at each point in space as [16]

$$E_{\text{xc}}^{LDA}[\rho] = \int d\mathbf{r} \rho(\mathbf{r}) \epsilon_{\text{xc}}[\rho(\mathbf{r})] \tag{2.3.52}$$

where ϵ_{xc} is the energy density of the exchange-correlation energy. This is the first term of a gradient expansion of E_{XC} which is exact in the limit of slowly varying electron density. This energy density can be split into contributions from exchange and correlation

$$\epsilon_{\text{xc}}[\rho] = \epsilon_{\text{x}}[\rho] + \epsilon_{\text{c}}[\rho]. \tag{2.3.53}$$

The exact behaviour of these terms are known from the homogeneous electron gas (HEG) [29], a system where the positive background charge is distributed uniformly throughout space. In the HEG the exchange energy is known analytically to have the form

$$\epsilon_{\text{x}}[\rho] = -C\rho(\mathbf{r})^{\frac{1}{3}} \tag{2.3.54}$$

where the coefficient C can be found from accurate simulations of the HEG [30]. The correlation energy density $\epsilon_{\text{c}}[\rho]$ can only be determined analytically for the high and low density limits of the HEG. Expressions can be constructed to interpolate between

these limits and comparison with accurate quantum Monte-Carlo calculations allows the construction of an accurate LDA [31–33]. Due to being derived from the HEG these approximations work well for homogeneous systems in which electrons are delocalised and the density varies slowly. This makes it well suited to periodic systems, especially metals, where electrons are delocalised. In molecular systems where electrons are more localised the LDA is less accurate and applications in these systems require further terms in the gradient expansion of $E_{\text{XC}}[\rho]$ [34, 35].

Generalised Gradient Approximations

An extension to the LDA approximation includes a dependence on the gradient of the density, $\nabla\rho(\mathbf{r})$ [36]. Functionals of this form are known as GGA [36–38] with energy functionals

$$E_{\text{XC}}^{GGA}[\rho] = \int d\mathbf{r}\rho(\mathbf{r})\epsilon_{\text{xc}}[\rho, \nabla\rho]. \tag{2.3.55}$$

Unlike LDA there is not a single choice for the parameterisation of the GGA energy density and many variants have been proposed. Some commonly used functionals are the functional of Perdew, Burke, and Ernzerhof (PBE) [39]; Lee, Yang, and Parr (LYP) [40]; and the Becke 88 functional (BP86) [41]. These functionals are constructed in terms of an enhancement factor [42] as

$$E_{\text{XC}}^{GGA}[\rho] = \int d\mathbf{r}\rho(\mathbf{r})\epsilon_{\text{xc}}^{\text{LDA}}[\rho(\mathbf{r})]F_{\text{XC}}\left[s(\mathbf{r}), r_s\right] \tag{2.3.56}$$

where

$$s(\mathbf{r}) = \frac{|\nabla\rho(\mathbf{r})|}{2k_F\rho(\mathbf{r})} \tag{2.3.57}$$

is a dimensionless gradient term and

$$r_s^3 = \frac{3}{4\pi\rho(\mathbf{r})} \tag{2.3.58}$$

is the Wigner-Seitz radius.

For the PBE functional the exchange component of this enhancement factor can be simply as

$$F_{\mathrm{X}}(s) = 1 + \kappa - \frac{\kappa}{1 + \frac{\mu s^2}{\kappa}} \tag{2.3.59}$$

with $\kappa = 0.804$ and $\mu = 0.21951$ where these quantities are determined from fundamental constants. PBE was developed to satisfy a set of known conditions of the behaviour of the correlation energy density using only fundamental constants, building on both LDA and earlier GGA methods. Because it does not depend on empirical properties, the PBE functional is not the best approximation for any specific property of a system, however in general it provides a reliable approximation for a range of systems, and as such remains one of the most widely used GGAs. More empirically determined approximations typically provide better approximations for specific properties in specific systems. For example, the LYP correlation functional is parameterised by a fitting to a helium atom [40] and is particularly accurate when applied to molecular systems, but performs much worse when applied to some metallic systems [43].

Some functionals are constructed to satisfy known exact conditions of the behaviour of the exchange-correlation energy density, though there is not a single parameterisation that satisfies every exact condition and many such parameterisations are available. There are also many empirical parameterisations that are fitted to experimental data enabling these functions to better represent certain sets of physical systems. However, this can lead to deficiencies when applied to systems that are outside the set of systems used to parametrise these functionals.

Meta-GGAs

An obvious further extension to GGAs is to include terms dependent on $\nabla^2 \rho$ or higher derivatives of the electron density, along with terms dependent on the kinetic energy density $\tau[\rho]$ [44, 45]. Such functionals are known as Meta-GGA functionals and have been shown to offer improvements over GGAs [46]. Meta-GGAs have had some successes such as the Minnesota set of functionals [47, 48] a highly parameterised set of Meta-GGA functionals which are widely used in the quantum chemistry community. For these meta-GGAs the empirical parameterisations used in their construction can lead to accurate energy predictions for specific sets of sys-

tems, but more accurate results may not mean the functionals are approaching the exact DFT solution. Improvements in DFT energetic results are not necessarily matched by an improvement in the quality of the predicted electron densities [49].

2.3.5 Spin Density Functional Theory

So far, the systems that have been considered are assumed to be spin neutral systems with an equal number of spin up and spin down electrons. These systems can be treated by having $\frac{N}{2}$ pairs of electrons. Each pair of electrons differ only in spin and these pairs of electrons share the same Kohn-Sham equation and Kohn-Sham orbitals. In such a spin symmetric system each Kohn-Sham orbital can be considered to be doubly occupied and only half the number of electrons need to be considered. In systems where the numbers of up and down spins are not symmetric the Kohn-Sham equations are modified to reflect that the behaviour of the differing spin channels may no longer be the same [25]. Unlike DFT, which depends on the electron density, these methods instead depend on the spin-densities and are known as spin-density functional theory (SDFT).

In unrestricted SDFT the Kohn-Sham potential is spin-dependent and the electron density is split into spin components

$$\rho^\sigma(\mathbf{r}) = \sum_i^{N^\sigma} |\phi_i^\sigma(\mathbf{r})|^2 \qquad (2.3.60)$$

where σ is a spin index. The total energy of the system depends on these spin densities and the exchange and correlation energy is written as $E_{\mathrm{XC}}[\rho^\uparrow, \rho^\downarrow]$. The total energy must be minimised with respect to the two spin density resulting in spin dependent Kohn-Sham equations

$$\left[-\frac{\nabla^2}{2} + v_{\mathrm{ext}}(\mathbf{r}) + V_{\mathrm{H}}[\rho](\mathbf{r}) + V_{\mathrm{KS}}[\rho^\sigma](\mathbf{r}) \right] \phi_i^\sigma(\mathbf{r}) = \epsilon_i^\sigma \phi_i^\sigma(\mathbf{r}). \qquad (2.3.61)$$

Each orbital in this case is distinct for spin up and spin down electrons. The difference in the potentials $V_{\mathrm{KS}}[\rho^\uparrow]$ and $V_{\mathrm{KS}}[\rho^\downarrow]$ defines a magnetic field aligned along the z axis [50]:

$$B_z(\mathbf{r}) = \frac{V_{\text{KS}}^{\uparrow}(\mathbf{r}) - V_{\text{KS}}^{\downarrow}(\mathbf{r})}{2\mu_0}. \tag{2.3.62}$$

Non-collinear SDFT will not be used in this thesis as these cases require a more involved mechanism to incorporate into the framework of DFT [51, 52].

2.4 Beyond Local Density Functional Theory

2.4.1 Hybrid Functionals

An extension to the DFT theory is to use the Hartree-Fock exact exchange energy as a component of the DFT energy, originally proposed by Becke [53–55] with a "half and half" functional with energy expression

$$E_{\text{XC}} = \frac{1}{2}E_{\text{X}} + \frac{1}{2}E_{\text{XC}}^{LDA}. \tag{2.4.63}$$

This representation is justified by the adiabatic connection path for which

$$E_{\text{XC}} = \int_0^1 d\lambda U_{\text{XC}}^{\lambda}, \tag{2.4.64}$$

where λ determines the interaction strength of the electron-electron interaction and U_{XC} is the exchange correlation energy. As λ varies from $\lambda = 0$ to $\lambda = 1$ it connects the non-interacting Kohn-Sham system ($\lambda = 0$) with the fully interacting system ($\lambda = 1$) by "switching on" the $1/|\mathbf{r}_1 - \mathbf{r}_2|$ Coulomb repulsion between electrons. This results in a continuous set of systems with varying electron-electron interaction strengths, all sharing the same ground state electron density ρ. Becke's "half and half" functional is a linear interpolation of this integral using the LDA DFT approximation for the fully interacting case and the Hartree-Fock term for the non-interacting exchange energy expression. In his original formulation Becke uses the orbitals from the local LDA Kohn-Sham potential. In subsequent formulations the orbitals are calculated self-consistently.

In order to have a self-consistent hybrid functional, consistent total energies and Kohn-Sham equations are required. Through appeals to the adiabatic connec-

tion [56, 57] a generalised Kohn-Sham equation, including a non-local Fock-exchange component, can be constructed. This generalised Kohn-Sham equation is

$$\left[-\frac{\nabla^2}{2} + v_{\text{ext}}(\mathbf{r}) + V_{\text{H}}(\mathbf{r}) + \alpha \hat{V}_F + (1 - \alpha)V_{\text{X}}^{KS}(\mathbf{r}) + V_{\text{C}}^{KS}(\mathbf{r}) \right] \phi_i(\mathbf{r}) = \epsilon_i \phi_i(\mathbf{r}).$$
(2.4.65)

The factor α determines the ratio of Hartree-Fock exchange to local Kohn-Sham exchange present in the method, $V_{\text{H}}(\mathbf{r})$ is the Hartree potential shared by both Hartree-Fock and Kohn-Sham DFT, $\hat{V}_F$ is the non-local Fock-exchange operator, and $V_{\text{X}}^{KS}(\mathbf{r}), V_{\text{C}}^{KS}(\mathbf{r})$ are the Kohn-Sham exchange and correlation potentials. Combining this generalised Kohn-Sham equation with the energy expression

$$E_{\text{HYB}}[\rho] = T_{\text{s}}[\rho] + E_{\text{ext}}[\rho] + E_{\text{H}}[\rho] + \alpha E_{\text{X}}^{HF}[\rho] + (1 - \alpha)E_{\text{X}}^{\text{DFT}}[\rho] + E_{\text{C}}^{\text{DFT}}[\rho] \quad (2.4.66)$$

allows the construction of a hybrid DFT method.

Due to the flexibility in the value of α and the choice of local exchange and correlation functionals, many hybrid formulations have been developed under the generalised Kohn-Sham scheme. The inclusion of non-local Fock exchange tends to improve descriptions of geometries and binding energies [58–60]. Some functionals make use of a single GGA functional such as the PBE0 [61] hybrid which uses full PBE correlation and 75% PBE exchange along with 25% Fock exchange, while the popular B3LYP functional [62] uses a combination of LDA and GGA functional approximations for both the correlation and local exchange components. These functionals are generally determined by empirically fitting the results of the calculation to experimental data allowing for the generation of accurate results. However, these empirical fittings come at the expense of an *ab-initio* formulation and may not apply outside the fitted systems. A method has been developed by which the optimum hybrid mixing can be determined from an analysis of an estimate of the behaviour of the hybrid under various hybrid mixing parameters [61, 63], this method allows for a more rigorous hybrid to be defined without relying on empirically fitted parameters.

2.4.2 The Optimised Effective Potential Method

As established by the Hohenberg-Kohn theorems, the energy of the system is uniquely determined by the electron density or the external potential. So far the energy expressions in the LDA and GGA methods have been explicit functionals of the density. It is still possible, however, to make use of the Kohn-Sham formalism with an energy expression that is not an explicit functional of the density. For some energy expressions, such as the Hartree-Fock energy, the energy depends explicitly on the electron orbitals and as such does not have an explicit density dependence

$$E[\rho] = T_{\mathrm{s}}[\rho] + E_{\mathrm{ext}}[\rho] + E_{\mathrm{H}}[\rho] + E_{\mathrm{XC}}[\{\phi_i[\rho]\}].$$
(2.4.67)

Here, the exchange-correlation potential depends explicitly on the electron orbitals which themselves are implicit functions of the electron density $\phi_i[\rho](\mathbf{r})$. By the Hohenberg-Kohn theorems the system has a unique electron density and consequently a unique Kohn-Sham potential V_{KS}. The ground state is determined by minimising the total energy expression with respect to the Kohn-Sham potential instead of the electron density and solving

$$\frac{\delta E[\{\phi_i[\rho]\}]}{\delta V_{\mathrm{KS}}(\mathbf{r})} = 0.$$
(2.4.68)

Using the chain rule this derivate can be performed with an intermediate derivative of the energy with respect to the Kohn-Sham orbitals as

$$\frac{\delta E[\{\phi_i[\rho]\}]}{\delta V_{\mathrm{KS}}(\mathbf{r})} = \int d\mathbf{r}' \sum_i^N \frac{\delta E[\{\phi_i[\rho]\}]}{\delta \phi_i(\mathbf{r}')} \frac{\delta \phi_i(\mathbf{r}')}{\delta V_{\mathrm{KS}}(\mathbf{r})} + \mathbf{c.c.}$$
(2.4.69)

where **c.c.** is the complex conjugate. The derivative of the orbital $\phi_i(\mathbf{r})$ with respect V_{KS} can be determined from the Kohn-Sham equations through first order perturbation theory shown in Appedix A.1. This method is known as the optimised effective potential (OEP) method, and was originally suggested by Sharp and Horton [64] for application to single atoms. This limited application was later expanded upon and applied in general to the Hartree-Fock energy functional [65]. This method is most often applied with the Hartree-Fock total energy functional. However, it is applicable to any orbital dependent functional, and allows a Kohn-Sham treatment of these

non-local, or orbital dependent, functionals. The case of the OEP method applied to the Hartree-Fock potential has been shown to be equivalent to an exact-exchange only Kohn-Sham method [66].

2.4.3 The OEP Exact Exchange Method

The most common use of the OEP method is including the Fock exchange energy from the Hartree-Fock method, and evaluating it with electron orbitals from a local potential. The total energy expression is

$$E[V_{\text{KS}}] = T_{\text{s}}[V_{\text{KS}}] + E_{\text{ext}}[V_{\text{KS}}] + E_{\text{H}}[V_{\text{KS}}] + E_{\text{X}}[V_{\text{KS}}] \tag{2.4.70}$$

where all these energies are implicit functionals of a local Kohn-Sham potential through the Kohn-Sham orbitals given by

$$\left[-\frac{\nabla^2}{2} + V_{\text{KS}}(\mathbf{r}) \right] \phi_i(\mathbf{r}) = \epsilon_i \phi_i(\mathbf{r}). \tag{2.4.71}$$

This energy functional neglects a correlation energy term and as such this will be a demonstration for exchange-only OEP, however the OEP method is flexible enough to allow for the inclusion of a correlation energy term if one is required. Minimising this expression with respect to the Kohn-Sham potential gives

$$\frac{\delta E[V_{\text{KS}}]}{\delta V_{\text{KS}}(\mathbf{r})} = \int d\mathbf{r}' \sum_i^N \frac{\delta E[V_{\text{KS}}]}{\delta \phi_i(\mathbf{r}')} \frac{\delta \phi_i(\mathbf{r}')}{\delta V_{\text{KS}}(\mathbf{r})} + \mathbf{c.c.} = 0. \tag{2.4.72}$$

From first order perturbation theory, shown in Appendix A.1, the derivative of the orbitals with respect to the Kohn-Sham potential is

$$\frac{\delta \phi_i(\mathbf{r}')}{\delta V_{\text{KS}}(\mathbf{r})} = \sum_{j \neq i}^\infty \frac{\phi_i(\mathbf{r})\phi_j^*(\mathbf{r})}{\epsilon_i - \epsilon_j} \phi_j(\mathbf{r}'). \tag{2.4.73}$$

The derivative of the energy expression can be taken by evaluating energies with an explicit density dependence through the chain rule

$$\frac{\delta E[V_{\text{KS}}]}{\delta \phi_i(\mathbf{r}')} = \int d\mathbf{r}'' \frac{\delta}{\delta \rho(\mathbf{r}'')} \Big[T_{\text{s}}[\rho] + E_{\text{ext}}[\rho] + E_{\text{H}}[\rho] \Big] \frac{\delta \rho(\mathbf{r}'')}{\delta \phi_i(\mathbf{r}')} + \frac{\delta E_{\text{X}}\big[\phi_i[V_{\text{KS}}]\big]}{\delta \phi_i(\mathbf{r}')} \tag{2.4.74}$$

the derivatives with respect to the density are known from DFT to be

$$\frac{\delta}{\delta\rho(\mathbf{r}'')}\Big[T_{\text{s}}[\rho] + E_{\text{ext}}[\rho] + E_{\text{H}}[\rho]\Big] = \frac{\delta T_{\text{s}}[\rho]}{\delta\rho(\mathbf{r}'')} + V_{\text{ext}}(\mathbf{r}'') + V_{\text{H}}(\mathbf{r}'')$$

$$= V_{\text{ext}}(\mathbf{r}'') + V_{\text{H}}(\mathbf{r}'') - V_{\text{KS}}(\mathbf{r}'') \quad (2.4.75)$$

where the derivative of the kinetic energy has been substituted with $-V_{\text{KS}}$ from the Kohn-Sham equation(2.4.71). This substitution neglects a constant term from the eigenvalues ϵ_i, however, as the potential can only be determined uniquely up to a constant by the Hohenberg-Kohn theorem, this term does not affect the calculation of the OEP potential. V_{KS} can be defined as

$$V_{\text{KS}}(\mathbf{r}'') = V_{\text{ext}}(\mathbf{r}'') + V_{\text{H}}(\mathbf{r}'') + V_{\text{X}}(\mathbf{r}''). \quad (2.4.76)$$

In DFT $V_{\text{X}}(\mathbf{r}'') = \frac{\delta E_{\text{X}}}{\delta\rho(\mathbf{r}'')}$ when E_{X} is an explicit functional of ρ, if instead E_{X} is not an explicit functional of the density, as it is here, this derivative is instead an effective local potential $V_{\text{eff}}(\mathbf{r})$ to be determined. Defining

$$V_{\text{KS}}(\mathbf{r}'') = V_{\text{ext}}(\mathbf{r}'') + V_{\text{H}}(\mathbf{r}'') + V_{\text{eff}}(\mathbf{r}'') \quad (2.4.77)$$

the derivative in (2.4.75) simplifies to

$$\frac{\delta}{\delta\rho(\mathbf{r}'')}\left[T_{\text{s}}[\rho[V_{\text{KS}}]] + E_{\text{ext}}[\rho[V_{\text{KS}}]] + E_{\text{H}}[\rho[V_{\text{KS}}]]\right] = -V_{\text{eff}}(\mathbf{r}''). \quad (2.4.78)$$

The derivative of the density with respect to the orbitals is simply

$$\frac{\delta\rho(\mathbf{r}'')}{\delta\phi_i(\mathbf{r}')} = \frac{\delta\sum_j^N |\phi_j(\mathbf{r}'')|^2}{\delta\phi_i(\mathbf{r}')} = \phi_i^*(\mathbf{r}'')\delta(\mathbf{r}' - \mathbf{r}'') \quad (2.4.79)$$

and substitution of this expression and equation (2.4.78) into the first half of equation (2.4.74) gives

$$\int d\mathbf{r}'' \frac{\delta}{\delta\rho(\mathbf{r}'')}\left[T_{\text{s}}\big[\rho[V_{\text{KS}}]\big] + E_{\text{ext}}\big[\rho[V_{\text{KS}}]\big] + E_{\text{H}}\big[\rho[V_{\text{KS}}]\big]\right]\frac{\delta\rho(\mathbf{r}'')}{\delta\phi_i(\mathbf{r}')}$$

$$= -\int d\mathbf{r}'' V_{\text{eff}}(\mathbf{r}'')\phi_i^*(\mathbf{r}'')\delta(\mathbf{r}' - \mathbf{r}'') = -V_{\text{eff}}(\mathbf{r}')\phi_i^*(\mathbf{r}'). \quad (2.4.80)$$

The derivative of the Fock-exchange energy with respect to the electron orbitals gives the Fock-exchange operator

$$\frac{\delta E_{\mathrm{X}}[\phi_i[V_{\mathrm{KS}}]]}{\delta \phi_i(\mathbf{r}')} = \sum_j \int d\mathbf{r}'' \frac{\phi_j(\mathbf{r}'')\phi_i^*(\mathbf{r}'')}{|\mathbf{r}'' - \mathbf{r}'|} \phi_j^*(\mathbf{r}') = \hat{V}_{\mathrm{X}} \phi_i(\mathbf{r}'). \tag{2.4.81}$$

The derivative of the total energy with respect to the Kohn-Sham orbitals is then

$$\frac{\delta E[V_{\mathrm{KS}}]}{\delta \phi_i(\mathbf{r}')} = \left[\hat{V}_{\mathrm{X}} - V_{\mathrm{eff}}(\mathbf{r}')\right] \phi_i^*(\mathbf{r}'). \tag{2.4.82}$$

Multiplying this result by the derivative of the Kohn-Sham orbitals and integrating to gives

$$\frac{\delta E[V_{\mathrm{KS}}]}{\delta V_{\mathrm{KS}}(\mathbf{r})} = \int d\mathbf{r}' \sum_i^N \sum_{j \neq i}^\infty \frac{\phi_i(\mathbf{r})\phi_j^*(\mathbf{r})}{\epsilon_i - \epsilon_j} \phi_j(\mathbf{r}') \left[\hat{V}_{\mathrm{X}} - V_{\mathrm{eff}}(\mathbf{r}')\right] \phi_i^*(\mathbf{r}') + \mathbf{c.c.} \tag{2.4.83}$$

which equals zero at the energy minimum. The expression under the integral is antisymmetric under exchange of i, j and the summations reduce to over occupied orbitals $i \leq N$ and unoccupied orbitals $a > N$, and can be rewritten as

$$\frac{\delta E[V_{\mathrm{KS}}]}{\delta V_{\mathrm{KS}}(\mathbf{r})} = \int d\mathbf{r}' \sum_i^N \sum_{j=N+1}^\infty \frac{\phi_i(\mathbf{r})\phi_j^*(\mathbf{r})}{\epsilon_i - \epsilon_j} \phi_j(\mathbf{r}') \left[\hat{V}_{\mathrm{X}} - V_{\mathrm{eff}}(\mathbf{r}')\right] \phi_i^*(\mathbf{r}') + \mathbf{c.c.} = 0. \tag{2.4.84}$$

Defining the function

$$\chi(\mathbf{r}, \mathbf{r}') = \sum_i^N \sum_{a=N+1}^\infty \frac{\phi_i(\mathbf{r})\phi_a^*(\mathbf{r})}{\epsilon_i - \epsilon_a} \phi_a(\mathbf{r}')\phi_i^*(\mathbf{r}') + \mathbf{c.c.} \tag{2.4.85}$$

which is known as the density-density response function and is also equal to,

$$\chi(\mathbf{r}, \mathbf{r}') = \frac{\delta \rho(\mathbf{r})}{\delta V_{\mathrm{KS}}(\mathbf{r}')}, \tag{2.4.86}$$

the variation of the density under perturbation of the Kohn-Sham potential. The resulting equation is

$$\frac{\delta E[V_{\mathrm{KS}}]}{\delta V_{\mathrm{KS}}(\mathbf{r})} = \sum_i^N \sum_{j=N+1}^\infty \frac{\phi_i(\mathbf{r})\phi_j^*(\mathbf{r})}{\epsilon_i - \epsilon_j} \int d\mathbf{r}' \phi_j(\mathbf{r}')\hat{V}_{\mathrm{X}}\phi_i^*(\mathbf{r}') - \int d\mathbf{r}' V_{\mathrm{eff}}(\mathbf{r}')\chi(\mathbf{r}, \mathbf{r}') + \mathbf{c.c.} = 0 \tag{2.4.87}$$

and defining

$$B(\mathbf{r}) = \sum_{i}^{N} \sum_{j=N+1}^{\infty} \frac{\phi_i(\mathbf{r})\phi_j^*(\mathbf{r})}{\epsilon_i - \epsilon_j} \int d\mathbf{r}' \phi_j(\mathbf{r}')\hat{V}_X\phi_i^*(\mathbf{r}') \tag{2.4.88}$$

allows Eq. (2.4.87) to be written as

$$\frac{\delta E[V_{\text{KS}}]}{\delta V_{\text{KS}}(\mathbf{r})} = B(\mathbf{r}) - \int d\mathbf{r}' V_{\text{eff}}(\mathbf{r}')\chi(\mathbf{r}, \mathbf{r}') + \textbf{c.c.} = 0 \tag{2.4.89}$$

which must be solved to find V_{eff}. The density-density response functional $\chi(\mathbf{r}, \mathbf{r}')$ has been shown to have only a single null eigenvector, being that of the constant function [67]. Thus it is possible to invert $\chi(\mathbf{r}, \mathbf{r}')$ and the minimising potential of the OEP equation can be determined by solving the equation

$$V_{\text{eff}}(\mathbf{r}) = \int d\mathbf{r}' \chi^{-1}(\mathbf{r}, \mathbf{r}') B(\mathbf{r}). \tag{2.4.90}$$

For methods where the basis set is used to represent $\phi(\mathbf{r})$ is small, such as with a Gaussian basis (see section 2.5.1), $\chi(\mathbf{r}, \mathbf{r}')$ can be inverted, and (2.4.90) can be directly calculated in order to obtain $V_{\text{eff}}(\mathbf{r})$. This inversion of $\chi(\mathbf{r}, \mathbf{r}')$ can be computed efficiently and the minimising local potential can be found quickly. However, while this inversion is well defined for a complete infinite orbital basis set, for a practical calculation there are finite basis set effects which cause serious mathematical difficulties [68–70].

In plane wave methods (see section 2.5.2) the inversion of $\chi(\mathbf{r}, \mathbf{r}')$ is often impractical due to the large basis sets used, and the potential $V_{\text{eff}}(\mathbf{r})$ can instead found by minimising the total OEP energy using a steepest descent, conjugate gradient, or other direct minimisation method (see section 2.6).

Calculation of the matrix $\chi(\mathbf{r}, \mathbf{r}')$ can pose difficulties in all methods as its construction requires knowledge of all the unoccupied orbitals. These orbitals require more accurate basis sets to be adequately represented, increasing computational cost. For a practical calculation the infinite sum must be truncated to a finite number of unoccupied orbitals, that can introduce discontinuous behaviour in the OEP. These difficulties have led to approximations which simplify the expression of $\chi(\mathbf{r}, \mathbf{r}')$, with the method of Krieger, Li, and Iafrate (KLI) [71] fixing the energy

difference $\epsilon_i - \epsilon_j = \Delta$ for all orbital energies giving

$$\chi(\mathbf{r}, \mathbf{r}') = \frac{1}{\Delta} \sum_{i=1}^{N} \sum_{j=1}^{\infty} \phi_i(\mathbf{r})\phi_a^*(\mathbf{r})\phi_a(\mathbf{r}')\phi_i^*(\mathbf{r}'). \tag{2.4.91}$$

Similarly, the common energy denominator method (CEDA) [72] makes use of the antisymmetry of exchanging i, j in Eq. (2.4.85) for $i, j \leq N$. This antisymmetry allows a cancellation of all terms with $j \leq N$. Once this cancelation has been performed the energy $\epsilon_i - \epsilon_a = \Delta$ is fixed for all occupied-unoccupied orbital pairs, giving

$$\chi(\mathbf{r}, \mathbf{r}') = \frac{1}{\Delta} \sum_{i=1}^{N} \sum_{a=N+1}^{\infty} \phi_i(\mathbf{r})\phi_a^*(\mathbf{r})\phi_a(\mathbf{r}')\phi_i^*(\mathbf{r}'). \tag{2.4.92}$$

These methods allow good approximations for the full OEP method with a reduced computational cost, with the CEDA method being improved compared to the KLI method as it ensures that the denominators approximated with Δ all have the same sign, whereas in KLI this denominator does not have the same sign, introducing errors. Methods have also been developed to calculate the full OEP without requiring an infinite summation using the Hylleraas variational principle [73] and the completeness relation of the Kohn-Sham orbitals to define an alternative way to calculate $\frac{\delta E[V_{\mathrm{KS}}]}{\delta V_{\mathrm{KS}}(\mathbf{r})}$ [74]. These methods are all applicable to a general OEP method that can be calculated for orbital dependent potential functions in a similar manner as that used for the Hartree-Fock potential.

2.5 Representing the Orbitals

In order to perform calculations using electronic structure methods the orbitals have to be represented in some form. The simplest representation is to construct the orbitals discretely on a grid. Adequately representing the gradient and integral terms necessary for a DFT calculation requires a fine mesh of grid points. This leads to computationally expensive calculations, both in terms of calculation time and memory required to store the large grids involved. Despite these drawbacks, grid based approaches remain a viable method for solving the DFT equations [75,76]. On

modern computers, which allow massive parallelisability, grid methods have shown promise in constructing order N DFT methods [77, 78].

In the vast majority of DFT calculations, and all those calculations considered in this thesis, the orbitals are expanded in a basis set. Basis sets reduce the need for a fine discrete grid and greatly reduce computational cost of the calculations. There are two main basis set types; the choice of which is largely dependent on the systems considered. For atomic or molecular systems a basis set which is localised on the individual atoms in the system is preferred. While for electrons in a periodic infinite system, periodic functions such as plane waves, which well represent delocalised electrons, are often used.

2.5.1 Molecular Systems

In molecular systems the electron orbitals are confined close to the atomic centres and thus the basis sets for describing these orbitals should also be localised around the atomic centres. For such localised orbitals an immediate first choice would be to begin with the solutions of the Schrödinger equations for a hydrogen like atom. These basis set elements, known as Slater-type orbitals (STOs) [79], have the form

$$\chi^{\text{STO}} = r^{n-1} Y_{lm}(\theta, \phi) e^{-\zeta r} \tag{2.5.93}$$

where Y_{lm} is the angular component of the basis and n, l, m are the quantum numbers of the electron. This choice of basis runs into difficulty when the number of atomic centres grows, and scales poorly when calculating integrals of several electrons, required to calculate the Hartree energy. An alternative was proposed by Foster and Boys [80] which utilised Gaussian functions to approximate certain, difficult to integrate, STOs and was further developed to approximate, in general, STOs [81, 82]. These Gaussian-type orbitals (GTOs) in Cartesian coordinates have the form

$$\chi^{\text{GO}} = x^l y^m z^n e^{-\zeta r^2}. \tag{2.5.94}$$

Because products of GTOs can be written as a linear combination of GTOs, inte-

grals have a closed form expression. Therefore GTOs allow for efficient calculations
of the integrals used in DFT methods. As these orbitals, unlike STOs, are not
physically motivated, they make a poorer approximation to electronic orbitals and
require several basis set elements to reasonably approximate the true electron or-
bitals. However, the ease of performing integrals with GTOs makes them ideal for
calculations with many interacting electrons with different atomic centres [83]. In
order to save computational time it is desirable that the set of Gaussian orbitals cho-
sen has as few basis set functions, while also containing enough elements to provide
reasonable accuracy. A basis set with few functions may adequately describe a lone
electron in a hydrogen-like atom, but will fail to properly describe an interacting
electron in a molecule. The more basis functions in a basis set, the more accurate
a representation the basis set provides. There are many basis sets available for
molecular calculations [81, 84–86] with varying trade-offs between speed and accu-
racy. A commonly used set of Gaussian basis sets are the correlation consistent basis
sets [87–89] which are designed to reproduce atomic natural orbitals from correlated
calculations. While GTOs are computationally easy to implement, they come with
some disadvantages. The basis sets are difficult to systematically improve as larger
basis sets have entirely different Gaussian expansion to a smaller set. GTOs are
also poor at describing diffuse, weakly bound electrons as they are constructed to
describe bound electron orbitals. Weakly bound orbitals often require augmented
basis sets containing additional, diffuse Gaussian functions.

2.5.2 Periodic Systems

In periodic systems there are an infinite set of orbitals to represent and we make use
of Bloch's theorem to define these orbitals in a plane wave basis set. In a periodic
system Bloch's theorem allows the wave function of the infinite electron orbitals to
be expressed as a number of Bloch functions equal to the number of electrons in the
unit cell. These Bloch functions are given by

$$\phi_{i,k}^{\sigma}(\mathbf{r}) = u_j^{\sigma}(\mathbf{r})e^{i(\mathbf{k}\cdot\mathbf{r})} \tag{2.5.95}$$

where the function $u_j^{\sigma}(\mathbf{r})$ is periodic over the unit cell of the system and $e^{i(\mathbf{k}\cdot\mathbf{r})}$ is a

phase factor dependent on the momentum vector $\mathbf{k}$. In a periodic system the choice of $\mathbf{r}$ and $\mathbf{k}$ are not unique choices but are both periodic under $\mathbf{r} + \mathbf{R}$ or $\mathbf{k} + \mathbf{G}$, where $\mathbf{R}$ is a vector of the Bravais lattice, and $\mathbf{G}$ is a reciprocal lattice vector. Due to these periodicities the choice of $\mathbf{r}$ can be restricted to inside the primitive unit cell, and $\mathbf{k}$ can be restricted to inside the first Brillouin zone. These restrictions ensure that each $\phi_{i,k}^{\sigma}(\mathbf{r})$ is unique for these choices of $\mathbf{r}, \mathbf{k}$. The function $u_j^{\sigma}(\mathbf{r})$ can further be represented as a Fourier series

$$u_j^{\sigma}(\mathbf{r}) = \sum_{\mathbf{G}} c_{j,\mathbf{G}} e^{i\mathbf{G} \cdot \mathbf{r}} \tag{2.5.96}$$

where $\mathbf{G}$ are the reciprocal lattice vectors of the system. The expansion of the orbitals can then be written as

$$\phi_{i,k}^{\sigma}(\mathbf{r}) = \sum_{\mathbf{G}} c_{j,\mathbf{G}} e^{i(\mathbf{G}+\mathbf{k}) \cdot \mathbf{r}}. \tag{2.5.97}$$

The plane-wave representation of the electron orbitals allows a flexible description of the wave functions which is independent of the location or type of molecules in the system. This picture of electron orbitals depends on the choice of k-point $\mathbf{k}$ which can take a continuum of values in the Brillouin zone and must be discretised. The choice k-points is made through the use of a Monkhorst Pack grid [90,91] which discretises the space in the Brillouin zone into a regular array of $N_x \times N_y \times N_z$ points, specified by N_x, N_y, N_z points in each axis.

The infinite summation over the reciprocal lattice vectors $\mathbf{G}$ must also be truncated in order to make the plane-wave basis set practical for use in computation. The electron wave function in a periodic system is expected to vary smoothly, and basis set elements for which $|\mathbf{G} + \mathbf{k}|$ is large will have a high kinetic energy

$$E_k = \frac{1}{2} |\mathbf{G} + \mathbf{k}|^2 \tag{2.5.98}$$

and will have a small contribution to the overall wave function. As most behaviour will be described by plane waves with a small kinetic energy a cutoff energy E_{cut} for basis elements can be introduced for which basis elements with energies above this will not be included. This cutoff energy can be determined by increasing the value

of E_{cut} until the total energy of a calculation converges sufficiently. This allows a controllable accuracy to be obtained using plane waves and, if further accuracy is required, the cutoff energy can be increased further, including more basis functions with higher kinetic energy. A higher cutoff energy will improve the representation of the electron wave function, at the expense of a larger and more computationally demanding basis set.

Plane wave basis sets are very efficient when treating slowly varying electron orbitals, however electrons close to atomic nuclei have a much higher kinetic energy and consequently have rapidly oscillating wave functions requiring a very large cutoff energy in order to sufficiently represent these orbitals. This rapid oscillatory behaviour is confined to regions near the atomic nuclei where electrons are well localised meaning that a high cut-off energy is being required to model high energy core electrons that are typically not involved in chemical bonding. In order to improve efficiency these high energy orbitals can be treated using pseudopotentials [92–94] that replace the potential of the nuclei and core electrons with a single fictitious potential. This potential is constructed such that it reproduces the correct potential corresponding to the nuclei plus core electrons outside a cut-off radius from the nuclei but inside this radius the potential is smoothly varying instead of rapidly oscillating resulting in a smoother wave function. As the rapidly oscillating core electrons and potentials have been removed from the calculation the cut-off energy required by the plane wave basis set is greatly reduced. The cut-off energy can be reduced by several orders of magnitude this way. The use of pseudopotentials also reduces the overall size of the calculation by removing the core electrons and replacing them with a screened nuclear potential. Treating some of the electrons in the systems with a pseudopotential reduces the number of electrons described using DFT, further speeding up the calculation.

2.6 Obtaining the Ground State

The Hatree-Fock, DFT, and the OEP methods are all variational methods where the ground state wave function must be found by minimising a total energy expression. For any wave function

$$\langle \boldsymbol{\Psi} | \hat{H} | \boldsymbol{\Psi} \rangle \geq E_0 \tag{2.6.99}$$

and this equation is only an equality for $\boldsymbol{\Psi} = \boldsymbol{\Psi}_0$, the ground state wave function. In order to calculate the ground state a trial wave function is generated, either randomly or as the solution to a preliminary calculation. From this trial wave function the electron density and the Kohn-Sham potential can be calculated using a particular approximate exchange and correlation function. The Kohn-Sham equations are constructed and diagonalised with the eigenvectors becoming the the new set of orbitals. Updating this way can lead to oscillations, or even divergence of the orbitals. As such a suitable minimisation method must be implemented in order to achieve convergence. There may be several different minimisation schemes employed at different levels in calculation and a single self-consistent cycle may make use of several methods to improve convergence. The techniques covered here are only some of the basic and most general methods and many more advanced minimisation schemes have been developed. It is important to note that even when convergence is achieved that the system may not necessarily be the global ground state and the minimisation may have instead converged to local minima.

2.6.1 Density Mixing

A simple method to prevent the electron density from oscillating between very different states is the density mixing scheme. In this method the electron density is averaged from iteration to iteration in order to smooth out oscillations in the convergence. In the simplest case the density at the nth step is given as

$$\rho_{\mathrm{T}}^n(\mathbf{r}) = \alpha \rho_{\mathrm{T}}^{n-1}(\mathbf{r}) + (1 - \alpha)\rho_{\mathrm{O}}^{n-1}(\mathbf{r}) \tag{2.6.100}$$

where $\rho_{\mathrm{T}}^{n-1}(\mathbf{r})$ is the trial density of the $(n-1)$th step and $\rho_{\mathrm{O}}^{n-1}(\mathbf{r})$ is the updated density outputted when solving the Kohn-Sham equations for the trial density $\rho_{\mathrm{T}}^{n-1}(\mathbf{r})$. α is a mixing parameter that determines the weighting of the density change. A larger α will give a slower but more stable convergence whereas a small alpha can produce faster convergence, but is more likely to find oscillatory behaviour.

2.6.2 Pulay Mixing(DIIS)

Simple density mixing that uses only the electron density from the current and previous cycles can be inefficient if the mixing parameter is small, which is often required to dampen oscillations in convergence. Extensions to mixing routines typically aim to speed convergence by including density information from several previous steps. Pulay mixing, also known as direct inversion of the iterative subspace (DIIS) was developed as a method to improve the convergence of Hartree-Fock self-consistent calculations [95, 96].

DIIS works by calculating an approximate error for each iteration and after a certain number of steps using these errors to mix the previous results in such a way that it minimises the error. The mixing is done by defining an error on the vector $\mathbf{p}_i$ for each iteration as

$$\Delta \mathbf{p}_i = \mathbf{p}_{i+1} - \mathbf{p}_i \tag{2.6.101}$$

and constructing the vector $\mathbf{p}$ at the next iteration as a sum of the previous m iterations

$$\mathbf{p} = \sum_{i=1}^{m} c_i \mathbf{p}_i. \tag{2.6.102}$$

The coefficients c_i are constrained such that

$$\sum_{i=1}^{m} c_i = 1. \tag{2.6.103}$$

An error vector of $\mathbf{p}$ is constructed as

$$\Delta = \sum_{i=1}^{m} c_i \Delta \mathbf{p}_i \tag{2.6.104}$$

and the coefficients c_i can be determined by minimising $\Delta \cdot \Delta$ with the constraint in (2.6.103):

$$L = \Delta \cdot \Delta - \lambda \sum_{i=1}^{m} c_i. \tag{2.6.105}$$

Minimising this expression with respect to c_i gives

$$2 \sum_{j=1}^{m} c_j \beta_{ij} - \lambda = 0 \tag{2.6.106}$$

where $\beta_i j$ is defined as

$$\beta_i j = \Delta \mathbf{p}_i \cdot \Delta \mathbf{p}_j. \tag{2.6.107}$$

The coefficients are then given as

$$c_j = \lambda \sum_{i=1}^{m} \beta^- 1_{ij}. \tag{2.6.108}$$

and λ can be calculated by summing over j and applying the condition in (2.6.103):

$$\lambda = \frac{2}{\sum_{ij} \beta^- 1_{ij}} \tag{2.6.109}$$

and then

$$c_j = \frac{\sum_{i=1}^{m} \beta^- 1_{ij}}{\sum_{ij} \beta^- 1_{ij}}. \tag{2.6.110}$$

This method allows the calculation of the optimal mixing of the previous m steps in order to reduce the error. There are several ways to apply the method [97] and this method can also be used in conjunction with other minimisation techniques to further accelerate convergence.

2.6.3 Gradient Methods

When minimising an objective functional if the derivative is available the minimisation can be performed by following the local gradient and stepping "downhill" towards a minima. The simplest method of these gradient methods is the steepest descent method which takes the negative of the gradient at a point as the next
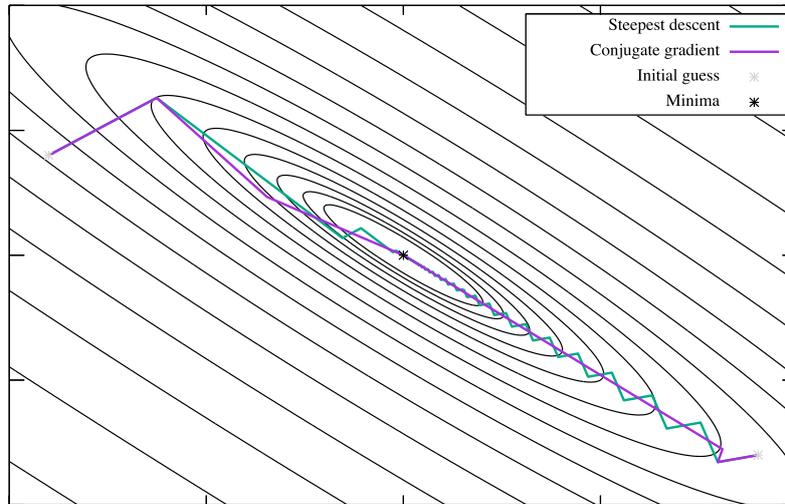
Figure 2.2: The convergence of the steepest descent method compared against the conjugate gradient method.

direction to step. For a objective functional $G[V]$ minimised with respect to some variable V the next iteration is determined by

$$V_{i+1} = V_i + \alpha V' \tag{2.6.111}$$

$$V' = - \left. \frac{\delta G}{\delta V} \right|_{V=V_i} \tag{2.6.112}$$

where the variable α is found by minimising $G[V_{i+1}]$. This method will minimise the objective functional at each step stepping towards the minimum, however this method can struggle when the objective functional landscape is very flat and the method takes many small steps.

To improve the convergence of the steepest descent method the conjugate gradient method is used, for which the step direction V' is chosen to be conjugate to previous V'. A comparison between the steepest descent and the conjugate gradient method can be seen in Figure 2.2 which shows that the convergence of the steepest descent method is strongly dependent on the starting guess, and converges poorly when

in a steep "valley" in the functional landscape. Figure 2.2 also shows the rapid convergence of the conjugate gradient method which converges much faster than the steepest descent method and requires fewer iterations to escape the "valley".

2.7 Codes Used

2.7.1 The HIPPO Local Basis Set Code

For molecular calculations in this thesis calculations were performed with the in-house Gaussian basis set code HIPPO [98], this code is used for the implementation of theoretical methods in DFT, OEP, and reduced density matrix functional theory(RDMFT). Written in FORTRAN 90 it makes use of the LibXC [99] functional library and uses one and two electron integrals calculated using the GAMESS molecular code [100,101]. The HIPPO code supports correlation-consistent Gaussian basis and these were taken from the Basis Set Exchange database [102].

2.7.2 The CASTEP Code

For periodic systems, calculations were performed with the CASTEP electronic structure code [103, 104]. This code is written in FORTRAN 90 and uses a plane wave basis to run DFT, Hartree-Fock, OEP, and other electron structure calculations. The code is fully parallelised, makes use of pseudopotentials, and can be efficiently applied to large and small periodic systems.

Chapter 3

Properties of the Kohn-Sham Potential

3.1 Introduction

This Chapter reviews the literature for some well known properties of the Kohn-Sham potential and the corresponding Kohn-Sham auxiliary system. These properties are shown for the exact DFT potential and the errors introduced when using approximate energy functionals are highlighted. These properties are included for completeness and background for work undertaken in this thesis.

3.2 Ensemble DFT for Systems With Fractional Occupation

The theorems established so far for DFT all treat the system of interest as containing a fixed, integer number of electrons. However it is possible to consider physical systems with an average non-integer number of electrons and DFT can be extended to describe such ensembles [105]. This fractional average number of $Z - \omega$ electrons, where $0 < \omega < 1$, is achieved as a statistical ensemble of two systems, one with Z electrons and another with $Z - 1$ electrons with a probability of being in found in either system. The total ensemble energy is minimised by appealing to

the constrained search method [19], minimising the total energy over all ensembles with a given density, then minimising over all densities that integrate to $Z - \omega$. The resulting ensemble energy is given by

$$E_{Z-\omega} = (1 - \omega)E_Z + \omega E_{Z-1} \tag{3.2.1}$$

where E_Z, E_{Z+1} are the ground state energies of the N and $N + 1$ systems. The ensemble density of this system is given by

$$\rho_{Z-\omega} = (1 - \omega)\rho_Z + \omega \rho_{Z-1} \tag{3.2.2}$$

where ρ_Z and ρ_{Z-1} are the ground state densities for the N and $N - 1$ systems. It should be noted that for an approximate functional such as LDA the exchange correlation energy can be evaluated for an arbitrary density which can integrate to some fractional number of electrons. Due to the approximate nature of DFT energy functionals, the energy obtained from a density which integrates to a fractional electron number is not equivalent to that which would be obtained by evaluating the ensemble energy as in Eq. (3.2.1). This ensemble formulation of DFT is particularly useful when treating the removal or addition of an electron in a system, along with the disassociation of a molecule. Both of these situations exhibit large errors when evaluated using approximate functionals without an ensemble approach due to the non-equivalence of

$$E[\rho_{Z-\omega}] \neq (1 - \omega)E[\rho_Z] + \omega E[\rho_{Z-1}] \tag{3.2.3}$$

for many approximate functionals, which holds for the exact energy functional.

3.3   The DFT Koopmans' Theorem

In the Hartree-Fock method it has been shown that the eigenvalue associated with the nth electron orbital is equal to the ionisation energy of the nth electron from the system under the frozen orbital approximation. In DFT there is no general relation for every electron orbital but there does exist an exact relation between the highest occupied molecular orbital (HOMO) and the first ionisation energy [105, 106]. The

DFT Koopmans' theorem is an exact relationship, which accounts fully for relaxation of the electronic orbitals after the removal of an electron. This is different to the Hartree-Fock Koopmans' theorem where the frozen orbital approximation is used which assumes electron orbitals remain fixed when an electron is removed.

This relation can be proved through a comparison of the asymptotic behaviour of the density expression in the interacting and non-interacting systems [107, 108]. Both have an exponential dependence on the ionisation energy for the exact interacting system and the negative of the highest Kohn-Sham eigenvalue for the non-interacting system as

$$\lim_{\mathbf{r}\to\infty} \rho \sim e^{-2\sqrt{2I_Z}|\mathbf{r}|} \tag{3.3.4}$$

$$\lim_{\mathbf{r}\to\infty} \rho_{\mathrm{KS}} \sim e^{-2\sqrt{-2\epsilon_Z}|\mathbf{r}|} \tag{3.3.5}$$

which, as the Kohn-Sham density is the same as that of the fully interacting system, immediately gives

$$I_Z = -\epsilon_Z. \tag{3.3.6}$$

The exact nature of the functionals is important when demonstrating the equivalence of the ionisation energy and the Kohn-Sham eigenvalue. This relationship is no longer satisfied exactly for approximate functionals resulting in significant errors when calculating the ionisation energy with an approximate functional.

3.3.1   Band Structures

In periodic systems the picture of electron excitations can be investigated through a band structure calculation. Electrons in a periodic system are represented differently to those in a molecular system and there are many solutions to the Kohn-Sham equations which depends on both the band number i and the wave vector k, with the one electron wave functions given by

$$\left[-\frac{\nabla^2}{2} + V_{\mathrm{KS}}^\sigma(\mathbf{r})\right] \phi_{i,k}^\sigma(\mathbf{r}) = \epsilon_{i,k}^\sigma \phi_{i,k}^\sigma(\mathbf{r}) \tag{3.3.7}$$

which defines the electron wave functions $\phi_{i,k}^{\sigma}(\mathbf{r})$ and the Kohn-Sham eigenvalues $\epsilon_{i,k}^{\sigma}$. The wave vector k is free to take any value but can always be mapped back into the first Brillouin zone of the crystal, which are a set of unique points in reciprocal space. By sampling points inside the first Brillouin zone the energy spectra can be determined from the Kohn-Sham eigenvalues $\epsilon_{i,k}^{\sigma}$ for every k-point k. In order to sample the behaviour of the Brillouin zone the band structure is typically calculated along paths between high symmetry points in the Brillouin zone [109].

The band structure of the Kohn-Sham non-interacting wave functions is often used to approximate the band structure of the fully interacting system. Much like for molecular systems this approximation has only been shown in Koopmans' theorem for DFT to hold when using the exact DFT functional to calculate the ionisation energy from the highest occupied band. However, the band structures generated this way are assumed to provide a qualitative insight into the physics of the system for all electron bands [110].

Because the energies of the Kohn-Sham orbitals can vary over the Brillouin zone this makes determining which bands are occupied when performing a calculation more difficult than for molecular systems. In molecular calculations the N lowest energy orbitals are all occupied by an integer number of electrons with the occupation number f_i^{σ} being either 0 or 1 (or 2 in the case of spin unpolarised systems). In periodic systems the Fermi energy ϵ_F defines an energy for which, at zero temperature, any state lower in energy is occupied and any state higher is unoccupied. In this picture bands may cross the Fermi energy at points in the Brillouin zone and to account for this, the band occupation numbers must be extended to include fractional occupation such that $0 \leq f_i^{\sigma} \leq 1$ (or $0 \leq f_i \leq 2$ in the case of a spin unpolarised system). In some calculations it can be useful to "smear" the occupancy of the bands to include occupied states above the Fermi energy. This can be seen as an extension of DFT to finite temperatures where the Fermi energy and the temperature of the system can be used in a distribution to determine the occupancy of each band. This extension of DFT to non-integer systems was introduced through

the use of Mermin's extension of Kohn-Sham DFT to finite temperatures [111, 112]. A typical choice for the distribution of energy states is the Fermi-Dirac distribution such that the occupancy of the ith band $f_{i,k}$ at a particular k-point is given by

$$f_{i,k}^{\sigma} = \left[\exp^{\frac{\left(\epsilon_{i,k}^{\sigma} - \epsilon_F\right)}{k_B T}} + 1 \right]^{-1} \tag{3.3.8}$$

where k_B is the Boltzmann constant and T is the temperature of the system. This "smearing" can be especially important in metals where bands are degenerate, or nearly degenerate, around the Fermi level [113]. The Fermi energy itself can be calculated by ensuring

$$\sum_{\sigma}^{\uparrow\downarrow} \sum_{i} \sum_{k \in BZ} f_{i,k}^{\sigma} = N. \tag{3.3.9}$$

This condition allows the Fermi energy to be determined by varying the Fermi energy and recalculating the occupancies from the chosen smearing regime (for example Eq. 3.3.8) until Eq. 3.3.9 is satisfied.

3.4 The Derivative Discontinuity

A consequence of the extension of DFT to ensembles of systems with fractional occupation numbers is the derivative discontinuity [105, 106]. This discontinuity appears simply from the expression in Eq. (3.2.1) which gives

$$\frac{\delta E_N[\rho]}{\delta N} = \frac{\delta E_N[\rho]}{\delta \omega} = E[\rho_{Z-1}] - E[\rho_Z] = -I_Z \tag{3.4.10}$$

which defines the ionisation energy I_Z. Using the relationship for the exact Kohn-Sham eigenvalue in Eq. (3.3.6) gives

$$\frac{\delta E_N[\rho]}{\delta N} = \epsilon_Z \qquad Z - 1 < N \leq Z \tag{3.4.11}$$

for $Z - 1 < N \leq Z$ this gradient is the Zth ionisation energy but upon crossing to $Z < N \leq Z+1$ this gradient becomes equal to the $(Z+1)$th ionisation energy. This results in the energy of a system being piecewise linear as electron number varies, with a discontinuous change of gradient at integer electron numbers.

One implication of this piecewise linearity is that molecules disassociate into fragments with integer electronic charge. This is the physically expected result when a molecular bond is stretched with its behaviour tending towards that of two isolated fragments. The piecewise linearity implies that the minimum energy state of each of these fragments is found at integer electron occupation [105], correctly tending towards the correct result in the limit of infinite separation. However, this property only holds true if the derivative discontinuity is correctly treated. For approximate methods the total energy is no longer piecewise linear and may not exhibit a discontinuity at integer electron numbers, instead varying smoothly. For molecular disassociation this can lead to a minimum energy state that does not have integer electron numbers on each fragment. This incorrect result is mainly attributed to a self-interaction error present in many approximate theories [114–117].

3.5 The Self-Interaction Problem

The electron density is the controlling quantity in DFT and the interactions of electrons with the density inherently contain interactions between an electron and its own contribution to the density resulting in self-interactions [114–117]. The largest contributions to self-interaction error comes from terms in the Hartree and exchange energy. When exchange is treated exactly, as in Hartree-Fock, these terms in the Hartree and exchange energies cancel and such methods are generally considered to be self-interaction free. Additional self-interaction errors can be found in the correlation energy, however, such errors are generally smaller than those found in the Hartree and exchange terms.

The Hartree energy can be written as

$$
\begin{aligned}
E_{\mathrm{H}} = \frac{1}{2} \int d\mathbf{r} d\mathbf{r}' \sum_{(i,\sigma) \neq (j,\sigma')}^{N} & \frac{\left[\phi_i^{\sigma}(\mathbf{r})\right]^* \phi_i^{\sigma}(\mathbf{r}) \phi_j^{\sigma'}(\mathbf{r}') \left[\phi_j^{\sigma'}(\mathbf{r}')\right]^*}{|\mathbf{r} - \mathbf{r}'|} \\
& + \frac{1}{2} \int d\mathbf{r} d\mathbf{r}' \sum_i^N \sum_\sigma \frac{\left[\phi_i^{\sigma}(\mathbf{r})\right]^* \phi_i(\mathbf{r}) \left[\phi_i^{\sigma}(\mathbf{r}')\right]^* \phi_i(\mathbf{r}')}{|\mathbf{r} - \mathbf{r}'|} \quad (3.5.12)
\end{aligned}
$$

where the final term is a self-interacting term giving the energy of an electron experiencing electrostatic repulsion from itself. When the exchange exactly is treated

exactly the energy is given by the Fock exchange energy in Eq. (2.2.21), which can be expressed as

$$
\begin{aligned}
E_{\mathrm{X}} = -\frac{1}{2} \int d\mathbf{r} d\mathbf{r}' \sum_{\sigma} \sum_{i,j}^{N^{\sigma}} & \frac{\left[\phi_i^{\sigma}(\mathbf{r})\right]^* \phi_j^{\sigma}(\mathbf{r}) \phi_i^{\sigma}(\mathbf{r}') \left[\phi_j^{\sigma}(\mathbf{r}')\right]^*}{|\mathbf{r} - \mathbf{r}'|} \\
& -\frac{1}{2} \int d\mathbf{r} d\mathbf{r}' \sum_{\sigma} \sum_{i}^{N^{\sigma}} \frac{\left[\phi_i^{\sigma}(\mathbf{r})\right]^* \phi_i^{\sigma}(\mathbf{r}) \left[\phi_i^{\sigma}(\mathbf{r})\right]^* \phi_i^{\sigma}(\mathbf{r}')}{|\mathbf{r} - \mathbf{r}'|} \quad (3.5.13)
\end{aligned}
$$

where the same self-interacting term appears with the opposite sign. The self-interaction energy introduced in the Hartree term cancels exactly resulting in a total energy expression free from self-interactions. In DFT methods where the exchange energy term is approximated, the approximate energy expressions fail to account for these self-interacting contributions and the self-interacting energy terms remain in the total energy expression. The inclusion of the self-interacting term therefore introduces an error into the energy expression. The error introduced by self-interactions depends on the choice of approximation used to calculate the exchange energy, some functionals partially cancel this interaction while others fail to account for self-interactions at all. The incorrect treatment of self-interactions in density functional approximations contributes towards some well known errors in DFT including: artificial stabilisation of delocalised states [114, 114], underestimating electron affinities [118] and the underestimation of ionisation energies and band gaps [33, 119–121].

3.5.1 One Electron Self-Interaction

In a one-electron system self-interaction effects are easy to identify as there are no electron-electron interactions and the exact energy is given only by the kinetic and external potential energies. Therefore, for the exact energy functional, contributions from the Hartree energy and exchange and correlation energy must cancel exactly. As the exact behaviour of the exchange-correlation energy is known for a one-electron system the self-interaction error of the system can be defined as

$$E_{\text{SIE}}[\rho^{(1)}] = E_{\text{H}}[\rho^{(1)}] + E_{\text{XC}}[\rho^{(1)}] \tag{3.5.14}$$

with $\rho^{(1)}$ as the one-electron density $|\phi_1(\mathbf{r})|^2$. If an approximate functional fails to have full cancellation between Hartree and exchange-correlation energies for a single electron then it exhibits self-interactions. Many commonly used density functional approximations have a non-zero self-interaction error despite providing accurate total energies. Typically non-local Hartree-Fock exchange terms are needed to begin accounting for self-interactions.

3.5.2 Self-Interaction Errors

The effects of self-interactions go beyond the incomplete cancellation of the Hartree and exchange energy for a one electron system, and functionals which are one electron self-interaction free can still exhibit many electron self-interaction effects [122–124]. In a multi-electron system the self-interaction energy is less well defined than for one-electron systems. The exact total energy expression is unknown, along with the self-interacting energy contribution from the exchange-correlation approximation. However, defining the Hartree self-interaction energy, as

$$E_{\text{H,SIE}} = \frac{1}{2} \sum_i^N \sum_\sigma \int d\mathbf{r} d\mathbf{r}' \frac{[\phi_i^\sigma(\mathbf{r})]^* \phi_i^\sigma(\mathbf{r}) [\phi_i^\sigma(\mathbf{r})]^* \phi_i^\sigma(\mathbf{r}')}{|\mathbf{r} - \mathbf{r}'|} \tag{3.5.15}$$

allows general insight into the energy error introduced by self-interactions. This term is a positive quantity that is larger when electrons are localised and smaller when electrons are delocalised. It is therefore energetically more favourable for states in which the Kohn-Sham electron wave functions are more delocalised. The tendency for the Kohn-Sham electrons to be more delocalised introduces errors which significantly affect properties calculated from the Kohn-Sham system [114].

Kohn-Sham Orbital Energies

The self-interaction error energetically favours systems where the Kohn-Sham orbitals are delocalised. This favouring of delocalised states changes not only the shape of the orbitals but also the eigenvalue associated with these states. In the case of the

eigenvalue of the HOMO this energy corresponds to the ionisation energy through the DFT Koopmans' theorem. However it has long been observed that local and semi-local DFT functionals give particularly poor approximations of the ionisation energy despite this theorem. Typical errors of several eV are largely associated with the self-interaction error in approximate DFT functionals. In these systems the delocalisation of the orbitals due to self-interaction error leads to an artificial raising of the potential, which in turn leads to smaller Kohn-Sham eigenvalues and a general underestimation of the ionisation energies. The Hartree-Fock method, which is free from self-interaction error, has much smaller errors when calculating ionisation energies using Koopmans' theorem. This is due in part to the cancellation between orbital relaxation effects and the errors from neglecting correlation.

Asymptotic Behaviour of the Kohn-Sham Potential

In molecular system, the asymptotic behaviour of the exact Kohn-Sham potential is known from a simple argument that Kohn-Sham electrons at long distances from the system should experience the Coulombic potential of a point charge centred on the system with a charge corresponding to $N-1$ electrons. Therefore at large distances from the centre of a molecule the Kohn-Sham potential should decay as $(N-1)/r$. The asymptotic behaviour of the Hartree potential is

$$\lim_{|\mathbf{r}|\to\infty} \int d\mathbf{r}' \frac{\rho(\mathbf{r}')}{|\mathbf{r}-\mathbf{r}'|} = \frac{\int d\mathbf{r}'\rho(\mathbf{r}')}{|\mathbf{r}|} = \frac{N}{|\mathbf{r}|} \qquad (3.5.16)$$

in order to have the correct asymptotic behaviour the exchange and correlation potentials should decay as $-1/r$.

This asymptotic behaviour is not seen with many functionals with Fig. 3.1 showing the asymptotic behaviour V_{xc} for the LDA potential in a n atom. It is clear that the LDA functional does not have the correct asymptotic behaviour and this is a common error in many density functional approximation (DFA)s [125, 126]. As can be seen in Fig. 3.1 the LDA Kohn-Sham potential has exponential asymptotic behaviour as opposed to the $-1/r$ decay that the exact functional should exhibit. The exponential behaviour is due to the exponential asymptotic decay of the electron density given in Eq. 3.3.4. The incorrect asymptotic behaviour of the Kohn-Sham
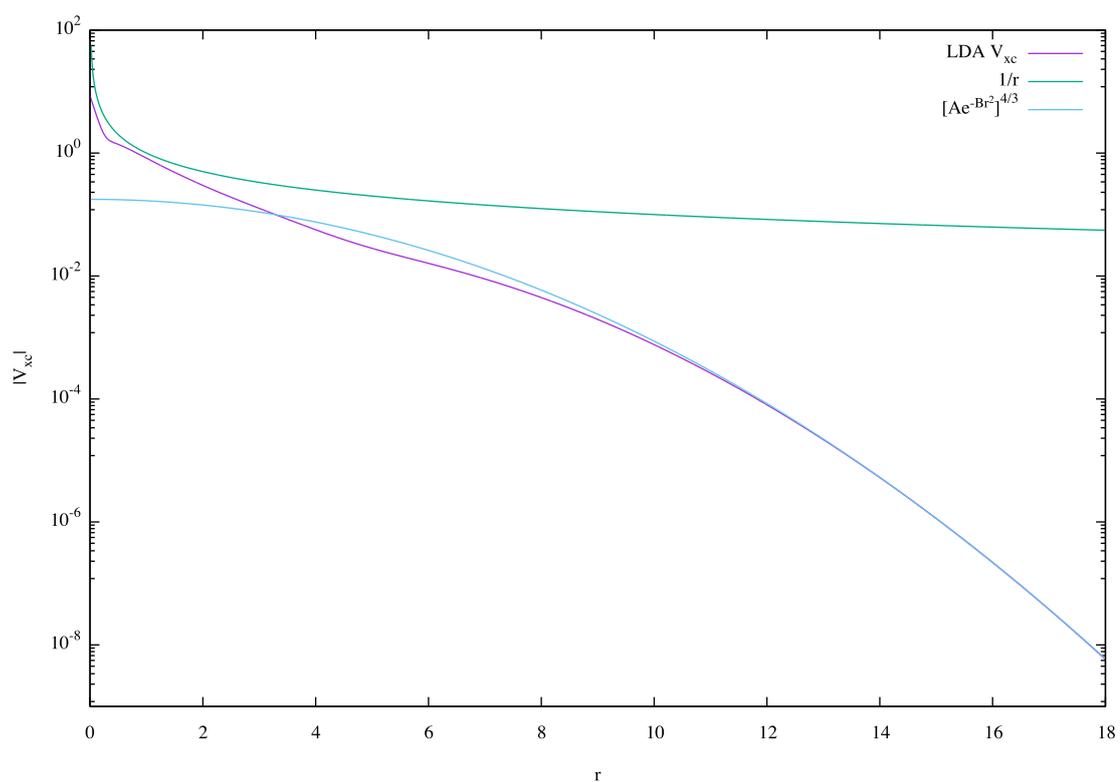
Figure 3.1: The asymptotic decay of the LDA potential compared to the self-interaction free correct decay of $1/r$. Calculated for a neon atom with a cc-pVQZ basis set.

potential means that a Kohn-Sham electron at large r experiences an electrostatic repulsion that corresponds to N electrons, including an image of the electron itself. In this case the electron is less tightly bound to the molecule than in the self-interaction free case, directly affecting the ionisation energies of molecular systems as the asymptotic behaviour of the potential at long range strongly determines the energy required to remove an electron from a system.

Molecular Disassociation

The erroneous result in which molecules disassociate into fractionally charged fragments is also due in part to self-interaction errors [123, 127, 128]. Self-interaction effects allow a lower energy configuration to be obtained by delocalising electrons over all fragments in order to minimise the self-interaction of the electrons. This is opposed to the localisation of full electronic charge onto a single fragment, expected in the exact system. This results in spurious charges present on disassociated fragments that can significantly affect the disassociation energies or energies of formation.

3.5.3 Self-Interaction Corrections

As self-interactions contribute significant errors to DFT there have been many attempts to correct for them without having to resort to a more expensive method such as a full exact exchange treatment [70, 114, 119, 120, 129–135]. A portion of this thesis will be investigating a novel self-interaction correction but there also exist other methods that aim to correct for self-interactions or construct functionals that are self-interaction free [33, 136–138].

3.6 Summary

The importance of self-interaction effects has been highlighted in approximate DFT with the errors due to self-interactions affecting ionisation energies, energies of disassociation, and the derivative discontinuity. These errors have been investigated with the main cause of errors being a non-zero one-electron, and many-electron

self-interaction error and an incorrect asymptotic behaviour of the Kohn-Sham potential.

Chapter 4

Constrained Method of Self-interaction Correction

4.1 Introduction

As we saw in the previous Chapter, the presence of self-interactions in approximate DFT methods lead to large errors in properties related to the Kohn-Sham potential. This Chapter will introduce a self-interaction correction in which the behaviour of the Kohn-Sham potential is constrained such that it has the correct asymptotic behaviour. This method was introduced by Gidopoulos and Lathiotakis [70, 139] in 2012 and I improved and extended this method. This Chapter will present results from my application of this method to a wide variety of systems and functional approximations [140].

4.2 Theory

As has been shown self-interaction error in a DFA can manifest in the asymptotic behaviour of the Kohn-Sham potential, with the correct behaviour being

$$\lim_{r \to \infty} V_{\mathrm{KS}}(\mathbf{r}) = \frac{N - 1}{r} \tag{4.2.1}$$

where N is the number of electrons in the system. In DFT the Kohn-Sham potential is given by $V_{\mathrm{KS}}(\mathbf{r}) = V_H(\mathbf{r}) + V_{\mathrm{XC}}(\mathbf{r})$ and the asymptotic behaviour of the Hartree

potential V_H is

$$\lim_{r \to \infty} V_{\mathrm{H}}(\mathbf{r}) = \lim_{r \to \infty} \int d\mathbf{r}' \frac{\rho(\mathbf{r})}{|\mathbf{r}' - \mathbf{r}|} = \frac{N}{r}. \qquad (4.2.2)$$

Therefore, in a self-interaction free method the exchange-correlation potential should decay as $-1/r$ in order to give the correct overall asymptotic behaviour. Hence, self-interaction errors are present when $V_{\mathrm{XC}}(\mathbf{r})$ does not decay as $-1/r$. This does not guarantee that a method with the correct decay is self-interaction free, as it may still exhibit self-interactions in its short range behaviour. In many popular and well used density functional approximations $V_{\mathrm{XC}}(\mathbf{r})$ is found to decay exponentially fast as seen in Section 3.5.2. In these approximations the overall asymptotic behaviour of the Kohn-Sham potential decays incorrectly as N/r, therefore a long distance from the system an electron sees a potential which includes an interaction with itself. These self-interactions in the Kohn-Sham potential has significant effects on the ionisation energy predicted by the DFT Koopmans' theorem [70].

4.2.1   Quantifying Self-Interactions With Poisson's Law

The presence of self-interactions in a DFT approximation can be quantified in terms of an effective charge density $\rho_{\mathrm{HXC}}(\mathbf{r})$ whose electrostatic potential gives $V_{\mathrm{HXC}}(\mathbf{r})$ [70]. That such a charge density exists is justified through Poisson's law, with which we define the charge density ρ_{HXC} as

$$\nabla^2 V_{\mathrm{HXC}}(\mathbf{r}) = -4\pi \rho_{\mathrm{HXC}}(\mathbf{r}), \ V_{\mathrm{HXC}}(\mathbf{r}) = \int d\mathbf{r}' \frac{\rho_{\mathrm{HXC}}(\mathbf{r}')}{|\mathbf{r}' - \mathbf{r}|}. \qquad (4.2.3)$$

Eq. 4.2.3 holds for a sufficiently well behaved potential. The presence of self-interactions can be seen from the behaviour of the potential in the limit of large r, and can be found by integrating the charge density $\rho_{\mathrm{HXC}}(\mathbf{r})$. If $\int d\mathbf{r} \rho_{\mathrm{HXC}}(\mathbf{r}) = N - 1$ the asymptotic behaviour of the system is correct, while if $\int d\mathbf{r} \rho_{\mathrm{HXC}}(\mathbf{r}) > N - 1$ then there are self-interactions present in the approximation.

4.2.2 A Modification to the Kohn-Sham Equations

A method for correcting for SI effects in the KS potential (but without correcting the energy) was proposed by Gidopoulos and Lathiotakis [70, 139]. In place of $V_{\mathrm{KS}}(\mathbf{r}) = V_{\mathrm{HXC}}(\mathbf{r})$, it employs an effective local potential which represents the electronic repulsion, denoted by $V_{\mathrm{KS}}(\mathbf{r}) = V_{\mathrm{rep}}(\mathbf{r})$. This new potential is constructed as

$$V_{\mathrm{rep}}(\mathbf{r}) = \int d\mathbf{r}' \frac{\rho_{\mathrm{rep}}(\mathbf{r}')}{|\mathbf{r}' - \mathbf{r}|} \qquad (4.2.4)$$

the Hartree potential of some auxiliary density $\rho_{\mathrm{rep}}(\mathbf{r})$ which is distinct from the electron density of the interacting system. This change allows for easy control of the asymptotic behaviour of the Kohn-Sham potential while leaving the energy expression of an approximation unchanged. Constructing the Kohn-Sham potential this way, it is clear that the asymptotic behaviour, and therefore the level of self-interaction error, in the method is determined by the value of $\int d\mathbf{r} \rho_{\mathrm{rep}}(\mathbf{r})$. To ensure the method is self-interaction free constraints must be placed on this auxiliary density. It should be noted that the potential V_{rep}, which plays the role of V_{HXC} in the KS equations, is not defined as the functional derivative of the approximate HXC energy with respect to the density and must be determined in a different way.

4.2.3 Constraints on ρ_{rep}

Despite a change in the Kohn-Sham expression, performing an unconstrained minimisation of the total energy with respect to the effective potential $V_{\mathrm{rep}}(\mathbf{r})$ would result in $V_{\mathrm{rep}}(\mathbf{r}) = V_{\mathrm{HXC}}(\mathbf{r})$, returning the DFT result with the same self-interactions as the original method. Therefore constraints must be applied in the minimisation of the total energy in order to obtain a self-interaction free potential. There are two constraints that are required on the auxiliary density

$$\int d\mathbf{r} \rho_{\mathrm{rep}}(\mathbf{r}) = N - 1 \qquad (4.2.5)$$

$$\rho_{\mathrm{rep}}(\mathbf{r}) \geq 0. \qquad (4.2.6)$$

The first of these constraints ensures that $V_{\text{rep}}(\mathbf{r})$, the electrostatic potential of $\rho_{\text{rep}}(\mathbf{r})$ has the $(N-1)/r$ asymptotic behaviour of a self-interaction free potential. For approximate functionals that exhibit self-interaction errors, the constraint in Eq. (4.2.5) on its own is not sufficient to yield physical potentials: in the minimisation of the total energy, it is energetically favourable for the charge of -1 to be distributed far away from the system where the effect on the Kohn Sham potential near the molecule is negligible. In order to make the constraint in Eq. (4.2.5) have an effect, the additional positivity constraint of Eq. (4.2.6) is introduced that forces the charge of -1 to be distributed in regions where electrons are present. This positivity constraint is motivated by requiring the auxiliary density to represent a system of $N-1$ electrons with a density $\rho_{\text{rep}}(\mathbf{r})$ which repels the Kohn-Sham electrons, and will therefore be a positive definite quantity. Additionally the combination of the constraints in Eq. 4.2.5 and Eq. 4.2.6, when applied to a one electron system, gives the exact $V_{\text{rep}}(\mathbf{r}) = 0$.

4.2.4 Method

In order to obtain self-interaction-free results the total energy of the system

$$E_{\text{V}_{\text{ext}}}[\rho] = T_{\text{s}}[\rho] + E_{\text{ext}}[\rho] + E_{\text{H}}[\rho] + E_{\text{XC}}^{\text{DFA}}[\rho] \tag{4.2.7}$$

where $E_{\text{XC}}^{\text{DFA}}$ is the exchange-correlation energy of a DFA which may or may not contain self-interactions. As in the Kohn-Sham scheme there is a non-interacting system satisfying

$$\left[-\frac{\nabla^2}{2} + V_{\text{ext}}(\mathbf{r}) + V_{\text{rep}}(\mathbf{r}) \right] \phi_i(\mathbf{r}) = \epsilon_i \phi_i(\mathbf{r}) \tag{4.2.8}$$

where $V_{\text{rep}}(\mathbf{r})$ has the form in Eq. (4.2.4) and is subject to the constraints in Eqs. (4.2.5),(4.2.6). By the Hohenberg-Kohn theorem the energy is an implicit functional of the Kohn-Sham potential which, by construction, is itself a functional of the auxiliary density ρ_{rep}. The total energy is therefore a functional of this density

$$E_{\text{V}_{\text{ext}}}[\rho_{\text{rep}}] = T_{\text{s}}[\rho_{\text{rep}}] + E_{\text{ext}}[\rho_{\text{rep}}] + E_{\text{H}}[\rho_{\text{rep}}] + E_{\text{XC}}^{\text{DFA}}[\rho_{\text{rep}}]. \tag{4.2.9}$$

This energy can be minimised under constraints through the use of a Lagrange multiplier and a penalty function. The Lagrange energy term is

$$E_{\mathcal{L}}[\rho_{\text{rep}}] = -\lambda \left[\int d\mathbf{r} \rho_{\text{rep}}(\mathbf{r}) - (N-1) \right] \tag{4.2.10}$$

enforcing the constraint that the auxiliary density must integrate to $N-1$. The penalty term

$$E_{\mathcal{P}}[\rho_{\text{rep}}] = \Lambda \left[\int d\mathbf{r} |\rho_{\text{rep}}(\mathbf{r})| - (N-1) \right] \tag{4.2.11}$$

in conjunction with Eq. (4.2.10) enforces the positivity constraint on the auxiliary density ρ_{rep} by imposing an energy penalty when the auxiliary density has negative components. These energy terms allow an objective functional to be constructed for this method

$$G[\rho_{\text{rep}}] = E_{\text{V}_{\text{ext}}}[\rho_{\text{rep}}] + E_{\mathcal{L}}[\rho_{\text{rep}}] + E_{\mathcal{P}}[\rho_{\text{rep}}] \tag{4.2.12}$$

which, when minimised with respect to the auxiliary density, gives a constrained, self-interaction free Kohn-Sham potential. At the minimum of $G[\rho_{\text{rep}}]$ the derivative with respect to the auxiliary density must vanish

$$\frac{\delta G[\rho_{\text{rep}}]}{\delta \rho_{\text{rep}}(\mathbf{x})} = \frac{\delta E_{\text{V}_{\text{ext}}}[\rho_{\text{rep}}]}{\delta \rho_{\text{rep}}(\mathbf{x})} + \frac{\delta E_{\mathcal{L}}[\rho_{\text{rep}}]}{\delta \rho_{\text{rep}}(\mathbf{x})} + \frac{\delta E_{\mathcal{P}}[\rho_{\text{rep}}]}{\delta \rho_{\text{rep}}(\mathbf{x})} = 0 \tag{4.2.13}$$

The derivative for the constraint terms are simple to evaluate

$$\frac{\delta E_{\mathcal{L}}[\rho_{\text{rep}}]}{\delta \rho_{\text{rep}}(\mathbf{x})} = -\lambda \tag{4.2.14}$$

$$\frac{\delta E_{\mathcal{P}}[\rho_{\text{rep}}]}{\delta \rho_{\text{rep}}(\mathbf{x})} = \Lambda \text{sgn}\left[\rho_{\text{rep}}(\mathbf{x})\right] \tag{4.2.15}$$

where sgn is the sign function. The derivative of the DFT energy is more difficult as it is not an explicit functional of the auxiliary density and is calculated in a similar manner to the OEP method. The derivative is given by applying the chain rule as

$$\frac{\delta E_{\text{V}_{\text{ext}}}[\rho_{\text{rep}}]}{\delta \rho_{\text{rep}}(\mathbf{x})} = \int d\mathbf{r} d\mathbf{r}' \frac{\delta E_{\text{V}_{\text{ext}}}[\rho_{\text{rep}}]}{\delta \rho(\mathbf{r})} \frac{\delta \rho(\mathbf{r})}{\delta V_{\text{rep}}(\mathbf{r}')} \frac{\delta V_{\text{rep}}(\mathbf{r}')}{\delta \rho_{\text{rep}}(\mathbf{x})} \tag{4.2.16}$$

where $\rho(\mathbf{r})$ is the electron density. These derivatives can be evaluated using results previously derived in section 2.4.3 for the OEP method, these derivatives are

$$\frac{\delta E_{\text{V}_{\text{ext}}}[\rho_{\text{rep}}]}{\delta\rho(\mathbf{r})} = V_{\text{HXC}}(\mathbf{r}) - V_{\text{rep}}(\mathbf{r}) \tag{4.2.17}$$

$$\frac{\delta\rho(\mathbf{r})}{\delta V_{\text{rep}}(\mathbf{r}')} = \chi(\mathbf{r}, \mathbf{r}') \tag{4.2.18}$$

$$\tag{4.2.19}$$

where $\chi(\mathbf{r}, \mathbf{r}')$ is the density-density response function of the non-interacting system from Eq. (2.4.85). The final derivative can be evaluated from the definition of $V_{\text{rep}}(\mathbf{r}')$ in Eq. (4.2.4) as

$$\frac{\delta V_{\text{rep}}(\mathbf{r}')}{\delta\rho_{\text{rep}}(\mathbf{x})} = \frac{1}{|\mathbf{r}' - \mathbf{x}|}. \tag{4.2.20}$$

This allows the derivative of the objective functional to be evaluated as

$$\frac{\delta G[\rho_{\text{rep}}]}{\delta\rho_{\text{rep}}(\mathbf{x})} = \int d\mathbf{r}' \frac{1}{|\mathbf{r}' - \mathbf{x}|} \int d\mathbf{r}\chi(\mathbf{r}, \mathbf{r}') \left[V_{\text{HXC}}(\mathbf{r}) - V_{\text{rep}}(\mathbf{r})\right] - \lambda + \Lambda\text{sgn}\left[\rho_{\text{rep}}(\mathbf{x})\right] = 0 \tag{4.2.21}$$

using the definition of V_{rep} this can be written as a function of the auxiliary density as

$$\int d\mathbf{r}' \frac{1}{|\mathbf{r}' - \mathbf{x}|} \int d\mathbf{r}\chi(\mathbf{r}, \mathbf{r}') \left[V_{\text{HXC}}(\mathbf{r}) - \int d\mathbf{y}\frac{\rho_{\text{rep}}(\mathbf{y})}{|\mathbf{r} - \mathbf{y}|}\right] - \lambda + \Lambda\text{sgn}\left[\rho_{\text{rep}}(\mathbf{x})\right] = 0. \tag{4.2.22}$$

Introducing

$$\tilde{b}(\mathbf{x}) = \int d\mathbf{r}' \frac{1}{|\mathbf{r}' - \mathbf{x}|} \int d\mathbf{r}\chi(\mathbf{r}, \mathbf{r}')V_{\text{HXC}}(\mathbf{r}) \tag{4.2.23}$$

and

$$\tilde{\chi}(\mathbf{x}, \mathbf{y}) = \int d\mathbf{r}' \int d\mathbf{r}\frac{\chi(\mathbf{r}, \mathbf{r}')}{|\mathbf{r}' - \mathbf{x}||\mathbf{r} - \mathbf{y}|} \tag{4.2.24}$$

the derivative of the objective functional can be written as

$$\int d\mathbf{y} \tilde{\chi}(\mathbf{x}, \mathbf{y}) \rho_{\text{rep}}(\mathbf{y}) = \tilde{b}(\mathbf{x}) - \lambda + \Lambda \text{sgn} \left[\rho_{\text{rep}}(\mathbf{x}) \right] \qquad (4.2.25)$$

which, as the electron orbitals are implicitly determined by the auxiliary density, this defines an equation that allows the auxiliary density to be determined in a self-consistent manner. This concludes the theoretical review of the self-interaction method of Gidopoulos and Lathiotakis.

4.2.5 Implementation With Molecular Basis Sets

This method was implement in a molecular basis set code HIPPO by Lathiotakis [70, 98]. In this implementation the auxiliary density must be represented in terms of molecular orbital basis set $\xi_k(\mathbf{x})$. The auxiliary density is expanded in this basis set as

$$\rho_{\text{rep}}(\mathbf{x}) = \sum_k \nu_k \xi_k(\mathbf{x}) \qquad (4.2.26)$$

and the minimisation with respect to $\rho_{\text{rep}}(\mathbf{x})$ becomes a search for the minimising coefficients ν_k. Substituting the basis set expansion of Eq. (4.2.26) into Eq. (4.2.25) multiplying by $\xi_l(\mathbf{x})$ and integrating with respect to $\mathbf{x}$ to remove the spatial dependence gives

$$\sum_l \nu_l \int \int d\mathbf{x} d\mathbf{y} \xi_k(\mathbf{x}) \tilde{\chi}(\mathbf{x}, \mathbf{y}) \xi_l(\mathbf{y})$$
$$= \int d\mathbf{x} \tilde{b}(\mathbf{x}) \xi_k(\mathbf{x}) - \lambda \int d\mathbf{x} \xi_k(\mathbf{x}) + \Lambda \int d\mathbf{x} \xi_k(\mathbf{x}) \text{sgn} \left[\rho_{\text{rep}}(\mathbf{x}) \right]. \quad (4.2.27)$$

Defining:

$$A_{kl} = \int \int d\mathbf{x} d\mathbf{y} \xi_k(\mathbf{x}) \tilde{\chi}(\mathbf{x}, \mathbf{y}) \xi_l(\mathbf{y}) \qquad (4.2.28)$$

$$b_k = \int d\mathbf{x} \tilde{b}(\mathbf{x}) \xi_k(\mathbf{x}) \qquad (4.2.29)$$

$$X_k = \int d\mathbf{x} \xi_k(\mathbf{x}) \qquad (4.2.30)$$

$$\tilde{X}_k = \int d\mathbf{x} \xi_k(\mathbf{x}) \text{sgn} \left[\rho_{\text{rep}}(\mathbf{x}) \right], \qquad (4.2.31)$$

Eq. (4.2.27) becomes:

$$\sum_l A_{kl}\nu_l = b_k - \lambda X_k + \Lambda \tilde{X}_k. \tag{4.2.32}$$

The minimising coefficients are found by inverting the matrix A_{kl}:

$$\nu_l = \sum_k A_{lk}^{-1} b_k - \lambda \sum_k A_{lk}^{-1} X_k + \Lambda \sum_k A_{lk}^{-1} \tilde{X}_k. \tag{4.2.33}$$

The Lagrange multiplier can be determined from the constraint in Eq. 4.2.5 on the auxiliary density. Writing Eq. (4.2.5) in terms of the basis set

$$N - 1 = \int d\mathbf{x} \rho_{\text{rep}}(\mathbf{x}) = \sum_l \nu_l \int d\mathbf{x} \xi_l(\mathbf{x}) = \sum_l \nu_l X_l \tag{4.2.34}$$

substituting in Eq. (4.2.33) gives an expression for the Lagrange multiplier

$$\lambda = \frac{\sum_{kl} X_l A_{kl}^{-1} \left[b_k + \Lambda \tilde{X}_k \right] - (N - 1)}{\sum_{kl} X_l A_{kl}^{-1} X_k} \tag{4.2.35}$$

which can be used in conjunction with Eq. (4.2.33) to calculate the basis set coefficients ν_l.

4.2.6 Numerical Considerations

When represented in a finite orbital basis, the matrix A_{kl} has vanishingly small eigenvalues and when performing the inversion this requires a singular value decomposition (SVD) in order to remove projections to the (almost) null eigenvalues from the matrix. The choice of cutoff point for the nonzero eigenvalues is often ambiguous. Including too many small, but non-zero, eigenvalues, leads to a slower and likely non-convergent calculation, while omitting too many may not provide the correct inversion of the matrix A_{kl}. Different cutoffs may result in slightly different ground states being obtained and a cutoff of $\sim 10^{-5}$ was found to be a good choice for most molecules. For a better way to determine the cutoff point for the singular eigenvalues, see Ref. [141].

Start with initial guess
for the KS orbitals

From the KS orbitals
find $\tilde{\chi}$, A_{kl}, b_k, X_k, $\bar{X}_k$

Keeping the orbitals
fixed calculate ν_l
via Eq. (4.2.33)

Use ν_m to find ρ_{rep}
from Eq. (4.2.26)

Is the negative
component
of ρ_{rep} suffi-
ciently small?

no

yes

Recalculate V_{rep} from ρ_{rep}

Update KS orbitals and
calculate total energy

Has the energy
converged
sufficiently?

no

yes

Calculate final properties

Figure 4.1: A flow diagram showing the procedure for a constrained calculation.

4.2.7 Iterative Procedure

The iterative procedure to minimise the objective functional is shown in Fig. 4.1, in this iterative procedure an initial guess is not needed for ρ_{rep} instead the calculation is initialised with the Kohn-Sham orbitals from an initial guess, e.g. LDA orbitals. The iterative scheme consists of two loops, an outer and inner loop, beginning from an initial choice of orbitals the outer loop is entered and the quantities $\tilde{\chi}$, A_{kl}, b_k, X_k, $\tilde{X}_k$ are calculated for the particular orbitals. The calculation then enters an inner loop where the coefficients of the basis set representation of the auxiliary density are calculated from Eq. (4.2.33), this allows the auxiliary density to be calculated from Eq. (4.2.26). From the new auxiliary density X_k and $\tilde{X}_k$ can be recalculated along with a measure of the negative component of the auxiliary density defined to be

$$Q_{\text{neg}} = \int d\mathbf{x} \left[\rho_{\text{rep}}(\mathbf{x}) - |\rho_{\text{rep}}(\mathbf{x})|\right] \tag{4.2.36}$$

which from the constraint in Eq. (4.2.6) was desired to be as small as possible. Practically, a criterion for positivity $Q_{\text{neg}} < 10^{-6}$ was used.

In the inner loop a density mixing scheme was used when calculating ρ_{rep} and the efficiency/convergence were controlled by the values of the penalty parameter, Λ, and the mixing parameter, x_m. Typically, for Λ, a value of the order of ~ 100 a.u. worked well when combined with a small starting value for x_m ($\sim 10^{-8}$). This mixing parameter was dynamically increased and decreased based on the change of Q_{neg} at each successive iteration in order to aid convergence.

Once the auxiliary density had converged with a sufficiently small negative component this was then used to recalculate the potential V_{rep} and with this updated potential the Kohn-Sham orbitals were obtained to be used for the next iteration of calculation. Kohn-Sham orbitals were updated until the total energy given by Eq. (4.2.7) had converged and convergence can be aided by a density mixing procedure.

4.3 Results

4.3.1 Implementation

For my application of the constrained method I made use of the HIPPO code [70, 98] and applied the method to a wide variety of systems with various functional approximations. The HIPPO implementation of the constrained method makes use of Gaussian basis sets to expand both the orbitals and the auxiliary effective density; for the expansion of the orbitals the cc-pVDZ basis set was used as a compromise between accuracy and speed for the calculations. The auxiliary density was found to require a larger basis in order to allow the variational flexibility for the minimisation to be successful. This density, unlike the electron density, is represented with only a single basis set element while the electron density uses a product of two basis set elements. In order to provide a large enough basis set the uncontracted version of the orbital basis set was chosen to represent the auxiliary density.

4.3.2 Asymptotic Behaviour

The aim of the correction is to fix the asymptotic behaviour of the DFT exchange potential such that it has the correct decay at long range of $-1/r$. From Fig. 4.2 it is clear to see that the constrained potential has the correct asymptotic behaviour following in the $-1/r$ decay. The effect of the constraint appears to manifest as a shift in the potential such that the asymptote tends to $-1/r$ with the main features of the potential remaining unchanged. This shift in the potential will have a corresponding shift in the electron orbital eigenvalues and consequently a shift in the ionisation energies.

4.3.3 Ionisation Energies

The ionisation energies as calculated from the Kohn-Sham eigenvalues are used as an indicator of self-interaction errors. These results are compared to experimental results from the NIST computational chemistry comparison and benchmark database (CCCBDB) [1]. To show the applicability of this method to different approxima-
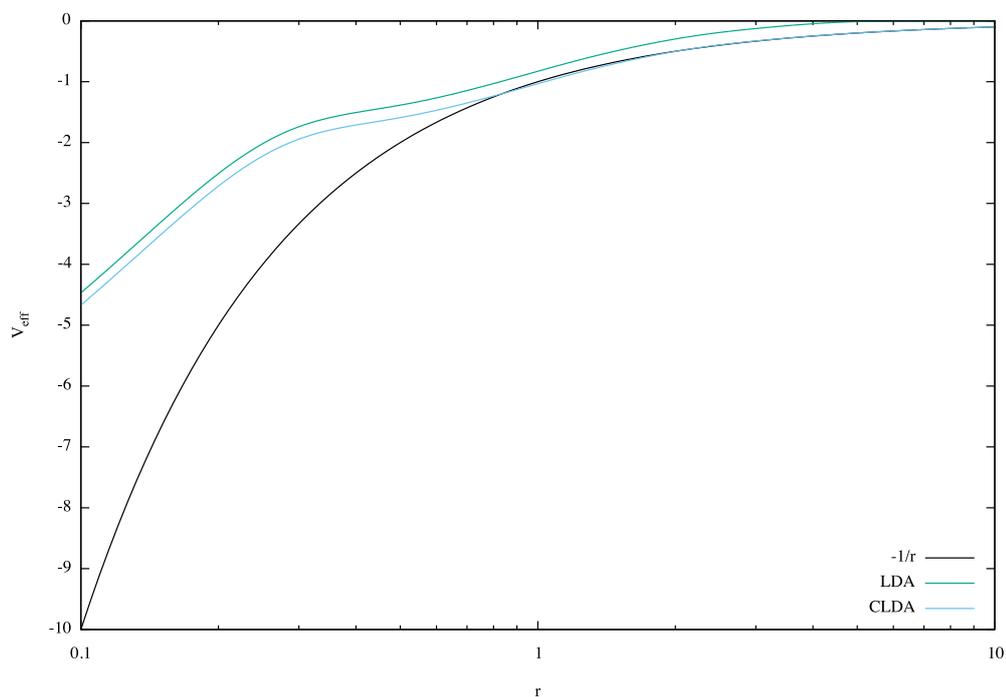
Figure 4.2: The behaviour of the LDA and the Constrained LDA (CLDA) exchange-correlation potentials compared to the $-1/r$ behaviour of the exact exchange-correlation potential.
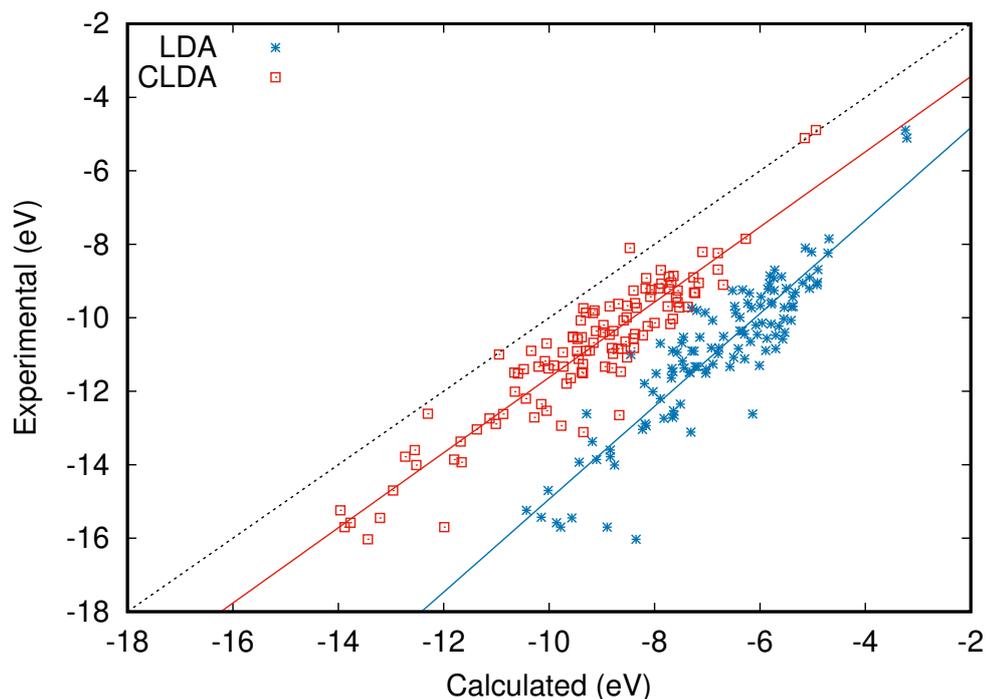
Figure 4.3: Calculated ionisation energies(IEs) using the LDA compared with experimental values [1]. Blue stars show results from unconstrained minimisation; red boxes show results of the constrained minimisation. Red and blue lines are guides to the eye. The IE is found as the negative of the HOMO energy. The black dotted line corresponds to the ideal correlation between an exact calculation and experiment.

tions, three DFAs were investigated, LDA, PBE, and the hybrid functional B3LYP. These DFAs are among the most popular functionals for electronic structure calculations and they all contain self-interaction effects, to some degree.

The results for the calculated HOMO energies are plotted against the experimental results in Fig. 4.3 for LDA, Fig. 4.4 for PBE and Fig. 4.5 for B3LYP. From these plots, it is clear that the results of all the unconstrained methods give poorer fits to the experimental results than the constrained, with the latter being closer to the ideal correlation between calculation and experiment. For all three approximate functionals, the calculated IE almost always underestimates the experimental IE. This well-known underestimation of the IE [142] continues to be present, but substantially reduced, in the constrained results except in a handful of cases.

In Fig. 4.6, the error in the calculated ionisation energy(IE) ΔI_N is plotted, where
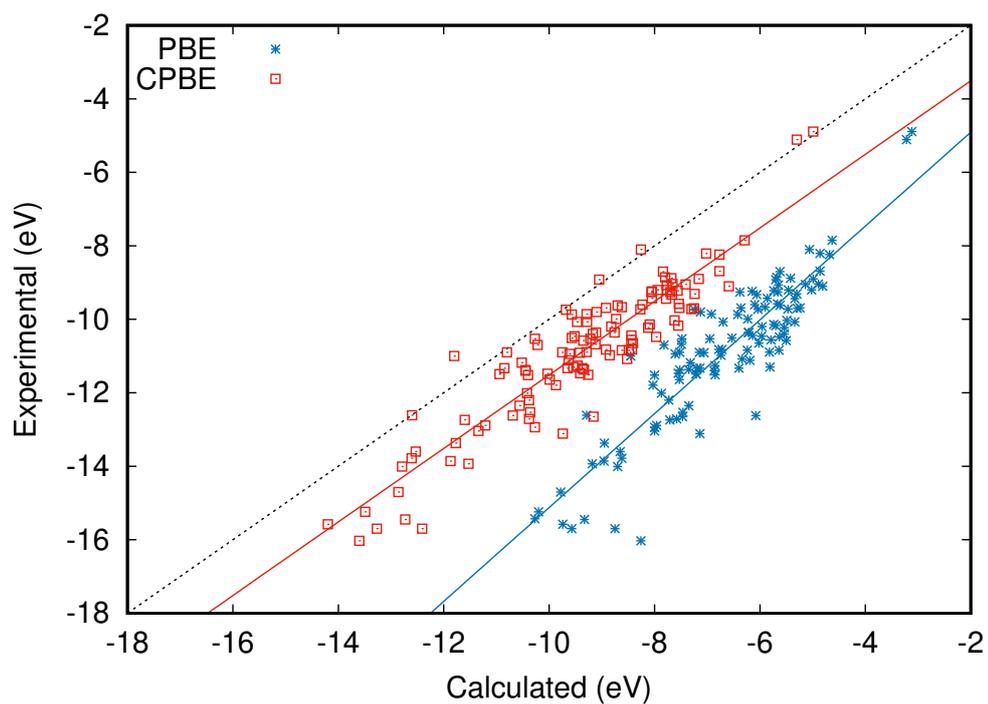
Figure 4.4: Calculated IEs using the PBE functional compared with experimental values [1]. Blue stars show results from unconstrained minimisation; red boxes show results of the constrained minimisation. Red and blue lines are guides to the eye. The IE is found as the negative of the HOMO energy. The black dotted line corresponds to the ideal correlation between an exact calculation and experiment.
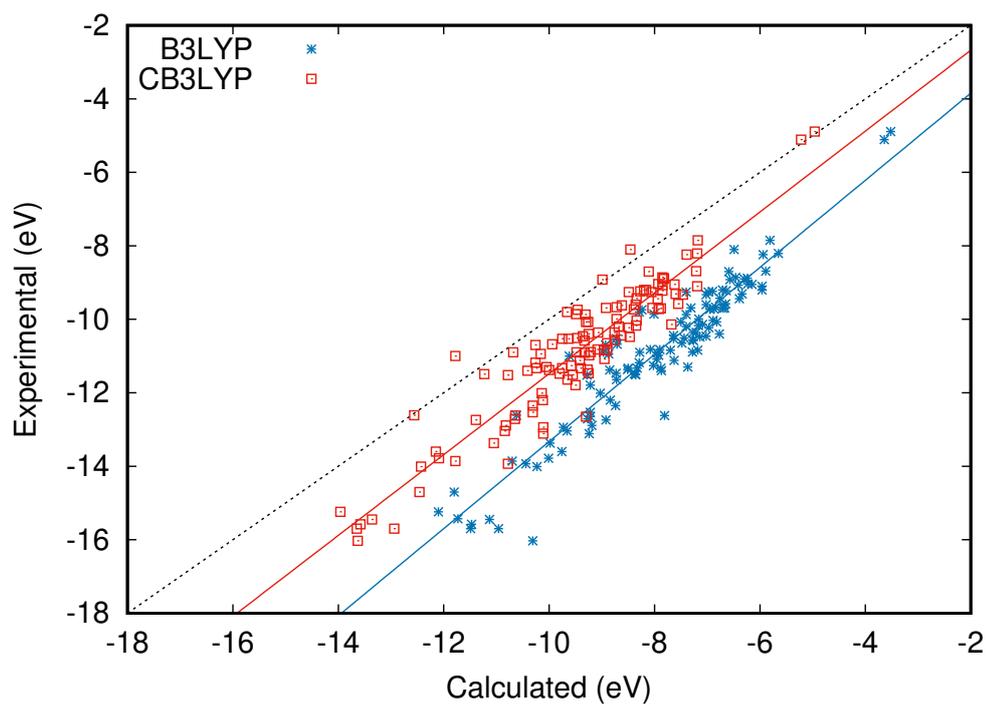
Figure 4.5: Calculated IEs using the B3LYP hybrid functional compared with experimental values [1]. Blue stars show results from unconstrained minimisation; red boxes show results of the constrained minimisation. Red and blue lines are guides to the eye. The IE is found as the negative of the HOMO energy. The black dotted line corresponds to the ideal correlation between an exact calculation and experiment.

this error is given by the difference between the experimental and calculated values, $\Delta I_N = I_N^{\text{calc}} - I_N^{\text{exp}}$. The inferior performance of the unconstrained relative to constrained minimisation, is seen clearly in this figure, with IE errors of 4 eV or more occurring frequently in the unconstrained case. The improvement of (unconstrained) B3LYP results over LDA and PBE is also evident, due to the partial cancellation of SIs in B3LYP due to a component of the exact exchange energy included in the hybrid method. This improvement, however, is surpassed and offset by the constrained minimisation technique to obtain the effective potential, with the three approximations giving similar results to each other.

A quantitative summary of the observations of the graphs in Figs. 4.3 - 4.6 can be found in Table 4.1. There, the average error, $\bar{\Delta}$, and the percentage error $\bar{\delta}$, defined by averaging over the absolute value of ΔI_N from Fig. 4.6, and $|\Delta I_N|/I_N$ is shown. The standard deviations σ and $\bar{\sigma}$ of the absolute values of the ΔI_N and $|\Delta I_N|/I_N$ are also shown. The improvements of the constrained methods amount to a reduction in the average error for LDA and PBE by ~ 2.5 eV while the B3LYP average error is halved to ~ 1.5 eV. For LDA and PBE these reductions correspond to a percentage improvement of 25% and for B3LYP the improvement is 14% over the unconstrained result. The standard deviation of the constrained results are smaller than the unconstrained for LDA and PBE and almost equal for B3LYP. The quality of the results improves not only because the average error decreases but also the standard deviation, reducing the spread of these results.

An important result that is evident in Fig. 4.6 and Table 4.1 is the similarity of the results of the constrained optimizations, with all three approximations giving similar averages and similar deviations. One might expect this for the CLDA and CPBE calculations, since the unconstrained results are similar. However, although the B3LYP results are shifted by approximately 1 eV compared to the LDA and PBE results, the CB3LYP results show no such shift when compared to CLDA and CPBE. This demonstrates that the potential that is constructed as a result of the constrained method appears relatively independent of the functional approximation used.
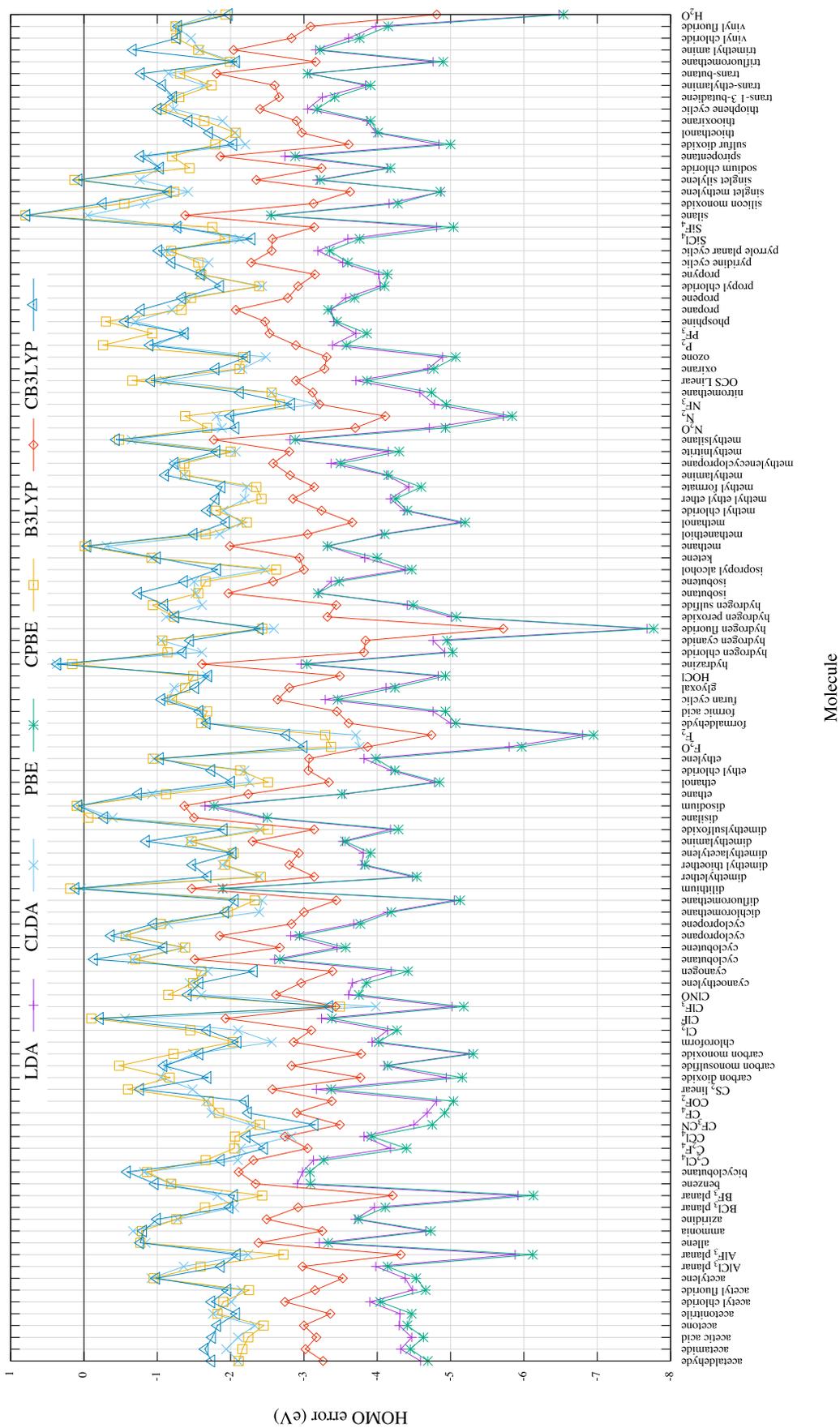
Figure 4.6: The differences between the calculated HOMO energy level and the experimental values [1] for the ionisation energy, comparing the unconstrained and constrained minimisation of the LDA, PBE and B3LYP approximations. A positive value corresponds to an underestimation of the IE.

Table 4.1: The average error, $\bar{\Delta}$, standard deviation of the error, σ, average percentage error, $\bar{\delta}$, and standard deviation of the percentage error, $\bar{\sigma}$, from experimental results [1] for the ionisation energy (IE) for the molecules in Fig. 4.6. The IE was approximated by the energy of the HOMO calculated using unconstrained functionals LDA, PBE, B3LYP and the constrained minimisation of the functionals CLDA, CPBE, CB3LYP. The average energy increase, ΔE, of the total energies of the constrained calculations compared to the unconstrained are also shown.

	LDA	CLDA	PBE	CPBE	B3LYP	CB3LYP
$\bar{\Delta}$ (eV)	-4.08	-1.61	-4.20	-1.51	-2.94	-1.42
σ (eV)	0.93	0.74	0.94	0.77	0.71	0.73
$\bar{\delta}$	38%	15%	39%	14%	27%	13%
$\bar{\sigma}$	6%	6%	5%	7%	5%	6%
ΔE (meV)		0.1		0.2		0.3

Calculations have also been performed on a set of closed-shell anions where the IE coincides with the electron affinity (EA) of the neutral system. The results found in Table 4.3 demonstrate a clear advantage of these calculations over unconstrained calculations. As can be seen from Table 4.2 a cc-pVDZ basis set is unsuitable for calculations involving anions due to the diffuse nature of the HOMO. For these calculations the augmented cc-pVTZ basis containing additional diffuse functions was deemed sufficiently well converged for application to anions.

With most approximate density functionals, the HOMO of the ions is found positive, i.e. they are predicted to have unbound electrons in most cases. This is a well known failure of many density functional approximations. With the constrained minimisation method, the same density functional approximations now correctly predict that these anions have bound electrons, in agreement with experimental results. These results demonstrate that the improvements in the ionisation energies are not limited to neutral molecules but can also be applied to anions.

Table 4.2: The convergence of the ionisation energy with respect to basis set for the Cl⁻ anion. Where each calculation was performed using a contracted orbital basis set and uncontracted auxiliary basis set of the same basis set type. The prefix "aug" indicates an augmented basis set.

Basis	IE(eV)
cc-pVDZ	0.812
cc-pVTZ	2.034
cc-pVQZ	2.402
cc-pV5Z	2.652
aug-cc-pVDZ	2.583
aug-cc-pVTZ	2.615
aug-cc-pVQZ	2.604
aug-cc-pV5Z	2.619

4.3.4 Energetics

Due to the introduction of constraints the total energy of the constrained method will be increased over an unconstrained calculation. In the last row of Table 4.1 the average increase is shown in the total energy, ΔE, from the corresponding unconstrained KS calculation. This increase is rather small, therefore, by enforcing the constraints of Eqs. (4.2.5), (4.2.6), total energies very close to the unconstrained KS minimum are obtained while on the other hand the orbital energies of the HOMO are substantially improved. The price of this improvement is that the optimal potential is no longer the functional derivative of the potential energy with respect to the electron density. The almost negligible increase in total energy for the constrained calculation is consistent with the observation [143] that potential terms with minimal influence in the total energy are responsible for the large deviation of the HOMO energies from the IEs. Thus, a viable path for correcting the HOMO energies is the identification and correction for such erroneous terms, as is achieved with this correction.

Table 4.3: The calculated IEs (in eV) for a set of anions using both constrained and unconstrained methods for the functionals LDA, PBE, B3LYP compared with experimental values [1] for the electron affinities of the neutral systems. The average error, $\bar{\Delta}$, the average percentage error, $\bar{\delta}$, and the average increase in the total energies, ΔE, are shown for each of the functionals. All ionisation energies in eVs.

system	LDA	CLDA	PBE	CPBE	B3LYP	CB3LYP	Exp
CH_3^-	-	0.30	-	0.26	-	0.51	0.08
CN^-	0.17	2.96	0.05	2.78	1.33	3.45	3.86
Cl^-	-	2.62	-	2.63	0.86	3.07	3.61
F^-	-	2.24	-	2.16	0.01	2.62	3.40
NH_2^-	-	0.23	-	0.15	-	0.50	0.77
OH^-	-	1.07	-	0.98	-	1.42	1.83
PH_2^-	-	0.74	-	0.75	-	0.91	1.27
SH^-	-	1.57	-	1.57	-	1.91	2.31
SiH_3^-	-	1.30	-	1.30	-	1.50	1.41
$\bar{\Delta}$ (eV)		0.66		0.70		0.41	
$\bar{\delta}$ (*)		35%		38%		20%	
ΔE (meV)		0.015		0.052		0.15	

(*)The result for CH_3^- is excluded as it dominates the percentage error.

4.3.5 Conclusions

A novelty of this self-interaction correction method is the proposition that deficiencies of approximate KS potentials can be corrected by replacing the KS potentials with variationally optimized effective potentials that satisfy certain properties. In this method, these properties are that the electron repulsion density integrates to N-1 and is everywhere positive, Eqs (4.2.5), (4.2.6).

The constrained minimisation method was tested on its prediction for the ionisation energy of a large set of molecules. Based on these results, the constrained method is found to offer substantial improvements for all approximate functionals tested, with a reduction of the average error for LDA from 4.08 eV in the unconstrained case to 1.61 eV with the constrained method. Similar reductions are found for PBE, while for the hybrid B3LYP functional the average error is almost halved from 2.94 eV to 1.42 eV. The method is also applied the method to the calculation of the HOMO energies of a group of anions which are found to be correctly negative. In addition to the improvements in the prediction of ionisation energies, it was found that, in all cases, the imposition of the constraints only marginally affects the total energy of the system.

It must be mentioned that the corrected IEs obtained with this method are still not very accurate, reflecting the limitations of the underlying DFAs. These results suggest that improved results for the IEs can be obtained either by a more refined DFA or through a direct modelling of the effective single particle potential [143–145]. These results show the importance of correcting for SI effects when calculating ionisation energies, and demonstrate the applicability of the constrained method in order to remove these self interaction effects in the KS potential. The constrained local potential is found to be a powerful method for improving the results of approximate functionals that contain self interactions.

Importantly, the constrained minimisation results appear to be independent of the particular approximation, as can be seen from Fig. 4.6 and Table 4.1, where the constrained optimisation results for the three DFAs give similar results. This property can be used to allow for more efficient calculations using a DFA that has a low computational cost but is of similar accuracy, once the constrained minimisation
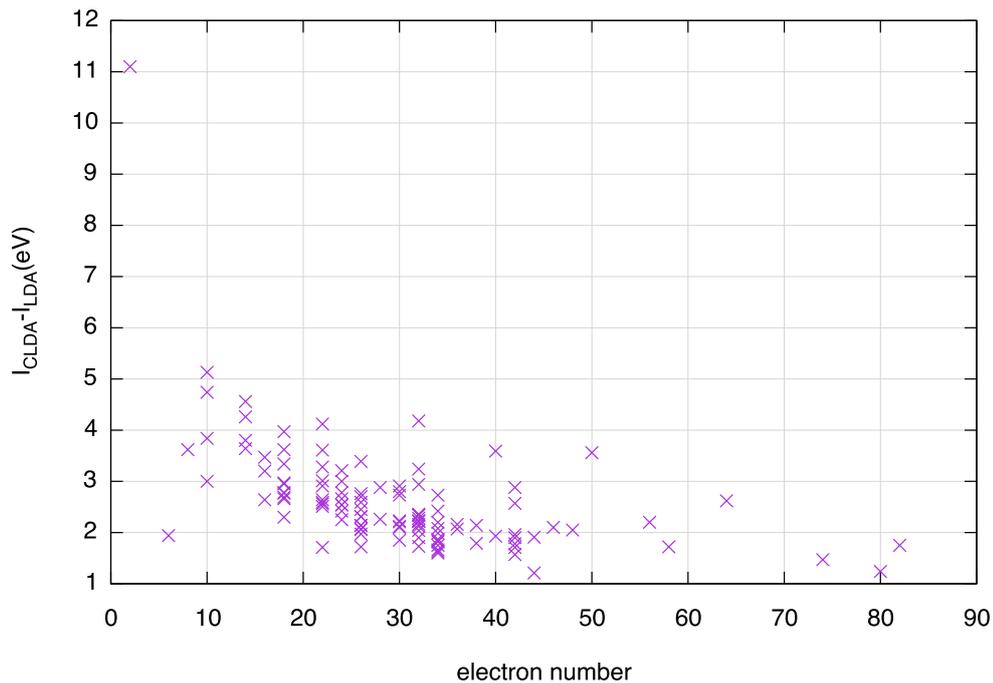
Figure 4.7: The change in the ionisation energy between unconstrained LDA and Constrained LDA (CLDA) as the number of electrons in the system increases.

method is used.

A consequence of the constraint of Eq. (4.2.5) is the introduction of size inconsistency, making this method most applicable to localised systems of atoms or molecules. This size inconsistency can be seen in Fig. 4.7 where the change in ionisation energy under the self-interaction correction is plotted against the electron number. The effect on ionisation energy is more pronounced for smaller systems and the effect of the correction reduces as the size of the system increases. This would be expected as the correction depends on the difference between N and $N-1$ and as the system size increases this difference reduces. A size inconsistency can be demonstrated by considering the treatment of two well separated atoms, each atom should behave as an isolated system with N electrons and an effective density which integrates to $N-1$. However, this correction would also treat the whole system as having $2N$ electrons and an effective density that integrates to $2N-1$ leading to a size inconsistency. In this two atom case the size consistency can be restored through distributing a charge of 1 between the atoms. How such a charge would be-

have as the atoms approach each other is unknown and would require investigation but may allow for a size consistent method to be obtained.

4.4   Summary

This Chapter has demonstrated the applicability of constraining the Kohn-Sham potential through an OEP like approach to have the correct $(N-1)/r$ asymptotic behaviour using the self-interaction correction of Gidopoulos and Lathiotakis. In the start of the original work in this thesis I have demonstrated that this method of correcting for self-interactions significantly improve ionisation energies of many molecular systems for a range of approximate functionals [140]. I also show that the use of this correction only increases the total energy compared to an unconstrained calculation on the order of m eV, preserving the energetics of the uncorrected functional while improving the ionisation energies significantly.

Chapter 5

Extensions to the Constrained Correction Method

5.1 Introduction

This chapter takes the constrained method of the previous chapter, that provides a basis for a self-interaction free theory, and investigates extensions to this method that improve or refine the technique further. A self-interaction free hybrid will also be constructed that combines the constrained method with exact exchange, and improvements when performing calculations with this method will be presented.

5.2 Finite Basis Set Correction

A problem with OEP based methods, of which the constrained method is an example, is an incompleteness in the representation of $\chi(\mathbf{r}, \mathbf{r}')$ the density response function given by

$$\chi(\mathbf{r}, \mathbf{r}') = 2 \sum_{i}^{occ} \sum_{a}^{unocc} \frac{\phi_i(\mathbf{r})\phi_i(\mathbf{r}')\phi_a(\mathbf{r})\phi_a(\mathbf{r}')}{\epsilon_i - \epsilon_a}. \qquad (5.2.1)$$

For simplicity the orbitals here are taken to be real, however the method shown here generalises to complex orbitals. When represented with a complete infinite set of orbitals $\chi(\mathbf{r}, \mathbf{r}')$ has no null eigenfunctions, except the constant function and hence can be inverted in order to solve the integral equation

$$\int d\mathbf{r} \chi(\mathbf{r}, \mathbf{r}') \left[\hat{V}_{HXC} - V_{\text{eff}}(\mathbf{r}) \right] = 0 \tag{5.2.2}$$

allowing V_{eff} to be determined up to a constant.

For practical purposes the infinite sum over the unoccupied orbitals must be truncated at some point. However, doing so introduces elements in the null space of $\chi(\mathbf{r}, \mathbf{r}')$, with any finite truncation introducing an infinite null space corresponding to the missing components of the infinite sum. One effect of this truncation is then the introduction of "zero" (or very small) eigenvalues in the matrix representation of $\chi(\mathbf{r}, \mathbf{r}')$ leading to the associated eigenvectors dominating when the matrix inversion is performed. This can lead to difficulties in converging the calculation as the minimisation is attempting to minimise along eigenvectors that, when varied, have arbitrarily small contributions to the total energy. In order to avoid difficulties with the inversion of $\chi(\mathbf{r}, \mathbf{r}')$ to obtain a converged V_{eff}, the eigenvectors in the null space of $\chi(\mathbf{r}, \mathbf{r}')$ must be removed through a singular value decomposition (SVD). For simple systems there is a clear distinction in magnitude between eigenvalues of eigenvectors in the null space as seen in Fig. 5.1. This is due to there being a large overlap between the representation of $\chi(\mathbf{r}, \mathbf{r}')$ and that of the potential and as such there are fewer null eigenvectors. If the basis set for the potential is too small then the potential will not be flexible enough to fully minimise the total energy. For large potential basis sets the distinction between eigenvalues in and out of the null space becomes harder and requires careful determination of the cutoff used in the SVD.

Even with an unambiguous SVD cutoff, the converged potential V_{eff} will often exhibit unphysical behaviour with large oscillations as seen in Fig. 5.2.
These unphysical results were shown by Gidopoulos and Lathiotakis [68] to be due to further finite basis set effects in the representation of $\chi(\mathbf{r}, \mathbf{r}')$. For simplicity we take a large(complete) auxiliary basis set and we define $\chi(\mathbf{r}, \mathbf{r}')$ as

$$\chi(\mathbf{r}, \mathbf{r}') = \chi_0(\mathbf{r}, \mathbf{r}') + \lambda \tilde{\chi}(\mathbf{r}, \mathbf{r}') \tag{5.2.3}$$

where for $\lambda = 1$
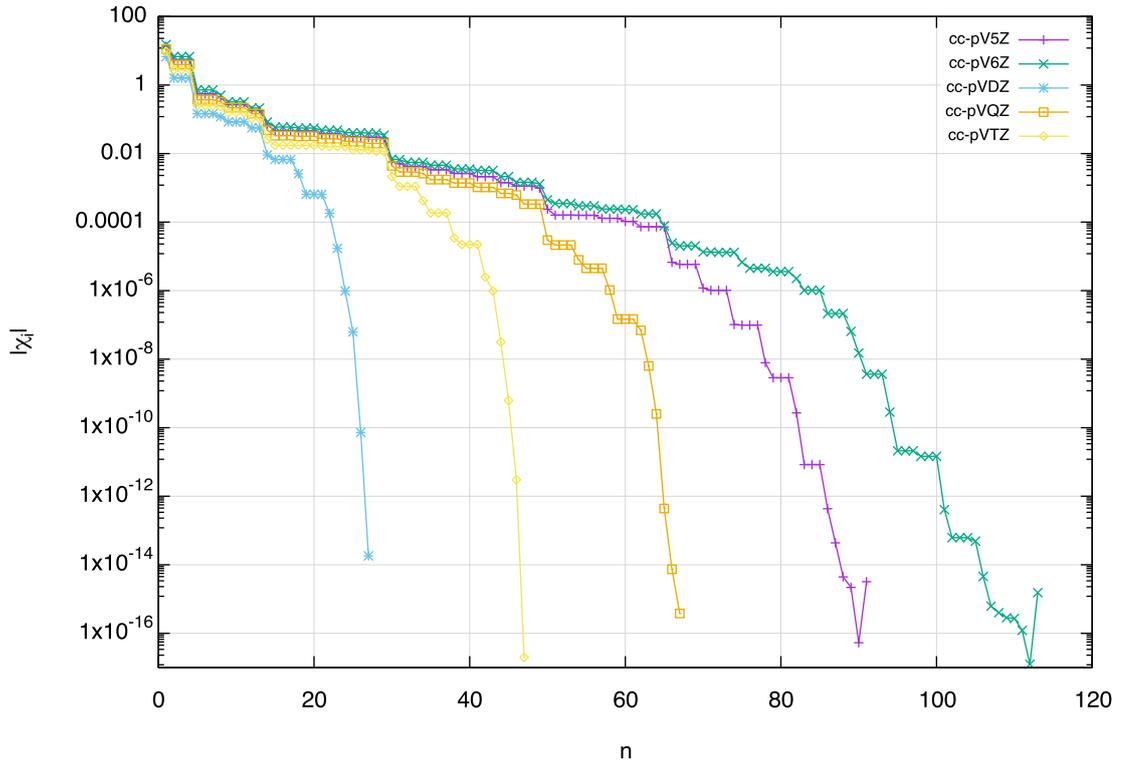
Figure 5.1: The absolute value of the eigenvalues χ_i of the matrix $\chi(\mathbf{r}, \mathbf{r}')$ for the n atom represented using a variety of uncontracted potential basis sets, for the orbital basis cc-pVQZ.

$$\chi_0(\mathbf{r}, \mathbf{r}') = 2 \sum_i^{occ} \sum_{a \in \mathcal{B}}^{unocc} \frac{\phi_i(\mathbf{r})\phi_i(\mathbf{r}')\phi_a(\mathbf{r})\phi_a(\mathbf{r}')}{\epsilon_i - \epsilon_a} \tag{5.2.4}$$

$$\tilde{\chi}(\mathbf{r}, \mathbf{r}') = 2 \sum_i^{occ} \sum_{b \notin \mathcal{B}}^{unocc} \frac{\phi_i(\mathbf{r})\phi_i(\mathbf{r}')\phi_b(\mathbf{r})\phi_b(\mathbf{r}')}{\epsilon_i - \epsilon_a} \tag{5.2.5}$$

$\chi_0(\mathbf{r}, \mathbf{r}')$ consists of all orbitals in the finite orbital basis set $\mathcal{B}$ while $\tilde{\chi}(\mathbf{r}, \mathbf{r}')$ corresponds to orbitals outside the orbital basis set. $\tilde{\chi}(\mathbf{r}, \mathbf{r}')$ will be denoted as the "complement" of $\chi(\mathbf{r}, \mathbf{r}.)$. Unphysical oscillations in OEP methods are a result of a distinct difference between the $V_{\text{eff}}(\mathbf{r})$ calculated using $\chi(\mathbf{r}, \mathbf{r}')$ with $\lambda \to 0$, $\lambda > 0$ and the $V_{\text{eff}}(\mathbf{r})$ calculated at $\lambda = 0$. Therefore, the potential calculated in a finite orbital basis set i.e. $\lambda = 0$ will not converge to the complete basis set result $\lambda = 1$ regardless of the size of the finite orbital basis set used, unless the orbital basis set becomes complete.
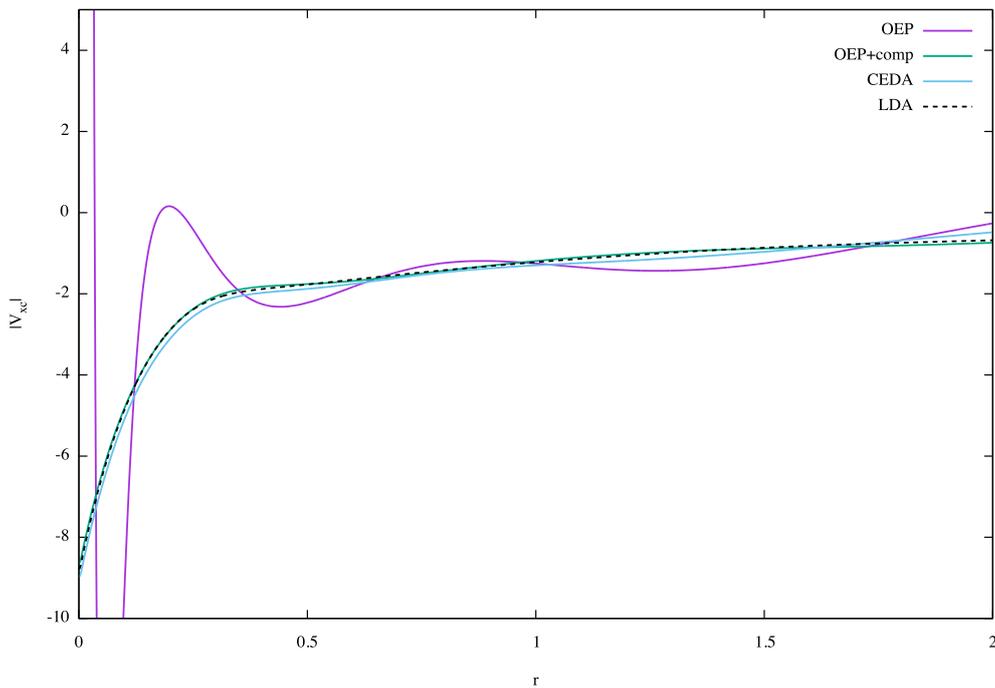
Figure 5.2: The XC potential for a n atom using the OEP method to calculate the LDA potential, with $\tilde{\lambda} = 0$ (OEP), $\tilde{\lambda} = 1 \times 10^{-7}$ (OEP+comp) and $\tilde{\lambda} \to \infty$ (CEDA), these are compared to a grid calculated LDA potential. These calculations are performed with a cc-pVDZ orbital basis set and an uncontracted cc-pVDZ auxiliary basis set.

Gidopoulos and Lathiotakis further demonstrated that the incompleteness in $\chi(\mathbf{r}, \mathbf{r}')$ in a finite basis set can be corrected by approximating the complement $\tilde{\chi}(\mathbf{r}, \mathbf{r}')$ [68]. This is achieved with an Ünsold approximation [146] for which the denominator $\epsilon_i - \epsilon_a$ is approximated as a constant $-\Delta > 0$, independent of i, a. The denominator is no longer involved in the summation over i, a giving

$$\tilde{\chi}(\mathbf{r}, \mathbf{r}') = -\frac{2}{\Delta} \sum_i^{occ} \phi_i(\mathbf{r})\phi_i(\mathbf{r}') \sum_{b \notin \mathcal{B}}^{unocc} \phi_b(\mathbf{r})\phi_b(\mathbf{r}'). \qquad (5.2.6)$$

The Kohn-Sham orbitals form a complete basis set and therefore have a completeness relation

$$\sum_i^{\infty} \phi_i(\mathbf{r})\phi_i(\mathbf{r}') = \delta(\mathbf{r} - \mathbf{r}'). \qquad (5.2.7)$$

This completeness relation can be used to relate the sum over orbital elements outside the basis set onto elements in the basis set by

$$\sum_i^\infty \phi_i(\mathbf{r})\phi_i(\mathbf{r}') = \delta(\mathbf{r} - \mathbf{r}') = \sum_i^{occ} \phi_i(\mathbf{r})\phi_i(\mathbf{r}') + \sum_{a \in \mathcal{B}}^{unocc} \phi_a(\mathbf{r})\phi_a(\mathbf{r}') + \sum_{b \notin \mathcal{B}}^{unocc} \phi_b(\mathbf{r})\phi_b(\mathbf{r}').$$
(5.2.8)

$\tilde{\chi}$ is then

$$\tilde{\chi}(\mathbf{r},\mathbf{r}') = -\frac{2}{\Delta} \sum_i^{occ} \phi_i(\mathbf{r})\phi_i(\mathbf{r}') \left[\delta(\mathbf{r} - \mathbf{r}') - \sum_j^{occ} \phi_j(\mathbf{r})\phi_j(\mathbf{r}') - \sum_{a \in \mathcal{B}}^{unocc} \phi_a(\mathbf{r})\phi_a(\mathbf{r}') \right].$$
(5.2.9)

This evaluates the response function in a complete orbital basis allowing a well defined inverse to be calculated. The final term in 5.2.9 adds terms that already appear in $\chi_0(\mathbf{r},\mathbf{r}')$ and can be neglected as its contribution goes to zero as $\lambda \to 0$, a limit that will be taken. The other terms account for the missing elements from the orbital basis set for any non-zero λ and as such must be included in the complement of $\chi(\mathbf{r},\mathbf{r}')$. The parameter Δ can also be combined with λ in order to leave a single variable $\tilde{\lambda}$ controlling the strength of the finite basis set correction. For a small value of λ, and therefore small $\tilde{\lambda}$, the complement of $\chi_0(\mathbf{r},\mathbf{r}')$ is

$$\lambda\tilde{\chi}(\mathbf{r},\mathbf{r}') = -2\tilde{\lambda} \sum_i^{occ} \phi_i(\mathbf{r})\phi_i(\mathbf{r}') \left[\delta(\mathbf{r} - \mathbf{r}') - \sum_j^{occ} \phi_j(\mathbf{r})\phi_j(\mathbf{r}') \right]$$
(5.2.10)

where, by varying $\tilde{\lambda}$, the strength of the finite basis set correction can be varied. Any non-zero $\tilde{\lambda}$, even as $\tilde{\lambda}$, tends to zero will complete the space of $\chi(\mathbf{r},\mathbf{r}')$. For large values of λ the contribution of the complement dominates the inversion of $\chi(\mathbf{r},\mathbf{r}')$ and the matrix $\chi(\mathbf{r},\mathbf{r}')$ tends to

$$\chi(\mathbf{r},\mathbf{r}') = \sum_i^{occ} \phi_i(\mathbf{r})\phi_i(\mathbf{r}') \left[\delta(\mathbf{r} - \mathbf{r}') - \sum_j^{occ} \phi_j(\mathbf{r})\phi_j(\mathbf{r}') \right]$$
(5.2.11)

which is identical to the CEDA approximation [71].

For computational purposes, a value of λ must be chosen such that it is large enough that the complement stabilises the inversion of $\chi(\mathbf{r},\mathbf{r}')$, but small enough such that

$\chi(\mathbf{r}, \mathbf{r}')$ is not dominated by the complement.

The inclusion of the complement removes the sensitivity of the method to the incompleteness of $\chi(\mathbf{r}, \mathbf{r}')$, this can be seen in Fig.5.2 where the oscillations in the OEP potential are significantly reduced by the addition of the complement even for a small $\tilde{\lambda}$.

5.2.1 Relaxing the Positivity Constraint

The use of the complement of $\chi(\mathbf{r}, \mathbf{r}')$ is important when performing OEP calculations without constraints. However, in the constrained method, the constraint on the positivity of ρ_{eff} results in smooth functions without the large oscillations present in other OEP methods. This suggests that the additional constraint of positivity on the effective density helps to stabilise the calculation of V_{eff}. Satisfying this positivity constraint adds an additional step in the computation of V_{eff}, increasing the computational cost to the method. This motivated an investigation into the behaviour of the constrained method when we performed calculations without the positivity constraint [147]. The removal of this constraint reintroduces the large unphysical oscillations observed in Fig. 5.2 and the complement of $\chi(\mathbf{r}, \mathbf{r}')$ is required to stabilise $V_{\text{eff}}(\mathbf{r})$.

The results for this method in Table 5.1 show that performing this calculation without the positivity constraint gives results very similar to using the constraint for most systems. The complement stabilises the calculation of V_{eff} in a similar manner to the positivity constraint, localising the distribution of the effective charge of -1 in the constrained method. The exception to this is when the method is applied to helium where this method shows a large deviation from the constrained result.

Analysis of the effective density as seen in Fig. 5.3b shows that the large error in Helium is due to a negative contribution to the effective density that is distributed at a larger and larger distance from the centre of the Helium atom with increasing basis set sizes. This negative charge corresponds to a charge of -1 introduced when constraining the effective density to integrate to a charge of $N - 1$. At a large distance from the atom this negative charge contributes a small energy cost and has little effect on the potential close to the atom. In this case the system will

Table 5.1: The ionisation energies (IEs) of selected atoms, molecules (top) and electron affinities (EAs) of negative ions (bottom) are shown in columns 3-5 . The IEs and EAs are obtained as the negative of the HOMO eigenvalue ϵ_N of the neutral system or the anion. The positivity constraint is employed in the constrained method for the results in column 4 and relaxed for the results in column 5. Experimental IEs and EAs are shown in the sixth column [1]. In the second column, X-Y stands for basis sets cc-pVXZ and un-contracted cc-pVYZ for the expansion of orbitals and screening charge densities(For the negative ions the screening charge is expanded in an un-contracted aug-cc-pVYZ basis set). All energies in eV..

	Basis	LDA	CLDA pos	CLDA no pos	Exp
He	T-Q	15.46	23.14	21.57	24.6
Be	T-T	5.59	8.62	8.11	9.32
Ne	T-T	13.16	18.94	18.94	21.6
H_2O	T-T	6.96	11.24	11.34	12.8
NH_3	T-T	6.00	9.81	9.77	10.8
CH_4	D-D	9.28	12.52	10.51	14.4
C_2H_2	D-D	7.02	10.63	10.31	11.5
C_2H_4	D-D	6.67	9.57	9.35	10.7
CO	D-D	8.75	12.73	12.11	14.1
NaCl	D-D	5.13	7.87	7.82	8.93
F^-	T-T	$\epsilon_H > 0$	2.23	2.16	3.34
Cl^-	T-T	$\epsilon_H > 0$	2.61	2.59	3.61
OH^-	T-T	$\epsilon_H > 0$	0.99	0.93	1.83
CN^-	T^1-T	0.13	2.87	2.86	3.77

adopt the potential of the unconstrained DFA near the atom and the constraint that $\rho_{eff} = N - 1$ will have little effect.

The large error for Helium can be attributed to the comparatively large difference between N and $N - 1$ for Helium due to its small number of electrons. For n, with a larger number of electrons, the effective density in Fig. 5.3a shows that a larger

(a) neon

(b) helium
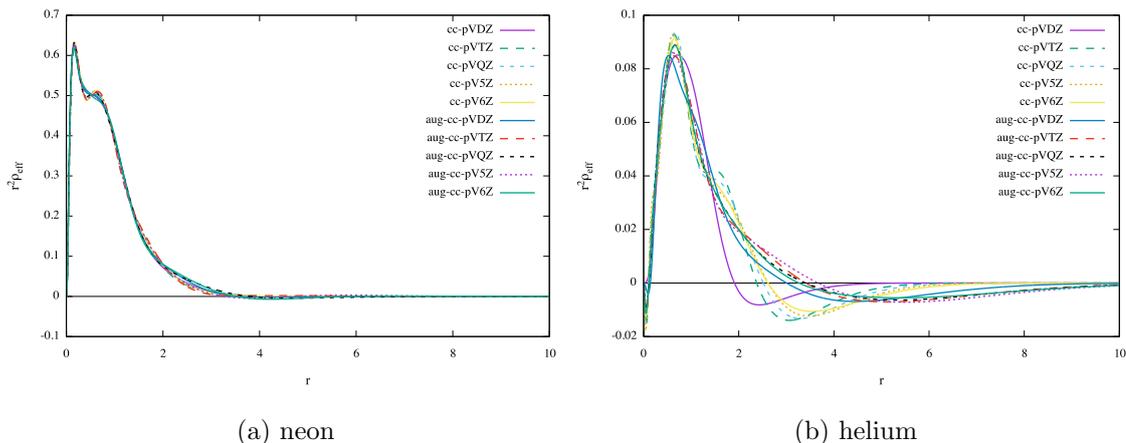
Figure 5.3: CLDA effective densities $\rho_{\text{eff}}(\mathbf{r})$ expanded in various auxiliary basis sets using a cc-pV5Z orbital basis set. For these calculations the complement of $\chi(\mathbf{r}, \mathbf{r}')$ is used with $\tilde{\lambda} = 10^{-4}$.

auxiliary basis set does not distribute the charge of -1 away from the atomic centre and is effectively stabilised by the complement of $\chi(\mathbf{r}, \mathbf{r}')$.

Therefore, for systems with many electrons the use of the complement of $\chi(\mathbf{r}, \mathbf{r}')$ helps obtain a smooth potential, performing a similar role as the positivity constraint, without the need for additional computational steps. However this method may produce results that are similar to the unconstrained DFT if the charge of -1 is distributed away from the system and care must be taken to ensure that the effective density is localised correctly. This effect of distributing the charge a long way from the system is only expected to occur, in systems with many electrons, for a very large, flexible auxiliary basis set, making this method a practical alternative to the positivity constraint for most applications.

5.3 The Effective Orbital Method

Enforcing the positivity constraint (4.2.6) using a penalty function adds an additional step in the calculation of the minimisation routine of the constrained method. This minimisation, with the use of a penalty function, is highly non-linear and, in some cases, was unable to achieve stable convergence to an effective density that

satisfied the positivity constraint. Another limitation is that the effective density consists of a linear combination of basis functions. Typically, the basis functions used to represent the electron orbitals do not allow sufficient variational freedom to correctly describe the auxiliary density. This requires an additional, larger set of basis set functions to adequately describe this auxiliary density. Both these limitations can be addressed by a redefinition of the auxiliary density to

$$\rho_{\text{rep}}(\mathbf{x}) = |f(\mathbf{x})|^2 \tag{5.3.12}$$

with

$$\int d\mathbf{x} |f(\mathbf{x})|^2 = N - 1 \tag{5.3.13}$$

where $f(\mathbf{x})$ is some "effective orbital" and the total energy can be minimised with respect to this "orbital". This construction guarantees that the auxiliary density is a positive quantity everywhere. Additionally, the auxiliary density is constructed as a product of basis set elements as

$$f(\mathbf{x}) = \sum_k \xi_k(\mathbf{x}) f_k \tag{5.3.14}$$

$$\rho_{\text{rep}}(\mathbf{x}) = \sum_{k,l} \xi_k(\mathbf{x}) \xi_l(\mathbf{x}) f_k f_l \tag{5.3.15}$$

increasing the variational freedom of the auxiliary density. This increase in variational freedom results in the effective potential being represented at a similar level as the Hartree potential, which is itself a product of the electron orbitals. This increase in the variational freedom of the auxiliary density allows a smaller auxiliary basis set to be used to represent the effective orbital. Some elements of the calculation can be simplified when using the same basis set for both the orbital and auxiliary basis sets. This was found in general to have sufficient variational freedom. Care must still be taken however to ensure that the auxiliary basis has the variational freedom required, making larger auxiliary basis sets necessary for particular systems. When using the effective orbital representation, the objective functional from (4.2.12) becomes

$$G[f] = E[f] + E_{\mathcal{L}}[f] \tag{5.3.16}$$

where $E_{\mathcal{L}}[f]$ is the Lagrange term ensuring that the auxiliary density integrates to $N-1$. This Lagrange term is

$$E_{\mathcal{L}}[f] = -\lambda \left[\int d\mathbf{x} \sum_{k,l} \xi_k(\mathbf{x})\xi_l(\mathbf{x}) f_k f_l d\mathbf{r} - (N-1) \right] \tag{5.3.17}$$

and the objective functional no longer contains a penalty function (equivalent to $\Lambda = 0$), because the positivity of the auxiliary density is guaranteed by the construction from the effective orbital. The derivative of the objective functional $G[f]$ with respect to the effective orbital $f(\mathbf{y})$ is

$$\frac{\delta G[f]}{\delta f(\mathbf{y})} = \int d\mathbf{x} \frac{\delta G[f]}{\delta \rho_{\text{rep}}(\mathbf{x})} \frac{\delta \rho_{\text{rep}}(\mathbf{x})}{\delta f(\mathbf{y})}. \tag{5.3.18}$$

Where, at the minimum value of the objective functional G, this derivative is equal to zero

$$4 \int d\mathbf{r}' \frac{f^*(\mathbf{x})}{|\mathbf{r}' - \mathbf{x}|} \int d\mathbf{r}\chi(\mathbf{r},\mathbf{r}') \left[V_{HXC}(\mathbf{r}) - \int d\mathbf{y} \frac{f^*(\mathbf{y})f(\mathbf{y})}{|\mathbf{r} - \mathbf{y}|} \right] - 2\lambda f^*(\mathbf{x}) = 0. \tag{5.3.19}$$

Using the definitions of $\tilde{\chi}(\mathbf{x},\mathbf{y})$ (4.2.24) and $\tilde{b}(\mathbf{x})$ (4.2.23), the derivative can be written as

$$4 \int d\mathbf{y} f^*(\mathbf{x})\tilde{\chi}(\mathbf{x},\mathbf{y})f^*(\mathbf{y})f(\mathbf{y}) = 4\tilde{b}(\mathbf{x})f(\mathbf{x}) - 2\lambda f(\mathbf{x}). \tag{5.3.20}$$

Expanding the effective orbital in a basis set as in (5.3.14), substituting into (5.3.19), multiplying by $\xi_l(\mathbf{x})$, and integrating over $\mathbf{x}$ gives

$$4 \sum_{kmn} \int d\mathbf{x} \int d\mathbf{y} f_k^* f_m^* f_n \xi_k^*(\mathbf{x})\xi_l(\mathbf{x})\tilde{\chi}(\mathbf{x},\mathbf{y})\xi_m^*(\mathbf{y})\xi_n(\mathbf{y})$$

$$= 2 \sum_k f_k^* \int d\mathbf{x}\xi_k^*(\mathbf{x})\xi_l(\mathbf{x}) \left[2\tilde{b}(\mathbf{x}) - \lambda \right]. \tag{5.3.21}$$

Defining,

$$\tilde{A}_{klmn} = \int d\mathbf{x} \int d\mathbf{y} \xi_k^*(\mathbf{x}) \xi_l(\mathbf{x}) \tilde{\chi}(\mathbf{x}, \mathbf{y}) \xi_m^*(\mathbf{y}) \xi_n(\mathbf{y}), \qquad (5.3.22)$$

along with

$$B_{kl} = \int d\mathbf{x} \xi_k^*(\mathbf{x}) \xi_l(\mathbf{x}) \tilde{b}(\mathbf{x}), \qquad (5.3.23)$$

and

$$O_{kl} = \int d\mathbf{x} \xi_k^*(\mathbf{x}) \xi_l(\mathbf{x}) \qquad (5.3.24)$$

allows the derivative to be written as

$$4 \sum_{kmn} f_k^* f_m^* f_n \tilde{A}_{klmn} = 4 \sum_k B_{kl} f_k - 2\lambda \sum_k O_{kl} f_k. \qquad (5.3.25)$$

The Lagrange multiplier is found from the constraint

$$\int d\mathbf{x} \rho_{\text{rep}}(\mathbf{x}) = \sum_{kl} f_k f_l O_{kl} = N - 1, \qquad (5.3.26)$$

multiplying (5.3.25) by f_l and summing over l gives

$$\lambda = 2 \left[\frac{\sum_{klmn} f_m f_n f_k f_l A_{klmn} - \sum_{k,l} f_k f_l B_{kl}}{N - 1} \right]. \qquad (5.3.27)$$

Unlike when representing the auxiliary density with a single basis set this formulation does not result in a linear equation and cannot simply be inverted to obtain the minimising auxiliary density. The minimising coefficients f_k must be found through the use of a gradient method, directly minimising the objective functional and finding the minimising f_k.

5.3.1 Application and Discussion

This method was implemented in the Hippo code with a gradient descent method from the NAG numerical algorithms library [148] that allowed rapid and stable convergence of the auxiliary density. Use of this method greatly improved the stability of the calculations for systems that originally had poor convergence under the positivity constraint. In comparison with the constrained method utilising a penalty

function the results were very close for both methods with the effective orbital (EFO) method finding the same minimum. The EFO method has clear advantages over the penalty function, with no external penalty parameter to fix. The EFO method was found to have adequate convergence when using the same basis set for both electron orbitals and the effective orbital $f_k(\mathbf{x})$. Using this method, convergent calculations were able to be performed for the molecule LiH, where using a penalty function method did converge. Additionally, there were no systems where the EFO method struggled to converge the energy. While this method shows large improvements in convergence, the penalty function construction resulted in a linear equation which can be easily inverted. In general the EFO method is a slower, but more reliable, method than the use of a penalty function, and ensures the positivity is enforced in all cases unlike when using the complement of $\chi(\mathbf{r}, \mathbf{r}')$.

5.4   Separation of the Correlation Potential

When using the constrained method, both the exchange and correlation potentials are subject the constraints in (4.2.5),(4.2.6). However, the long range behaviour of the correlation potential is different to that of exchange. At long range the behaviour of the exact correlation potential can be obtained through an asymptotic expansion of the electron density, this demonstrated that the correlation potential decays as $1/r^4$ [108] unlike the exchange potential which has been shown to decay asymptotically as $1/r$. To leading order v_X and v_XC is dominated by the decay of the exchange potential therefore resulting in a $-1/r$ decay overall regardless of whether the correlation potential is present. The correlation potential is a much smaller contribution to the overall potential than the exchange potential and the constrained method may miss fine details in the correlation potential due to the dominance of the exchange potential. An alternative method is to apply the constraints to the Hartree-exchange potential only, representing the Hartree-exchange potential with an effecting potential v_rep and leaving the correlation potential v_C unmodified from the chosen approximation. The Kohn-Sham equation of this method is

$$\left[-\frac{\nabla^2}{2} + v_{\text{ext}}(\mathbf{r}) + v_{\text{rep}}(\mathbf{r}) + v_{\text{C}}(\mathbf{r})\right]\psi_i(\mathbf{r}) = \epsilon_i\psi_i(\mathbf{r}). \tag{5.4.28}$$

and total energy expression is unchanged. For clarity the Hartree and exchange energies have been grouped and separated from the correlation energy

$$E[\rho] = T_{\text{s}}[\rho] + E_{\text{ext}}[\rho] + E_{\text{HX}}[\rho] + E_{\text{C}}^{\text{DFA}}[\rho]. \tag{5.4.29}$$

With this modification the minimisation of the objective functional $G[v_{\text{rep}}]$ to determine ρ_{rep} becomes

$$\frac{\delta G[v_{\text{rep}}]}{\delta\rho_{\text{rep}}(\mathbf{x})} = \int d\mathbf{r}d\mathbf{r}'\chi(\mathbf{r},\mathbf{r}')[v_{\text{HX}}(\mathbf{r}') - v_{\text{rep}}(\mathbf{r}')]\frac{v_{\text{rep}}(\mathbf{r})}{\delta\rho_{\text{rep}}(\mathbf{x})} - \lambda \tag{5.4.30}$$

almost identical to the original constrained method. However, the potential that appears in this equation is now just the Hartree Exchange potential $v_{\text{DFA}}^{\text{HX}}(\mathbf{r}')$ as opposed to $v_{\text{DFA}}^{\text{HXC}}(\mathbf{r}')$ in the original formulation.

The inclusion of only V_{HX} in v_{rep} allows the correction to apply to only the exchange element where main self-interaction errors appear. The separation of the correlation potential is expected to only have a small effect on the total energies because the total energy expression remains unchanged. A consequence of this is that for a single electron system, unless the chosen correlation potential gives zero potential, this method will no longer be exact and the system will exhibit a small one-electron self-interaction error.

Table 5.2 demonstrates that considering correlation separately to the exchange energy does result in an upshift of the ionisation energies(IEs). For LDA this results in an average upshift of 0.90 eV, for PBE this average is 0.42 eV. Typically calculations of the HOMO energy, similar to unconstrained LDA calculations, are an underestimation of the ionisation energy, and therefore this upshift of calculated IEs slightly improves the overall energy approximations. This improvement is a cancellation of errors from the many-electron self-interaction error of the correlation energy with the systematic underestimation of ionisation energies in DFT methods.

Due to the cancellation of errors on the ionisation energy this method offers improved ionisation energies compared to the fully constrained method. This comes

Table 5.2: The errors in calculating HOMO ionisation energies for a sample of molecules for the constrained method with the correlation energies constrained (v_{XC}) and unconstrained (v_X). along with the average error (AE) for each method, the standard deviation (SD) and the change in energy between the two methods ΔE. All energies in eV..

Molecule	Expt	LDA		PBE	
		v_{XC}	v_X	v_{XC}	v_X
C_2H_2	11.4	-1.52	-0.74	-1.30	-1.03
NH_3	10.07	-0.92	-0.14	-0.84	-0.65
CO	14.01	-2.23	-1.22	-1.71	-1.24
C_2H_4	10.51	-1.34	-0.57	-1.28	-0.96
F_2	15.7	-4.79	-3.5	-4.07	-3.29
CH_2O	10.89	-2.31	-1.44	-2.04	-1.64
HCN	13.6	-1.85	-1.03	-1.84	-1.32
HF	16.03	-2.82	-1.89	-2.57	-2.06
CH_4	12.61	-0.1	0.66	0.01	0.31
N_2	15.58	-2.82	-1.74	-2.25	-1.71
H_2O	12.62	-2.1	-1.3	-1.97	-1.69
AE		-2.07	-1.17	-1.81	-1.39
AAE		2.07	1.29	1.81	1.45
SD		1.26	1.11	1.08	0.95
ΔE		7.9×10^{-6}		-3.3×10^{-5}	

at the expense of not enforcing the exact one-electron result of $E_{XC} = 0$, which is guaranteed when also constraining the correlation potential. When separating the correlation functional the exact one-electron self-interaction only holds for approximate functionals where the one-electron correlation energy is zero. Otherwise, this method will exhibit self-interaction errors present in the correlation energy expression. The separation of the correlation potential from the constrained minimisation of the exchange potential allow for the targeting of the exchange potential, which

is the dominant contribution to the asymptotic behaviour of the Kohn-Sham potential. With the correlation potential known to have a different exact asymptotic behaviour to the exchange potential.

5.5 Constrained Minimisation Hybrid Method

The constrained minimisation method has been shown to be able to correct for the effects of self-interactions in density functional approximations, improving the calculated ionisation energies. However, when using the constrained method, the calculated ionisation energies remain, in general, an underestimation of the experimental ionisation energies. This shows the same systematic behaviour as that exhibited by the unconstrained methods. For the constrained method, these errors are similar in magnitude to the systematic overestimation of ionisation energies given by the Hartree-Fock method as can be seen in Fig. 5.4. And these constrained results seem independent of functional choice as seen in Fig. 4.6. These results suggest that a hybrid method combining the potentials of a constrained DFA and Hartree-Fock should result in an improved calculation of ionisation energies. In much the same way as seen in the original hybrid method proposed by Becke [53]. And for this section of my thesis I developed, implemented and applied this new hybrid method. The constrained method has been applied to the conventional hybrid method B3LYP, in which the hybrid B3LYP energy functional was used with orbitals generated from a Kohn-Sham potential with the local potential v_{rep}. Constrained B3LYP was seen to give similar accuracy when calculating ionisation energies as when using constrained LDA or PBE as seen in Fig. 4.1. In contrast, the Kohn-Sham equation of the hybrid proposed in this thesis will have both a local constrained potential which will represent a self-interaction free DFA, and a non-local Hartree-Fock component. The Hartree-Fock potential is already known to be a self-interaction free potential and as such does not need constraining. In this hybrid method only the self-interaction contaminated exchange potential from the DFA is constrained.
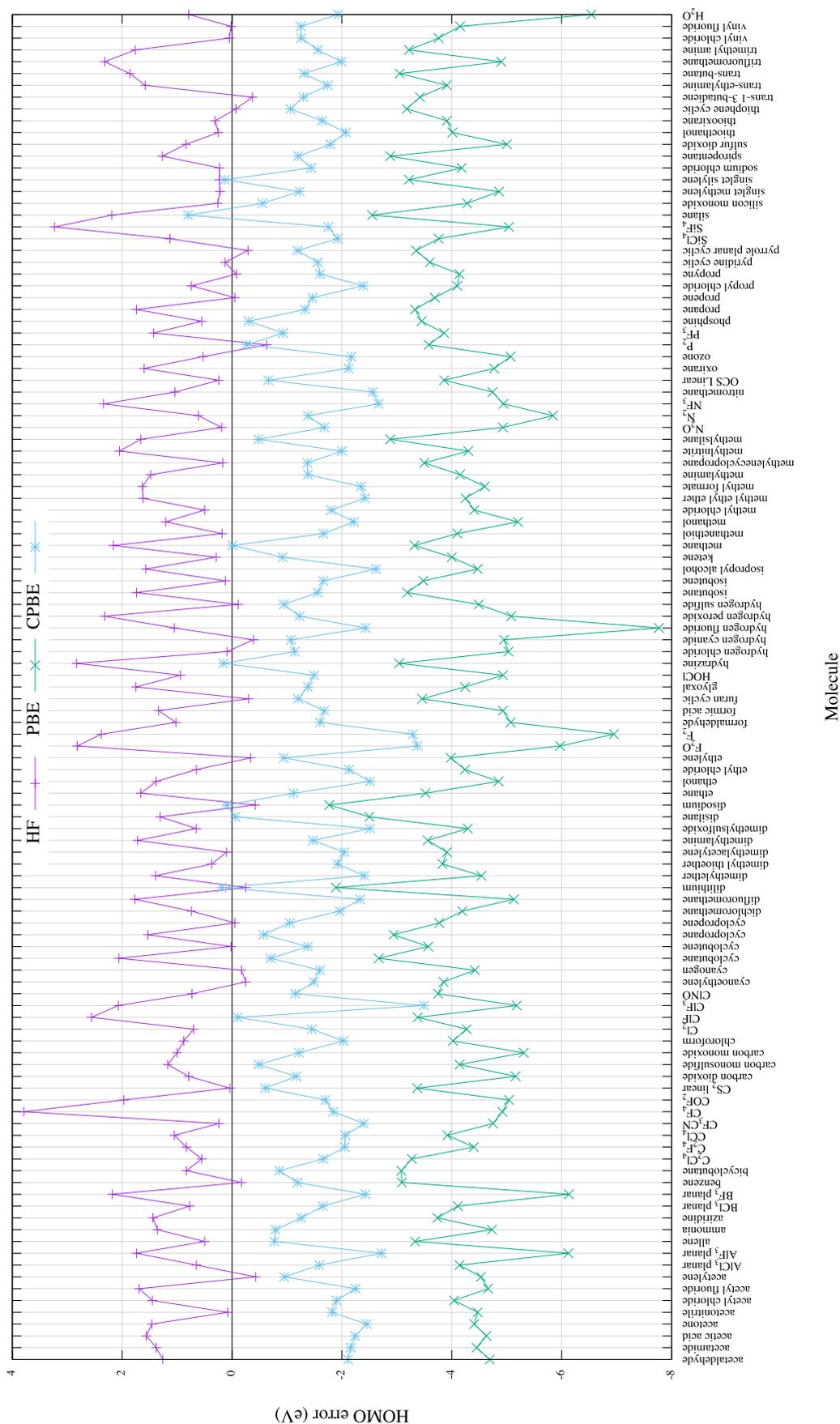
Figure 5.4: Graph showing the errors in Hartree-Fock, PBE and CPBE calculations of the ionisation energy compared with experimental results [1].

5.5.1 Constrained Generalised Kohn-Sham Equation

As we have seen the constrained method can be applied without constraining the correlation potential. Separating the correlation potential from the self-interaction corrected exchange potential leaves a constrained Hartree-exchange component of the Kohn-Sham potential that is self-interaction free. This allowed me to construct a generalised Kohn-Sham scheme where the self-interaction free potential is combined with the non-local Hartree Fock potential.

This new hybrid function can be constructed with a potential of the form

$$V_{\text{hyb}} = (1 - \alpha)V_{\text{HX}}^{\text{F}} + \alpha V_{\text{rep}}^{\text{DFA}} + V_{\text{C}}^{\text{DFA}} \tag{5.5.31}$$

where V_{HX}^{F} is the Fock Hartree-exchange potential, $V_{\text{C}}^{\text{DFA}}$ is the correlation potential from the chosen DFA and $V_{\text{rep}}^{\text{DFA}}$ is the self-interaction corrected Hartree and exchange potential from the chosen DFA. For the hybrid method discussed here the exchange and correlation potentials are taken from the same approximation. In principle, these potentials could be taken from different DFAs, allowing a further freedom in the hybrid formulation.

The hybrid total energy is constructed as

$$E_{\text{tot}}[\rho] = T_{\text{s}}[\rho] + E_{\text{ext}}[\rho] + E_{\text{H}}[\rho] + \alpha E_{\text{X}}^{\text{DFA}}[\rho] + (1 - \alpha)E_{\text{X}}^{\text{F}}[\rho] + E_{\text{C}}^{\text{DFA}}[\rho] \tag{5.5.32}$$

where T_{s} is the non-interacting kinetic energy, E_{ext} is the energy from the external potential, E_{H} is the Hartree energy, $E_{\text{X}}^{\text{DFA}}$ and $E_{\text{C}}^{\text{DFA}}$ are the exchange and correlation energy functional for the implemented DFA, and E_{X}^{F} is the Fock exchange energy. Correlation is treated separately to exchange in order to provide a method that has 100% correlation energy for all values of the hybrid parameter α.

This total energy can be minimised with respect to the potential ρ_{rep} with the constraints in (4.2.5),(4.2.6), as in the constrained method. This minimising potential is given by

$$\frac{\delta G[v_{\text{rep}}]}{\delta \rho_{\text{rep}}(\mathbf{x})} = \int d\mathbf{r} d\mathbf{r}' \chi(\mathbf{r}, \mathbf{r}')[v_{\text{HX}}^{\text{DFA}}(\mathbf{r}') - v_{\text{rep}}(\mathbf{r}')]\frac{\delta v_{\text{rep}}(\mathbf{r})}{\delta \rho_{\text{rep}}(\mathbf{x})} - \lambda, \tag{5.5.33}$$

Table 5.3: Table showing the change to the total energies as α is varied for both the LDA, PBE and B3LYP functionals for a range of molecules. Energies for $\alpha < 1$ are relative to the total energy at $\alpha = 1$. These results are obtained through averaging total energies over the molecules in Table 5.2. All energies are in eV.

α	LDA		PBE	
	V_{X}	V_{XC}	V_{X}	V_{XC}
1	-97.39	-97.39	-98.05	-98.05
0.75	-0.27	-0.06	-0.002	0.1
0.5	-0.55	-0.12	-0.01	0.21
0.25	-0.83	-0.18	0.01	0.31
0	-1.11	-0.25	-0.02	0.41

identical in form to (5.4.30), with no dependence on the hybrid parameter α. The difference for this hybrid method from the constrained method is that the the orbitals composing $\chi(\mathbf{r}, \mathbf{r}')$ are given by the hybrid Kohn-Sham potential in (5.5.31).

The parameter α determines the ratio of constrained local exchange to Fock exchange that is present in the method. For $\alpha = 1$ this method is just the constrained method with the correlation treated separately. For $\alpha = 0$ this method uses full non-local Hartree-Fock exchange with a correlation energy and potential determined by the choice of $E_{\mathrm{C}}^{\mathrm{DFA}}$. Intermediate values of α result in a hybrid method with contributions from both the constrained local potential and Fock exchange.

As α varies from 0 to 1 the total energy will vary from that of Hartree Fock + correlation (HF+C) energy to the constrained DFA energy. With a suitable choice of DFA the energy change from HF+C to the constrained DFA will be small. A small variation in total energy as α varies allows the total energy of the hybrid method to remain in good agreement with the DFT total energies. Where these total energies are generally a good representation of a systems energetics.

Table 5.3 demonstrates that for LDA there is a significant change in the total energy as α varies, with a change of 1.11 eV over $0 < \alpha < 1$. This energy change can be

attributed to the HF energy being lower than the LDA total energy. The addition of LDA correlation energy to HF further reduces the energy at $\alpha = 0$ therefore increasing the energy gap.

The results for the PBE approximation in Table 5.3 show a much smaller shift in energies of 0.02 eV between the CPBE total energy and the HF + E_c^{PBE}. Due to this preservation of the energetic properties by the PBE functional, all further investigation of the constrained hybrid will be performed with PBE as the local DFT exchange and correlation functional. Because the CPBE hybrid will preserve its energetics throughout the range $0 \leq \alpha \leq 1$ the effect of varying α on the orbital energies can be investigated while the value of the total energy will not be significantly affected.

This new hybrid of constrained PBE and HF, can be considered the self-interaction corrected analogue to the PBE0 hybrid [61, 149]. The PBE0 functional mixes 25% of exact exchange and 75% PBE exchange for the exchange potential along with a full contribution from the PBE correlation functional. For the constrained hybrid my choice of mixing parameter will be such that the method gives the best approximation of experimental ionisation energies.

5.5.2 Results

To determine the optimum value for the hybrid coefficient α the error on the orbitals for a range of molecules was compared. While the DFT Koopmans' theorem demonstrates that only the HOMO has any physical relation to the ionisation energy of a system. It has been argued that all the Kohn-Sham orbitals have an approximate relation to the ionisation energies of the orbitals [150]. The orbital energies and errors were investigated for all the valence orbitals to determine if a minimising quantity for the HOMO error also minimised the error in the valence orbitals.

The value of the hybrid parameter was determined by using the hybrid to calculate the ionisation energies for several systems for a range of values of α. Ionisation energies of lower lying orbitals were also computed and compared for this set of systems. A mixing parameter that minimises the ionisation energy error over all the
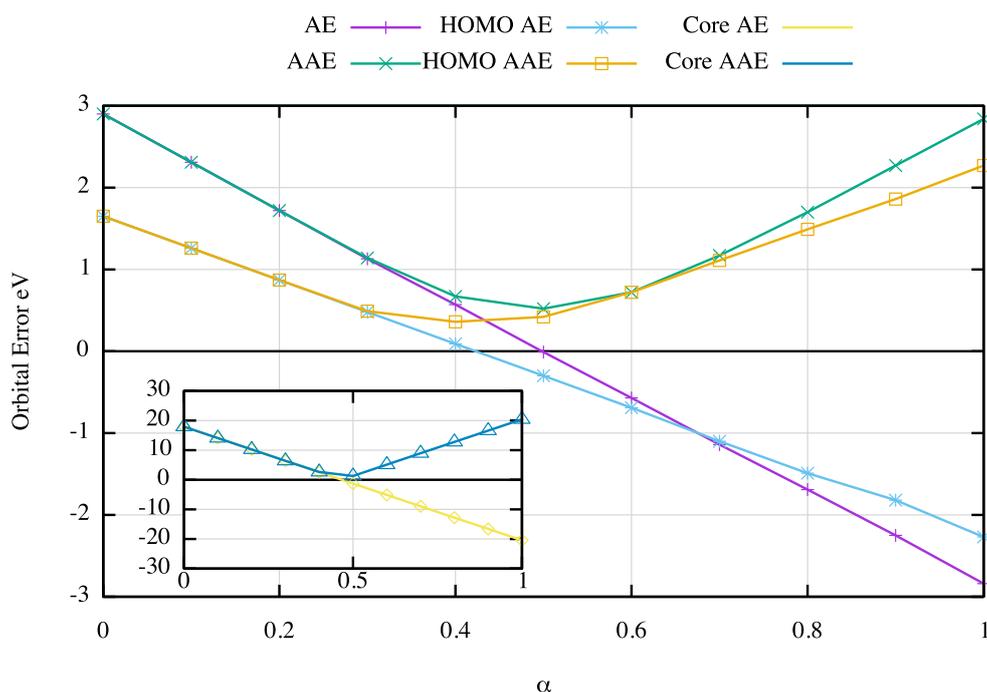
Figure 5.5: The errors on the orbital energies for a range of molecules over $0 < \alpha < 1$. Showing both average error (AE) and absolute average error (AAE) for the HOMO, valence orbitals (including HOMO). Inset, the average error and absolute average error for the core orbitals for the molecules in table 5.2.

orbitals was sought, to provide the best approximation to all orbitals from a single calculation.

The molecular geometries for these calculations were taken from the supplementary material of Ranasinghe [2] along with experimental and coupled cluster results. These results were calculated using the Hippo code utilising the EFO method 5.3, with a cc-pVDZ basis set (unless specified otherwise). From Fig. 5.5 it can be seen that the optimal value of α varies slightly depending on the orbital error considered and the basis set representation. However, a minimum appears around a mixing parameter of approximately $\alpha = 0.5$. This value was used for α to apply the method to a larger set of molecules to assess the general performance of the method.

Fig. 5.6 demonstrates the method with $\alpha = 0.5$ for a larger set of systems for the errors on the HOMO, valence and core orbitals compared to experiment. It can be seen that there is a good agreement in general with all results in close agreement

between calculation and experiment. Fig. 5.7 shows the improvement of the results with this method, relative to Hartree Fock and CPBE with an error lying between the overestimation of Hartree Fock and the underestimation of CPBE resulting in a smaller error in the majority of cases. Table 5.4 compares the hybrid method with results from unconstrained and constrained PBE, Hartree Fock, and coupled cluster(SD) results. These results demonstrate that this hybrid method has a significantly reduced error over the other DFT methods when calculating ionisation energies for all orbitals, and has accuracy comparable to the CCSD results. The change in total energy when applying this hybrid method compared to an unconstrained hybrid method, over all the systems in Table 5.4, was ~ 1 meV similar to the energy increase of CLDA over LDA. This implies that this functional will have the same energetic performance to that of a hybrid of 50% PBE exchange and 50% Fock exchange with full PBE correlation. This would result in energetic results comparable to the well used PBE0 hybrid function [61]. Of the molecules investigated with this hybrid, outlying results are for the molecules O_3 with a single valence orbital overestimated by 3 eV and SiF_4 where every occupied orbital eigenvalue has errors over 1 eV. The large error on these molecules requires further investigation. Similarly poor results were reported in the results for the CCSD calculations for O_3 [2], suggesting that these systems exhibit effects that make the ionisation energies particularly challenging to calculate.

Table 5.5 shows the full set of orbital energies for a small selection of molecules compared to experimental results [151]. The agreement of the self-interaction corrected hybrid functional method with experiment can clearly be seen for these molecules. A similar level of accuracy is found for the HOMO and valence orbitals. Core orbitals have a larger absolute error due to their large eigenvalues, however, even for orbitals with such large energies the constrained hybrid method still approximates these orbitals unexpectedly well with an error of the order of 1 eV.

5.5.3 Conclusions

From these results it is clear that a hybrid method utilising a constrained potential offers significant improvements in the approximation of orbital energies not just

Table 5.4: Table comparing calculated IEs to experimental valence [2] and HOMO [1] IEs for several methods, showing the number of orbitals analysed(#Orbs), the average error (AE), and the absolute average error(AAE). Results for core states are also shown for the cc-pVTZ basis set. CCSD results from the supplementary material or Ref [2]. All energies in eV.

	All Valence States			HOMO		
	#Orbs	AE	AAE	#Orbs	AE	AAE
cc-pVDZ						
HF	381	2.90	2.90	136	1.63	1.63
PBE	381	-5.02	5.02	136	-4.41	4.41
CPBE	381	-2.84	2.84	136	-2.06	2.06
HPBE	381	-0.01	0.52	136	-0.24	0.34
IP-EOM-CCSD	381	-0.07	0.34	136	-0.12	0.24
cc-pVTZ						
HF	91	2.58	2.58	28	1.62	1.62
PBE	91	-4.71	4.9	28	-4.79	4.79
CPBE	91	-1.6	1.63	28	-1.46	1.46
CHYB	91	0.48	0.54	28	0.11	0.25
IP-EOM-CCSD	91	0.15	0.27	28	-0.04	0.15
	Core States					
cc-pVTZ	#Orbs	AE	AAE			
HF	15	17.34	17.34			
PBE	15	-25.93	25.93			
CPBE	15	-22.06	22.06			
HPBE	15	-2.53	2.53			
IP-EOM-CCSD	15	0.98	0.98			

Table 5.5: Results for the full set of orbitals in the molecules N_2, CO, HF, H_2O for the cc-pVTZ basis set, comparing to experimental results [2]. With average errors(AE) and average absolute errors (AAE) for the subsets of orbitals. All energies in eV..

MOL	Expt	HF	PBE	CPBE	HPBE
N_2	15.58	0.72	-5.48	-1.78	0.22
	16.93	0.17	-5.63	-1.93	-1.13
	18.75	2.75	-5.15	-1.45	1.05
	37.3	2.10	-9.6	-5.9	-1.10
	409.98	17.02	-26.98	-22.98	1.02
	409.98	17.02	-26.98	-22.98	1.02
CO	14.01	1.09	-5.00	-1.41	0.09
	16.91	-0.23	5.3	1.72	0.56
	19.72	-2.1	5.65	2.07	-0.44
	38.3	-2.69	9.34	5.77	0.69
	296.21	-13.2	23.9	20.7	0.41
	542.55	-19.8	29.3	26.3	-1.35
HF	16.19	1.31	-7.17	-1.79	0.11
	19.9	0.6	-7.00	-1.70	-0.3
	39.6	3.6	-10.2	-4.9	0.2
	694.23	20.77	-34.23	-28.23	0.77
H_2O	12.62	1.08	-5.92	-1.52	0.08
	14.74	0.96	-5.9	-1.54	-0.04
	18.55	0.55	-5.85	-1.45	-0.25
	32.2	4.30	-7.40	-3.00	1.4
	539.9	19.1	-29.9	-25.9	1.1

		HF	PBE	CPBE	HPBE
ALL	AE	2.63	-5.95	-3.42	0.2
	AAE	4.44	3.5	2.69	0.42
HOMO	AE	1.05	-5.89	-1.63	0.13
	AAE	4.01	4.32	3.33	0.37
VALENCE	AE	1.8	-4.75	-2.3	0.15
	AAE	3.7	3.67	2.83	0.38
CORE	AE	2.91	-5.83	-3.58	0.3
	AAE	5.14	4.32	3.33	0.44
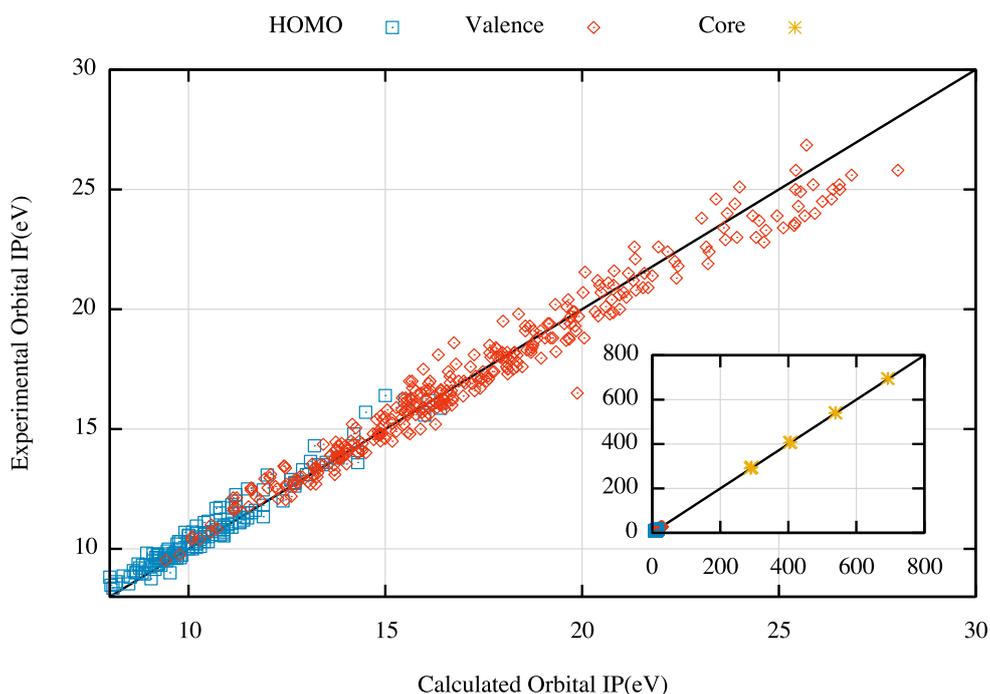
Figure 5.6: Experimental IEs [1, 2] against the IEs calculated from the orbital energies for the cc-pVDZ test set of molecules in 5.4.

for the HOMO but for the full range of occupied orbitals. The average error in orbital energies in the constrained hybrid method is below 1 eV. This is a major improvement when compared to the poor accuracy of traditional DFT methods that typically feature errors of ≈ 4 eV. This method has been demonstrated for the PBE functional but these improvements in the ionisation energies would be expected to be similar for a range of density functional approximations. This is due to the insensitivity of the orbital energies to the approximation used in the constrained method as seen in Chapter 4.

There is a slight change in total energies when using the constrained hybrid method; however with a suitable choice of correlation energy functional the energetics of the original DFA are preserved. The PBE functional was investigated here for this reason, but any functional where $E_{\text{tot}}^{\text{DFA}}$ and $E_{\text{tot}}^{\text{HF+C}}$ are close in energy will preserve the energetics of the original DFA in a hybrid formulation. This method therefore is an inexpensive way to obtain accurate orbital energies while preserving favourable energetics in a generalised Kohn-Sham scheme.
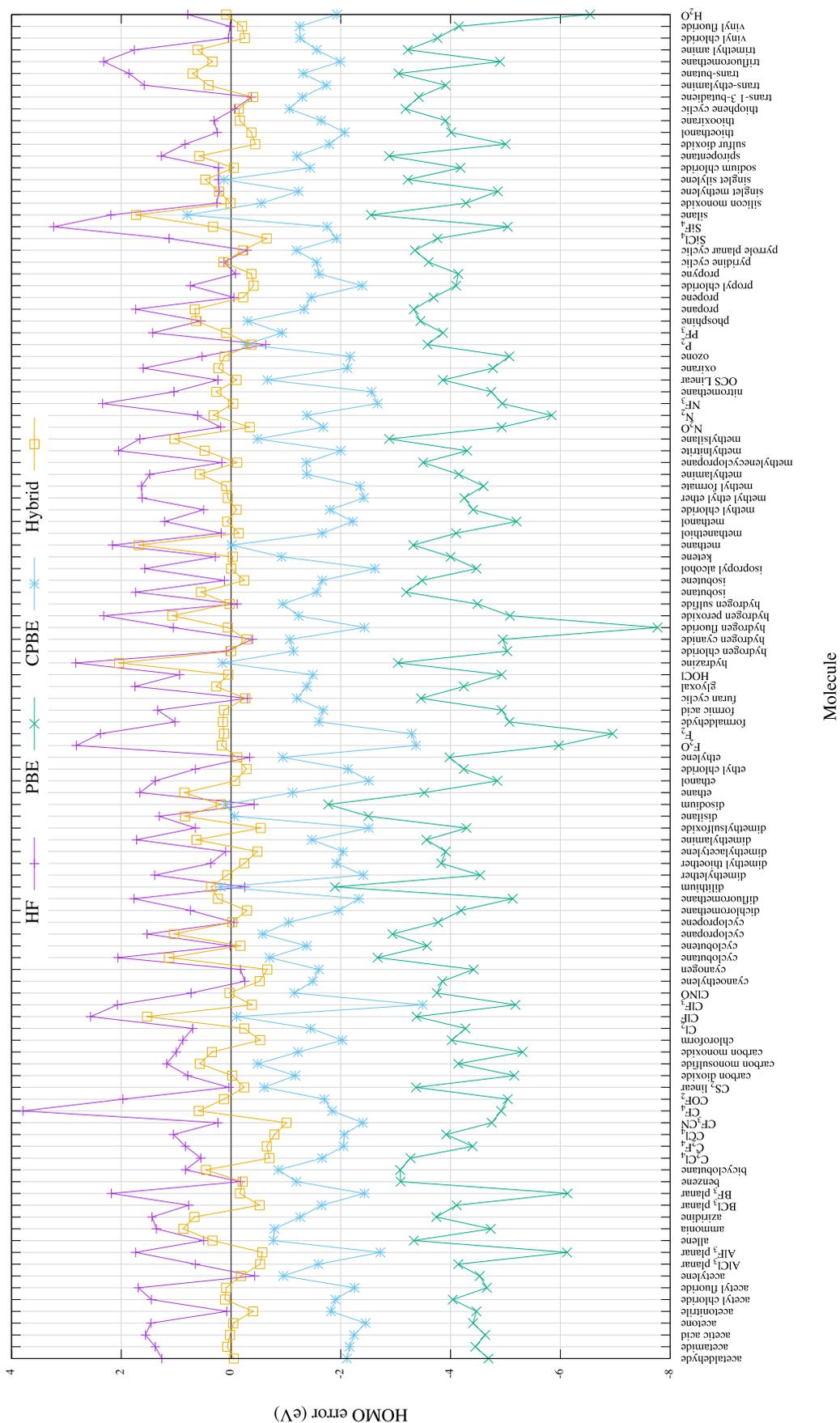
Figure 5.7: Graph showing the errors for Hartree-Fock, PBE, CPBE, and the hybrid method with $\alpha = 0.5$.

These results also challenge the often assumed interpretation of the Kohn-Sham orbital energies, for which the orbital energies below the HOMO have been considered to have no physical meaning. Similar agreement has been observed in other studies between on the Kohn-Sham orbital energies and the ionisation energies [151–153] suggesting there must exist some physical meaning to all the Kohn-Sham orbital eigenvalues. This is consistent with the suggested ionisation energy theorem by Bartlett that suggests that an accurate Kohn-Sham potential should give eigenvalues that are good approximations of ionisation energies [154–157].

The accuracy of this method at approximating all orbital energies suggest that the DFT orbitals have a systematic error that is compensated by an opposite error in the HF orbitals. It is very surprising that the error remains so small for high energy core orbitals where the relaxation effects of removing a core electron should introduce large errors in both theories. An investigation into the relation between the ionisation energies for lower lying orbitals and the Kohn-Sham eigenvalues will be performed in the following chapter. This investigation was unable uncover a fundamental reason for the hybrid ionisation energies to have such good agreement with experiment. These hybrid results are possibly attributed to a fortuitous cancellation of errors that account for relaxation effects. This cancelation of errors provides accurate predictions of ionisation energies that are improved over individual application of either Hartree-Fock or the constrained DFT methods.

5.6   Summary

In this chapter I have suggested several methods that help improve the constrained self-interaction correction method when dealing with the pathologies of finite molecular basis sets. The self-interaction corrected hybrid method presented here is the main result. It is a considerable improvement over simply applying the correction to a hybrid method. These corrections leads to significant improvements in the calculation of ionisation energies for a range of systems. The hybrid method is

also demonstrated to provide accurate ionisation energies for all occupied orbitals in accordance with the theoretical prediction of Bartlett [154–156].

Chapter 6

Orbital Energy Corrections

6.1 Introduction

This chapter introduces a novel post-SCF correction to the Kohn-Sham eigenvalues that corrects the Kohn-Sham eigenvalues towards the ionisation energy obtained from the difference in energy between an N and $N-1$ electron system.

6.2 Calculation of Ionisation Energies in DFT

As we saw in previous chapters the negative of the highest occupied Kohn-Sham orbital energy contains significant errors when compared to experimental ionisation energies. These errors arise from the approximate nature of DFT functionals and are mainly due to self-interactions in the Kohn-Sham potential. Despite the poor approximation of ionisation energies from Kohn-Sham HOMO eigenvalues, DFT methods are able to calculate accurate ionisation energies in finite systems using the Δ_{scf} method [158–160]. This method makes use of the accurate representation of total energies with DFT approximations [161]. The Δ_{scf} method calculates ionisation energies by taking the difference in total energy between a N and $N-1$ electron system. This difference in energies defines the ionisation energy(IE) and because approximate DFT functionals accurately approximate total energies they allow an accurate prediction of ionisation energies. For the exact DFT functional the ionisation energy of the highest energy electron is given exactly either by the Δ_{scf} method,

or by the negative of the highest occupied Kohn-Sham eigenvalue. This gives the following equality for the exact DFT functional

$$I_N = -\epsilon_N = E[\rho^{(N-1)}] - E[\rho^{(N)}] \tag{6.2.1}$$

where $\rho^{(N-1)}$ and $\rho^{(N)}$ are the electron densities of the $N-1$ and N electron systems respectively. When using an approximate DFT functional, the ionisation energy, the negative of the highest occupied Kohn-Sham eigenvalue, and the Δ_{scf} energy are no longer equivalent. As can be seen in Table 6.1, functionals typically approximate ionisation energies better when using the Δ_{scf} method compared to using the Kohn-Sham eigenvalue. This is due to DFT approximations primarily being optimised to accurately describe total energy properties. The Kohn-Sham eigenvalues have been shown to have large errors due to self-interaction effects. However, even when using a self-interaction correction such as the constrained minimisation method developed in Chapter 4, Table 6.1 demonstrates that these self-interaction corrected results are still less accurate than the Δ_{scf} method.

The work in thischapter aims to provide a post SCF correction to the Kohn-Sham eigenvalues that will improve ionisation energies calculated this way, bringing them in line with the Δ_{scf} results. A benefit of using the eigenvalue is that only a single DFT calculation is needed to calculate the ionisation energy; instead of a pair of calculations for the N and $N-1$ electron systems. This correction will take the form of a correcting term I_{corr} given by

$$I_N \sim E[\rho^{(N-1)}] - E[\rho^{(N)}] = -\epsilon_N + I_{\text{corr}} \tag{6.2.2}$$

where the target ionisation energy is approximated by the Δ_{scf} method. As shown in Table 6.1, the Δ_{scf} method is, in general, an accurate approximation of the ionisation energy. The ionisation energy can be partitioned as

$$I_N = I_{\text{frozen}} + I_{\text{relax}}, \tag{6.2.3}$$

where I_{frozen} corresponds to the Δ_{scf} result under the frozen orbital approximation. In this approximation the electron orbitals are held fixed and only the electron

Table 6.1: A comparison of the ionisation energies calculated using the Δ_{scf}, LDA, and the self-interaction corrected CLDA methods using a cc-pVTZ basis set. The CLDA results make use of the effective orbital method using the same auxiliary basis as the orbitals. All energies in eV.

MOL	EXP [1]	Δ_{scf}	LDA	CLDA
Acetylene	11.4	0.27	-4.12	-0.86
Ammonia	10.07	1.1	-4.07	-0.25
Carbon dioxide	13.78	0.19	-4.56	-1.44
Carbon monosulfide	11.33	0.18	-3.9	-0.87
Carbon monoxide	14.01	0.10	-4.91	-1.43
Cl2	11.48	-0.07	-4.05	-1.84
ClF	10.90	1.78	-2.95	0.13
Dilithium	5.11	0.16	-1.89	0.03
Disilane	9.74	0.77	-2.37	-0.11
Disodium	4.89	0.33	-1.69	0.12
Ethane	11.52	0.38	-3.41	-0.59
Ethylene	10.51	0.46	-3.61	-0.66
F2 molecule	15.70	-0.06	-6.22	-2.52
Formaldehyde	10.89	0.03	-4.65	-1.39
HOCl	11.12	-0.02	-4.46	-1.16
Hydrazine	8.10	1.83	-2.45	0.64
Hydrogen chloride	12.74	0.22	-4.68	-1.18
Hydrogen cyanide	13.60	0.61	-4.52	-1.20
Hydrogen fluoride	16.03	0.53	-6.70	-1.78
Hydrogen peroxide	10.58	0.70	-4.37	-0.8
Hydrogen sulfide	10.46	0.16	-4.13	-0.87
Lithium Fluoride	11.30	1.00	-5.04	-1.18
Lithium hydride	7.90	0.24	-3.54	-0.30
Methane	12.61	1.46	-3.16	0.22
Methanethiol	9.44	0.05	-3.80	-1.05
Methanol	10.84	-0.03	-4.65	-1.42
Methyl chloride	11.26	0.00	-4.15	-1.35
N2 molecule	15.58	-0.03	-5.29	-1.87
P2	10.53	0.29	-3.36	-0.40
Phosphine	9.87	0.69	-3.23	-0.19
Silane	11.00	1.18	-2.47	0.28
Silicon monoxide	11.49	0.01	-3.96	-1.00
Singlet methylene	10.40	0.22	-4.52	-0.99
Singlet silylene	8.92	0.54	-3.08	-0.21
Sodium Chloride	9.20	0.35	-3.90	-0.99
Water	12.62	0.37	-5.66	-1.33
		Δ_{scf}	LDA	CLDA
	AE	0.44	-3.99	-0.83
	AAE	0.46	3.99	0.91

number is changed. I_{relax} is related to the energy change due to the relaxation of the orbitals of the N electron system to those of the $N-1$ electron system. These two contributions to the ionisation energy can be written as

$$I_{\text{frozen}} = E[\rho_{\text{frozen}}^{(N-1)}] - E[\rho^{(N)}], \tag{6.2.4}$$

$$I_{\text{relax}} = E[\rho^{(N-1)}] - E[\rho_{\text{frozen}}^{(N-1)}]. \tag{6.2.5}$$

where $\rho_{\text{frozen}}^{(N-1)}$ is the $N-1$ electron density under the frozen orbital approximation. Here the frozen orbital approximation forms an intermediate step between the ground states of the N and $N-1$ electron systems.

From the frozen orbital approximation term in Eq. (6.2.4) a zero-order correction will be obtained for the Kohn-Sham eigenvalue, and from the relaxation term in Eq. (6.2.5) a first order correction can be derived. The terms in these corrections will correspond to an expansion of the energy of the $N-1$ electron system around the Kohn-Sham potential of the N electron system.

6.3 Method

6.3.1 Zero Order Correction

The frozen orbital approximation gives the zero order behaviour of the ionisation energy with respect to the Kohn-Sham orbitals of the N electron system. Under the frozen orbital approximation the ionised electron is assumed to be removed instantaneously such that the orbitals of the $N-1$ electron system remain unchanged from those of the N electron system. The orbitals of the N electron system are given by

$$\left[-\frac{\nabla^2}{2} + V_{\text{ext}}[\rho^{(N)}](\mathbf{r}) + V_{\text{KS}}^{(N)}(\mathbf{r}) \right] \phi_i^{(N)} = \epsilon_i^{(N)} \phi_i^{(N)} \tag{6.3.6}$$

where the Kohn-Sham potential $V_{\text{KS}}^{(N)}$ minimises the total energy of the N electron system, and for a DFT system would be given by $V_{\text{HXC}}^{(N)}$ the Hartree-exchange-correlation potential for the N electron system. The electron density of the $N-1$ electron system is given in terms of these orbitals by

$$\rho_{\text{frozen}}^{(N-1)}(\mathbf{r}) = \sum_{i \neq N} \left| \phi_i^{(N)}(\mathbf{r}) \right|^2 = \rho^{(N)}(\mathbf{r}) - \left| \phi_N^{(N)}(\mathbf{r}) \right|^2 = \rho^{(N)}(\mathbf{r}) - \rho_N(\mathbf{r}) \qquad (6.3.7)$$

where

$$\rho_N = \left| \phi_N^{(N)}(\mathbf{r}) \right|^2 \qquad (6.3.8)$$

is the one-electron density of the Nth electron using the orbitals of the N electron system. The frozen orbital ionisation energy given in Eq. (6.2.4) is given by

$$I_{\text{frozen}} = E[\rho^{(N)} - \rho_N] - E[\rho^{(N)}] \qquad (6.3.9)$$

where all quantities depend on the N electron Kohn-Sham orbitals. Evaluating the frozen orbital ionisation energy gives

$$I_{\text{frozen}} = - \langle \phi_N^{(N)} | - \frac{\nabla^2}{2} + V_{\text{ext}} | \phi_N^{(N)} \rangle + E_{\text{HXC}}[\rho^{(N)} - \rho_N] - E_{\text{HXC}}[\rho^{(N)}] \qquad (6.3.10)$$

where E_{HXC} is the Hartree-exchange and correlation energy density functional. Using the Kohn-Sham equations of the N electron system in Eq. (6.3.6) the kinetic energy term can be replaced, giving

$$I_{\text{frozen}} = -\epsilon_N^{(N)} + \langle \phi_N^{(N)} | V_{\text{KS}}^{(N)} | \phi_N^{(N)} \rangle + E_{\text{HXC}}[\rho^{(N)} - \rho_N] - E_{\text{HXC}}[\rho^{(N)}] \qquad (6.3.11)$$

relating the ionisation energy to the Kohn-Sham eigenvalue. As is known from the DFT Koopmans' theorem, the negative of the Kohn-Sham eigenvalue of the exact DFT functional is equal to the ionisation energy, as shown in Sec. 3.3. From this the additional terms in Eq. (6.3.11) form a zero order correction term to the Kohn-Sham eigenvalue for approximate functionals. Therefore, in an approximate functional the ionisation energy is given by

$$I_N = -\epsilon_N^{(N)} + I_{\text{corr}}^{(0)} + I_{\text{corr}}^{\text{relax}} \qquad (6.3.12)$$

with

$$I_{\text{corr}}^{(0)} = \langle \phi_N^{(N)} | V_{\text{KS}}^{(N)} | \phi_N^{(N)} \rangle + E_{\text{HXC}}[\rho^{(N)} - \rho_N] - E_{\text{HXC}}[\rho^{(N)}] \qquad (6.3.13)$$

being the zero-order correction to the Kohn-Sham eigenvalue, correcting towards the Δ_{scf} value. The higher order terms in $I_{\text{corr}}^{\text{relax}}$ take into account the change of the Kohn-Sham orbitals between the N and $N-1$ systems.

6.3.2   First Order Correction for DFT

The zero-order correction accounts for the instantaneous removal of an electron. Once the electron is removed the Kohn-Sham orbitals of the N electron system are no longer in the ground state of the $N-1$ electron system and a relaxation of the orbitals must occur to minimise the $N-1$ system's energy. The relaxation of the orbitals corresponds to a change in the Kohn-Sham potential from $V_{\text{KS}}^{(N)}$ to $V_{\text{KS}}^{(N-1)}$. These relaxed $N-1$ electron orbitals are defined by

$$\left[-\frac{\nabla^2}{2} + V_{\text{ext}}(\mathbf{r}) + V_{\text{KS}}^{(N-1)}(\mathbf{r}) \right] \phi_i^{(N-1)} = \epsilon_i^{(N-1)} \phi_i^{(N-1)} \qquad (6.3.14)$$

where $V_{\text{KS}}^{(N-1)}$ minimises the total energy functional for a $N-1$ electron system. The Kohn-Sham potential $V_{\text{KS}}^{(N-1)}$ can be found through a second DFT calculation for the $N-1$ electron system. It is possible, however, to approximate the Kohn-Sham potential for the $N-1$ electron system via perturbation theory. This is achieved by treating $V_{\text{KS}}^{(N-1)}$ as a perturbation of $V_{\text{KS}}^{(N)}$ by defining v', a perturbation in the potential, as

$$v' = V_{\text{KS}}^{(N-1)} - V_{\text{KS}}^{(N)}. \qquad (6.3.15)$$

This perturbation in the potential neglects that the derivative discontinuity would introduce a constant shift between these two potentials. This shift will not affect the electron orbitals, or the total energy and as such can be neglected when calculating this energy correction. The correction to the Kohn-Sham eigenvalues to first order is

$$I_{\text{relax}}^{(1)} = \int d\mathbf{r} \left. \frac{\delta E[\rho^{(N-1)}]}{\delta v'(\mathbf{r})} \right|_{v'=0} v'(\mathbf{r}) \qquad (6.3.16)$$

and the derivative can be evaluated through the chain rule as

$$\frac{\delta E[\rho^{(N-1)}]}{\delta v'(\mathbf{r})}\bigg|_{v'=0} = \sum_{j}^{N-1} \int d\mathbf{r}' \frac{\delta E[\rho^{(N)} - \rho_N]}{\delta \phi_j^{(N)}(\mathbf{r}')} \frac{\delta \phi_j^{(N)}(\mathbf{r}')}{\delta v'(\mathbf{r})} \tag{6.3.17}$$

where it has been used that at $v' = 0$ the orbitals are the orbitals of the N electron system. The derivatives in Eq. (6.3.17) are known from the OEP method as

$$\frac{\delta E[\rho^{(N)} - \rho_N]}{\delta \phi_j^{(N)}(\mathbf{r}')} = \left[-\frac{\nabla^2}{2} + V_{\text{ext}}(\mathbf{r}') + V_{\text{HXC}}[\rho^{(N)} - \rho_N](\mathbf{r}') \right] \phi_j^{(N)}(\mathbf{r}') \tag{6.3.18}$$

$$= \left[V_{\text{HXC}}[\rho^{(N)} - \rho_N](\mathbf{r}') - V_{\text{KS}}^{(N)}(\mathbf{r}') \right] \phi_j^{(N)}(\mathbf{r}') \tag{6.3.19}$$

$$\frac{\delta \phi_j^{(N)}(\mathbf{r}')}{\delta v'(\mathbf{r})} = 2 \sum_{k \neq j}^{\infty} \phi_k^{(N)}(\mathbf{r}') \frac{\phi_j^{(N)}(\mathbf{r}) \phi_k^{(N)}(\mathbf{r})}{\epsilon_j - \epsilon_k} \tag{6.3.20}$$

giving the first order correction in Eq. (6.3.16) as

$$I_{\text{relax}}^{(1)} = 2 \sum_{i}^{N-1} \sum_{a=N}^{\infty} \frac{\langle \phi_i^{(N)}| V_{\text{HXC}}[\rho^{(N)} - \rho_N] - V_{\text{KS}}^{(N)} |\phi_a^{(N)}\rangle \langle \phi_i^{(N)}| v' |\phi_a^{(N)}\rangle}{\epsilon_i - \epsilon_a} \tag{6.3.21}$$

where v' is given by Eq. (6.3.15). This equation for the first order correction assumes that the perturbation in the potential between the N and $N - 1$ electron system is known. V_{KS} can be determined exactly by performing a second DFT calculation, but for a DFT method $V_{\text{KS}} = V_{\text{HXC}}$. It is therefore possible to obtain an approximation of v' without the need for a second DFT calculation.

The $N - 1$ electron orbitals are treated as a perturbation of the N electron orbitals giving the $N - 1$ electron orbitals to first-order as

$$\phi_i^{(N-1)}(\mathbf{r}) \rightarrow \phi_i^{(N)}(\mathbf{r}) + \phi_i'(\mathbf{r}) \tag{6.3.22}$$

$$\phi_i'(\mathbf{r}) = \int d\mathbf{r}' \frac{\delta \phi_j^{(N)}(\mathbf{r})}{\delta v'(\mathbf{r}')}\bigg|_{v'=0} v'(\mathbf{r}') = \sum_{k \neq i}^{\infty} \frac{\langle \phi_i^{(N)}| v' |\phi_k^{(N)}\rangle}{\epsilon_i - \epsilon_k} \phi_k^{(N)}(\mathbf{r}) \phi_i^{(N)}(\mathbf{r}) \tag{6.3.23}$$

this perturbation in the orbitals has a corresponding first order perturbation in the $N - 1$ electron density as

$$\rho^{(N-1)}(\mathbf{r}) \rightarrow \rho^{(N)}(\mathbf{r}) - \rho_N(\mathbf{r}) + \rho'(\mathbf{r}) \tag{6.3.24}$$

$$\rho'(\mathbf{r}) = 2 \sum_i^{N-1} \sum_{a=N}^{\infty} \frac{\langle \phi_i^{(N)} | v' | \phi_a^{(N)} \rangle}{\epsilon_i - \epsilon_a} \phi_a^{(N)}(\mathbf{r}) \phi_i^{(N)}(\mathbf{r}) \tag{6.3.25}$$

where

$$\int d\mathbf{r} \rho'(\mathbf{r}) = 0 \tag{6.3.26}$$

which ensures that $\rho^{(N-1)}$ corresponds to a $N-1$ electron density regardless of the perturbation v'. The perturbation in the density ρ' allows a first order approximation to the $N-1$ electron density, from which $V_{\mathrm{HXC}}[\rho^{(N-1)}]$ can be approximated. ρ' can also be used to give an alternative expression for $I_{\mathrm{relax}}^{(1)}$ by rewriting Eq. (6.3.21) in terms of ρ' as

$$I_{\mathrm{relax}}^{(1)} = \int d\mathbf{r} \left[V_{\mathrm{HXC}}[\rho^{(N)} - \rho_N](\mathbf{r}) - V_{\mathrm{KS}}^{(N)}(\mathbf{r}) \right] \rho'(\mathbf{r}) \tag{6.3.27}$$

allowing calculation of the first-order correction from the perturbed density term. Once the perturbation in the density is calculated, the equivalence of $V_{\mathrm{HXC}}[\rho^{(N-1)}] = V_{\mathrm{KS}}^{(N-1)}$ for a DFT method can then be used to update v' by Eq. (6.3.15). The perturbation in the Kohn-Sham potential is given by

$$v' = V_{\mathrm{HXC}}[\rho^{(N)} - \rho_N + \rho'] - V_{\mathrm{HXC}}[\rho^{(N)}]. \tag{6.3.28}$$

This perturbed potential is updated until $I_{\mathrm{relax}}^{(1)}$ is converged, with the algorithm shown in Fig. 6.1.

In many systems the target Nth electron orbital is degenerate with an occupied orbital such that $\epsilon_i - \epsilon_a = 0$. This degeneracy would lead to an infinity in Eq. 6.3.21. In such cases the degenerate orbitals must be identified from the initial DFT calculation and treated using degenerate perturbation theory to obtain the derivative $\frac{\delta \phi_j^{(N)}(\mathbf{r}')}{\delta v'(\mathbf{r})}$. This technique for degenerate orbitals is covered in Appendix A.2.
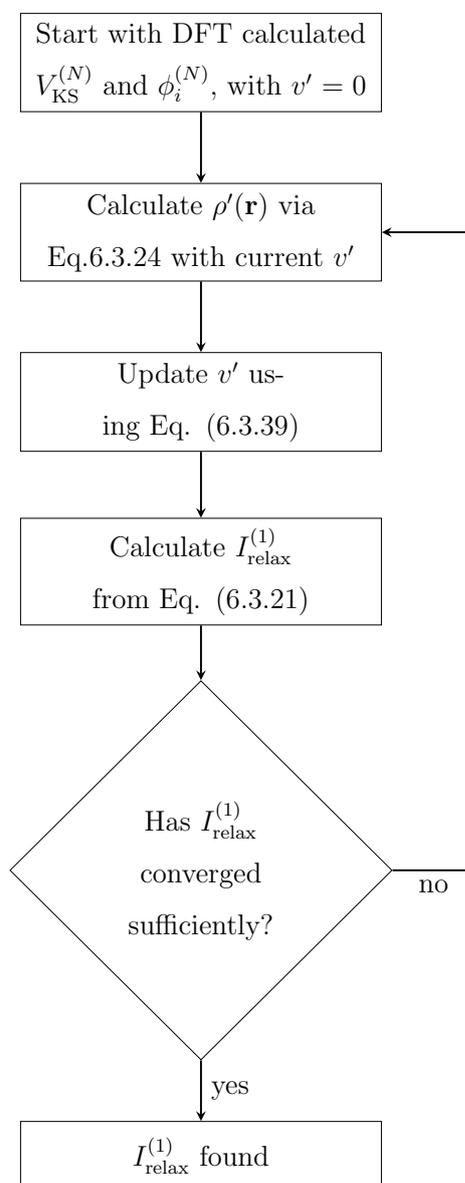
Figure 6.1: A flow diagram showing the procedure for a calculating the first order correction $I_{\text{relax}}^{(1)}$.

6.3.3 Corrections to Electron Affinities

Similar to the ionisation energy, a correction for the electron affinity can be constructed that will correct the $N + 1$ eigenvalue to the result of a Δ_{scf} calculation. The electron affinity is the energy gain when adding an additional electron to the system and is defined by the Δ_{scf} method as

$$A = E[\rho^{(N)}] - E[\rho^{(N+1)}]. \tag{6.3.29}$$

For the exact DFT functional the electron affinity can be related to the $(N + 1)$th Kohn-Sham eigenvalue of the N electron system as

$$A = -\epsilon_{N+1} + \Delta_{\mathrm{XC}} \tag{6.3.30}$$

where Δ_{XC} is the derivative discontinuity.

Similar to the ionisation energy the electron affinity can be broken into a frozen orbital term and an orbital relaxation term

$$A = A_{\mathrm{frozen}} + A_{\mathrm{relax}}, \tag{6.3.31}$$

where

$$A_{\mathrm{frozen}} = E[\rho^{(N)}] - E[\rho^{(N+1)}_{\mathrm{frozen}}], \tag{6.3.32}$$

$$A_{\mathrm{relax}} = E[\rho^{(N+1)}_{\mathrm{frozen}}] - E[\rho^{(N+1)}]. \tag{6.3.33}$$

Following the same steps as for the ionisation energy, the zero-order correction for the frozen orbital contribution to the electron affinity is found to be

$$A_{\mathrm{frozen}} = -\epsilon^{(N)}_{N+1} + \langle \phi^{(N)}_{N+1} | v^{(N)}_{\mathrm{KS}} | \phi^{(N)}_{N+1} \rangle + E_{\mathrm{HXC}}[\rho^{(N)}] - E_{\mathrm{HXC}}[\rho^{(N)} + \rho_{N+1}] \tag{6.3.34}$$

where

$$\rho_{N+1}(\mathbf{r}) = \left| \phi^{(N)}_{N+1}(\mathbf{r}) \right|^2 \tag{6.3.35}$$

is the density of the $N+1$ electron orbital using the orbitals from the N electron system. This equation for the electron affinity relates the electron affinity to the LUMO orbital for an approximate DFT functional. From this the zero order correction to the LUMO eigenvalue $A^{(0)}$ is defined as

$$A^{(0)} = \langle \phi_{N+1}^{(N)} | v_{\text{KS}}^{(N)} | \phi_{N+1}^{(N)} \rangle + E_{\text{HXC}}[\rho^{(N)}] - E_{\text{HXC}}[\rho^{(N)} + \rho_{N+1}]. \qquad (6.3.36)$$

A first-order correction can also be derived for the electron affinity, again using perturbation theory to obtain an approximation to the relaxed orbitals of the $N+1$ electron system. This first order correction is found by solving

$$A_{\text{relax}}^{(1)} = -2 \sum_{i}^{N-1} \sum_{a=N}^{\infty} \frac{\langle \phi_i^{(N)} | V_{\text{HXC}}[\rho^{(N)} + \rho_{N+1}] - V_{\text{KS}}^{(N)} | \phi_a^{(N)} \rangle \langle \phi_i^{(N)} | v' | \phi_a^{(N)} \rangle}{\epsilon_i - \epsilon_a} \qquad (6.3.37)$$

self-consistently. The perturbed potential v' is given by

$$v' = V_{\text{KS}}^{(N+1)}(\mathbf{r}') - V_{\text{KS}}^{(N)}(\mathbf{r}') \qquad (6.3.38)$$

where for a DFT method the Kohn-Sham potential $V_{\text{KS}}^{(N+1)}$ is equal to $V_{\text{HXC}}[\rho^{(N+1)}]$. This allows v' to be calculated at first order as

$$v' = V_{\text{HXC}}[\rho^{(N)} + \rho_{N+1} + \rho'] - V_{\text{HXC}}[\rho^{(N)}] \qquad (6.3.39)$$

similar to when calculating the perturbation for the ionisation energy. Applying both the zero- and first-order corrections to the $N+1$ Kohn-Sham eigenvalue gives the corrected electron affinity as

$$A = -\epsilon_{N+1} + A^{(0)} + A_{\text{relax}}^{(1)}. \qquad (6.3.40)$$

The self-consistent procedure for calculating the first order correction for the electron affinity follows a similar method as for the ionisation energy as shown in Fig. 6.1. Unlike the ionisation energy the correcting terms will not be equal to zero for the exact functional but will instead give the the value of the derivative discontinuity

$$\Delta_{\text{XC}} \sim A^{(0)} + A_{\text{relax}}^{(1)}. \qquad (6.3.41)$$

6.3.4   Correction for the mth Orbital

So far corrections have been derived for an electron being removed from the highest occupied orbital or added to the lowest unoccupied electron orbital. In both of these cases the exact DFT functional is known to have a relationship between these quantities, with $I_N = -\epsilon_N$ for the ionisation energy and $A = -\epsilon_{N+1} + \Delta_{\mathrm{XC}}$ for the electron affinity. However the Δ_{scf} method can be extended further to other occupied or unoccupied orbitals and the use of the Δ_{scf} method in this manner for non-ground state systems has been justified by Görling [162] who showed that the Δ_{scf} method can be used to calculate ionisation energies of the lower lying orbitals with a generalised adiabatic connection. It remains to be seen whether a direct relationship exists between the mth orbital eigenvalue and the corresponding ionisation energy of the fully interacting system. It has been argued [163] that an accurate DFT functional should predict excitation energies for all the orbitals and that a such a relationship exists for the exact DFT functional. As will be shown, the Δ_{scf} ionisation energy for the mth electron can always be written as the Kohn-Sham eigenvalue plus some correction with similar form to the ionisation energy/electron affinity. However, this correcting term will not vanish in general for the exact functional, and is only equal for the HOMO of the exact functional.

Considering two systems of N and $N-1$ electrons where the electron that has been removed in the $N-1$ electron system was in orbital m. The electron densities of the N and $N-1$ electron systems are $\rho^{(N)}$ and $\rho^{(N-1,m)}$ and the ionisation energy of the mth electron orbital is given by

$$I_m = E[\rho^{(N-1,m)}] - E[\rho^{(N)}].\tag{6.3.42}$$

This is an exact relationship for the exact energy functional and an approximation when using approximate energy functionals.

The frozen orbital approximation can be used to partition the ionisation energy into

$$I_{\mathrm{frozen}}{}^{(m)} = E[\rho_{\mathrm{frozen}}^{(N-1,m)}] - E[\rho^{(N)}]\tag{6.3.43}$$

$$I_{\mathrm{relax}}{}^{(m)} = E[\rho^{(N-1,m)}] - E[\rho_{\mathrm{frozen}}^{(N-1,m)}].\tag{6.3.44}$$

From Eq. (6.3.43) the zero order correction can be found by using

$$\rho_{\text{frozen}}^{(N)}(\mathbf{r}) = \rho^{(N)}(\mathbf{r}) - \rho_m(\mathbf{r}) \tag{6.3.45}$$

where $\rho_m(\mathbf{r}) = \left|\phi_m^{(N)}\right|^2$ is the electron density of the mth electron orbital. Making this substitution into Eq. (6.3.43) gives

$$I_{\text{frozen}}{}^{(m)} = -\langle\phi_m^{(N)}| - \frac{\nabla^2}{2} + V_{\text{ext}}|\phi_m^{(N)}\rangle + E_{\text{HXC}}[\rho^{(N)}(\mathbf{r}) - \rho_m(\mathbf{r})] - E_{\text{HXC}}[\rho^{(N)}(\mathbf{r})]. \tag{6.3.46}$$

Using the Kohn-Sham equation for the N electron system in Eq. (6.3.6) allows us to substitute the kinetic and external potential terms giving

$$I_{\text{frozen}}{}^{(m)} = -\epsilon_m^{(N)} + \langle\phi_m^{(N)}| V_{\text{KS}}^{(N)} |\phi_m^{(N)}\rangle + E_{\text{HXC}}[\rho^{(N)}(\mathbf{r}) - \rho_m(\mathbf{r})] - E_{\text{HXC}}[\rho^{(N)}(\mathbf{r})]. \tag{6.3.47}$$

This zero-order expression for the ionisation energy defines the zero-order correction to the Kohn-Sham eigenvalues as

$$I_{\text{m,corr}}^{(0)} = \langle\phi_m^{(N)}| V_{\text{KS}}^{(N)} |\phi_m^{(N)}\rangle + E_{\text{HXC}}[\rho^{(N)}(\mathbf{r}) - \rho_m(\mathbf{r})] - E_{\text{HXC}}[\rho^{(N)}(\mathbf{r})]. \tag{6.3.48}$$

As for the HOMO ionisation energy correction the first-order correction for a general ionisation energy is given by

$$I_{\text{m,corr}}^{(1)} = \int d\mathbf{r} \left.\frac{\delta E[\rho^{(N-1,m)}]}{\delta v'(\mathbf{r})}\right|_{v'(\mathbf{r})=0} v'(\mathbf{r}), \tag{6.3.49}$$

where $v' = V_{\text{KS}}^{(N-1,m)} - V_{\text{KS}}^{(N)}$. The chain rule can be used to split the derivative giving

$$I_{\text{m,corr}}^{(1)} = \int d\mathbf{r}d\mathbf{r}' \sum_{j}^{N}(1-\delta_{jm})\frac{\delta E[\rho^{(N-1,m)}]}{\delta\phi_j(\mathbf{r}')}\left.\frac{\delta\phi_j(\mathbf{r}')}{\delta v'(\mathbf{r}')}\right|_{v'(\mathbf{r}')=0} v'(\mathbf{r}') \tag{6.3.50}$$

where the summation runs over all orbitals. As the system has a vacancy in the mth electron orbital the factor $(1 - \delta_{jm})$ ensures that this orbital is not included. Using the results from Eqs. (6.3.19),(6.3.20) this expression can be written as

$$I_{\text{m,corr}}^{(1)} = 2 \sum_{i}^{N} \sum_{a=N+1}^{\infty} \frac{\langle \phi_i^{(N)} | V_{\text{HXC}}[\rho^{(N)} - \rho_m] - V_{\text{KS}}^{(N)} | \phi_a^{(N)} \rangle \langle \phi_i^{(N)} | v' | \phi_a^{(N)} \rangle}{\epsilon_i - \epsilon_a}$$
$$- 2 \sum_{a \neq m}^{\infty} \frac{\langle \phi_m^{(N)} | V_{\text{HXC}}[\rho^{(N)} - \rho_m] - V_{\text{KS}}^{(N)} | \phi_a^{(N)} \rangle \langle \phi_m^{(N)} | v' | \phi_a^{(N)} \rangle}{\epsilon_m - \epsilon_a}. \quad (6.3.51)$$

The perturbed potential defined for a DFT method is

$$v'(\mathbf{r}) = V_{\text{HXC}}[\rho^{(N)} - \rho_m + \rho'](\mathbf{r}) - V_{\text{HXC}}[\rho^{(N)}](\mathbf{r}) \quad (6.3.52)$$

and the perturbed density term ρ' given by

$$\rho'(\mathbf{r}) = 2 \sum_{i}^{N} \sum_{a=N+1}^{\infty} \phi_i^{(N)}(\mathbf{r}) \phi_a^{(N)}(\mathbf{r}) \frac{\langle \phi_i^{(N)} | v' | \phi_a^{(N)} \rangle}{\epsilon_i - \epsilon_a} - 2 \sum_{a \neq m}^{\infty} \phi_m^{(N)}(\mathbf{r}) \phi_a^{(N)}(\mathbf{r}) \frac{\langle \phi_m^{(N)} | v' | \phi_a^{(N)} \rangle}{\epsilon_m - \epsilon_a}.$$
$$(6.3.53)$$

This definition of $\rho'(\mathbf{r})$ allows the first-order correction in Eq. (6.3.51) to be alternatively written as

$$I_{\text{m,corr}}^{(1)} = \int d\mathbf{r} \left[V_{\text{HXC}}[\rho^{(N)} - \rho_m](\mathbf{r}) - V_{\text{KS}}^{(N)}(\mathbf{r}) \right] \rho'(\mathbf{r}). \quad (6.3.54)$$

This construction allows both the zero- and first-order corrections to be applied to every electron in the system. Each first order correction in the system will require a separate self-consistent cycle, that can be implemented as a modified version of Fig 6.1.

6.3.5 Application to Hartree-Fock

This ionisation energy correction can be extended to include the Hartree-Fock method. In this case the zero-order correction is known to be zero as the Hartree-Fock method satisfies Koopmans' theorem exactly. This result is the exact cancellation of

$$\langle \phi_m^{(N)} | \hat{V}_{\text{HX}}[\rho^{(N)}] | \phi_m^{(N)} \rangle + E_{\text{HX}}[\rho^{(N)} - \rho_m] - E_{\text{HX}}[\rho^{(N)}] = 0 \quad (6.3.55)$$

where $\hat{V}_{\text{HX}}$ is the Hartree and Fock-exchange potential operator. The first order correction allows for relaxation effects to be accounted for which are not included in

the Hartree-Fock Koopmans' theorem, due to the use of the frozen orbital approximation. Similar to the first-order correction for DFT methods, the correction can be expressed as

$$I_{\mathrm{m,corr}}^{(1)} = \int d\mathbf{r} \left[\hat{V}_{\mathrm{HX}}[\rho^{(N)} - \rho_m] - \hat{V}_{\mathrm{HX}}[\rho^{(N)}] \right] \rho'(\mathbf{r}) \tag{6.3.56}$$

where $\rho'(\mathbf{r})$ is defined with respect to a v' by Eq. (6.3.53). However, unlike when applied to a DFT method, v' is no longer a local potential and is instead a non-local operator determined by

$$v' |\phi_i^{(N)}\rangle = \left[\hat{V}_{\mathrm{HX}}[\rho^{(N-1,m)}] - \hat{V}_{\mathrm{HX}}[\rho^{(N)}] \right] |\phi_i^{(N)}\rangle \tag{6.3.57}$$

where $\rho^{(N-1,m)}$ is itself a function of v' through Eq. (6.3.53) and must be solved self-consistently. Calculation of the first-order correction allows relaxation effects to be included in Hartree-Fock results. As the Hartree-Fock ionisation energy is a result of the cancellation of errors due to correlation and relaxation this correction could result in less accurate results.

6.4 Results

6.4.1 Basis Set Convergence

Table 6.2 demonstrates the convergence of the correction term for the ionisation energy and electron affinity with increasing basis set size. The correction for the ionisation energy appears to be well converged for a pVTZ basis set, while the correction for the EA requires a larger basis for results to sufficiently converge. This is to be expected as the EA will depend on the representation of the diffuse LUMO, and will require a larger basis set to more accurately describe this unoccupied orbital.

6.4.2 The Importance of the First-Order Correction

Table 6.3 shows the effects of the zero- and first-order correction on the accuracy of the calculated IE and EA, demonstrating an immediate improvement when applying the zero-order correction. However, the zero-order correction tends to over

Table 6.2: The convergence of the IE and EA with increasing basis set size when calculated with the Δ_{scf} method. All energies in eV.

	IE		EA	
BASIS	ClF	LiH	ClF	LiH
pVDZ	12.56	8.15	-0.31	0.20
pVTZ	12.68	8.14	0.38	0.27
pVQZ	12.7	8.15	0.66	0.32
pV5Z	12.72	8.15	0.83	0.35
aug-pVDZ	12.74	8.16	0.97	0.42
aug-pVTZ	12.72	8.14	0.99	0.42
aug-pVQZ	12.73	8.15	1.01	0.42

correct the eigenvalue while the first-order correction is a negative correction that corrects the ionisation energy towards the Δ_{scf} eigenvalue. For EAs LDA typically overestimates the size of the electron affinity and the zero-order correction provides a negative correction. However, for many of these molecules the zero-order correction is too large and incorrectly predicts many of the molecules as having an unbound LUMO. The first-order correction is important in balancing out this over-correction. The zero-order correction provides a simple correction to both the ionisation energy and electron affinity, but it is greatly improved by the addition of the first-order correction. The correction that is the combination of the zero- and first-order terms will continue to be investigated here.

6.4.3   Ionisation Energy Correction

Ionisation energies are known to be poorly represented by the HOMO energy in the "DFT Koopmans' theorem", with typical errors of 4 eV seen for the LDA functional. While more complex GGAs and hybrid functionals succeed in reducing the error when calculating total energies there is little improvement in the HOMO error with these more advanced functionals.

Table 6.4 compares the error in IEs calculated via LDA, LDA+correction and the

Table 6.3: The average error(AE) and absolute average error (AAE) in the calcula-
tion of the ionisation energy or electron affinity with no correction(LDA), the zero
order correction or both the zero and first order correction. These were calculated
with an aug-pVTZ basis set for the list of molecules in Table 6.4. All energies in
eV.

	IE			EA		
	LDA	ZO	ZO+FO	LDA	ZO	ZO+FO
AE	-3.89	2.35	-0.86	2.37	-1.74	0.33
AAE	3.89	2.35	1.01	2.37	1.74	0.54

Δ_{scf} method. There is clear improvement in the absolute average error from ~ 4 eV
to ~ 1 eV, a similar level of accuracy as that of Hartree-Fock and approaching the
accuracy achieved through a Δ_{scf} calculation. On average the correction reduces the
difference between the HOMO energy and the Δ_{scf} IE by 75%.

6.4.4   Corrected Electron Affinities

Table 6.5 shows how the correction improves the LDA predicted electron affinities
from the LUMO energy level. The correction improves the LUMO energy prediction
of LDA significantly, with the corrected LDA having a smaller error than Hartree-
Fock. This improvement of the LUMO energy brings the error in these calculations
in line with results from a Δ_{scf} calculation. For the LUMO energies the correction
accounts for 82% of the energy difference between the LDA LUMO and the Δ_{scf} EA.
When compared to experimental results the corrected energies are improved over
the Δ_{scf} result. This can be attributed to a general overestimation of the electron
affinity by the Δ_{scf} method and the correction to first order being an underestimation
of the full correction.

6.4.5   Corrected Fundamental Gaps

Having accurate energies for of both the ionisation energy and electron affinities
allows fundamental gaps to be calculated. The fundamental gap is defined as the

Table 6.4: The errors in calculating the ionisation energy from the HOMO energies of LDA, LDA with the ionisation correction, Hartree Fock and ionisation energies from the Δ_{scf} method. Calculated with an aug-pVTZ basis set. Experimental results from Ref. [1]. All energies in eV.

MOL	EXP	LDA	Corr LDA	Δ_{scf}	HF
Acetylene	11.40	-4.12	-0.82	0.27	-0.33
Ammonia	10.07	-4.07	-0.60	1.10	1.57
Carbon dioxide	13.78	-4.56	-0.94	0.19	0.96
Carbon monosulfide	11.33	-3.90	-1.07	0.18	1.20
Carbon monoxide	14.01	-4.91	-0.79	0.10	1.13
Cl2	11.48	-4.05	-0.74	-0.07	0.66
ClF	10.90	-2.95	0.91	1.78	2.59
Dilithium	5.11	-1.89	-0.20	0.16	-0.22
Disilane	9.74	-2.37	0.01	0.77	1.32
Disodium	4.89	-1.69	0.12	0.33	-0.40
Ethane	11.52	-3.41	-0.35	0.38	1.70
Ethylene	10.51	-3.61	-0.65	0.46	-0.27
F2 molecule	15.70	-6.22	-1.62	-0.06	2.44
Formaldehyde	10.89	-4.65	-1.81	0.03	1.18
HOCl	11.12	-4.46	-1.14	-0.02	1.00
Hydrazine	8.10	-2.45	0.54	1.83	3.00
Hydrogen chloride	12.74	-4.68	-0.81	0.22	0.20
Hydrogen cyanide	13.60	-4.52	-0.85	0.61	-0.30
Hydrogen fluoride	16.03	-6.70	-2.10	0.53	1.45
Hydrogen peroxide	10.58	-4.37	-0.83	0.70	2.50
Hydrogen sulfide	10.46	-4.13	-0.69	0.16	0.00
Lithium fluoride	11.30	-5.04	-2.82	1.00	1.58
Lithium hydride	7.90	-3.54	-0.58	0.24	0.23
Methane	12.61	-3.16	0.19	1.46	2.21
Methanethiol	9.44	-3.80	-0.95	0.05	0.26
Methanol	10.84	-4.65	-2.26	-0.03	1.38
Methyl chloride	11.26	-4.15	-1.20	0.00	0.57
N2 molecule	15.58	-5.29	-1.06	-0.03	0.73
P2	10.53	-3.36	-0.49	0.29	-0.60
Phosphine	9.87	-3.23	0.06	0.69	0.59
Silane	11.00	-2.47	0.84	1.18	2.23
Silicon monoxide	11.49	-3.96	-1.14	0.01	0.38
Singlet methylene	10.40	-4.52	-0.77	0.22	0.35
Singlet silylene	8.92	-3.08	0.20	0.54	0.27
Sodium chloride	9.20	-3.90	-1.56	0.35	0.32
Water	12.62	-5.66	-1.88	0.37	1.11
		LDA	Corr LDA	Δ_{scf}	HF
AE		-3.99	-0.77	0.44	0.92
AAE		3.99	0.93	0.46	1.03

Table 6.5: The errors in calculating the electron affinity from the LUMO energies of LDA, LDA with the ionisation correction, Hartree Fock and ionisation energies from the Δ_{scf} method. Calculated with an aug-pVTZ basis set. Experimental results from Ref. [1]. All energies in eV.

MOL	EXP	LDA	LDA+corr	Delta E	HF
Carbon monosulfide	0.205	3.40	0.79	-1.12	-1.45
Cl2	2.50	2.15	-0.49	-1.32	-3.01
ClF	2.86	2.12	-0.74	-1.87	-3.67
Dilithium	0.437	1.41	0.08	0.03	-0.50
F2 molecule	3.005	3.33	0.00	-2.05	-4.62
Lithium Fluoride	0.371	1.00	0.26	0.06	-0.09
Lithium hydride	0.342	1.22	0.21	0.07	-0.13
P2	0.589	3.06	0.59	0.14	-0.87
Singlet methylene	0.652	4.73	2.16	0.88	-1.32
Singlet silylene	1.123	3.13	0.70	0.18	-1.04
Sodium Chloride	0.727	1.46	0.30	0.11	-0.16
		LDA	LDA+corr	Delta E	HF
	AE	2.46	0.35	-0.45	-1.53
	AAE	2.46	0.57	0.71	1.53

Table 6.6: The fundamental gap calculated via LDA, LDA with the ionisation correction, and through the Δ_{scf} method. Calculated with an aug-pVTZ basis set. Experimental results from the supplementary data in Ref. [2]. All energies in eV.

MOL	EXP	LDA	correction	Δ_{scf}	HF
Carbon monosulfide	11.13	-7.24	-1.97	1.30	2.68
Cl2	8.98	-6.15	-0.35	1.26	3.68
ClF	8.04	-4.95	1.52	3.70	6.3
Dilithium	4.67	-3.31	-0.29	0.14	0.28
F2 molecule	12.7	-9.36	-1.94	2.02	7.11
Lithium Fluoride	10.93	-5.95	-3.15	0.96	1.74
Lithium hydride	7.56	-4.75	-0.77	0.17	0.37
P2	9.94	-6.41	-1.19	0.14	0.31
Singlet methylene	9.75	-9.13	-3.03	-0.63	1.71
Singlet silylene	7.80	-6.20	-0.59	0.35	1.32
Sodium Chloride	8.47	-5.29	-1.92	0.26	0.53
GAP	LDA	LDA+corr	Δ_{scf}	HF
AE	-6.25	-1.24	0.88	2.37
AAE	6.25	1.52	0.99	2.37

energy difference between the HOMO and LUMO energies and is important in the prediction of optical properties of molecules. Table 6.6 demonstrates that the fundamental gaps calculated from LDA with the correction are greatly improved over LDA with no correction. These corrected gap energies also compare favourably with gaps calculated through Δ_{scf} calculations of the $N-1$, N, and $N+1$ electron systems, and are also improved over gaps calculated with the Hartree-Fock method. In general the correction overestimates the electron affinity and underestimates the ionisation energy, and results in an overall underestimation of the fundamental gap.

6.4.6   Corrected Ionisation Energies for All Orbitals

Tables 6.7 and 6.8 demonstrate the effect of the correction when applied to orbitals lower than the HOMO. Table 6.7 shows improvements in the core electron ionisation energies compared to uncorrected LDA and Hartree-Fock. Ionisation of these core electrons will have large relaxation effects due to the high energies of the core electrons and this can be observed in the large size of the first-order correction. This implies that higher orders of the correction may be important for these orbitals. Table 6.8 has ionisation energies of the full set of orbitals in several molecules. The correction reduces the percentage error on all these orbitals, and the full correction brings the average error to the level of Hartree-Fock across a range of orbitals.

6.4.7   Application to Hartree-Fock

The correction was also applied to the Hartree-Fock method where the zero order correction is exactly zero. Therefore, the first-order term is the smallest component of the relaxation correction. This term incorporates relaxation effects that are neglected in the Hartree-Fock Koopmans' theorem. Table 6.7 shows that for core electron orbitals the correction significantly improves the Hartree-Fock results. This can be attributed to the large relaxation effects present when ionising a core electron. However, for orbitals where relaxation is less significant the correction can worsen the results, as seen in Table 6.8. This is due to the Hartree-Fock method neglecting correlation effects. The poor total energies lead to a correspondingly poor Δ_{scf} result for Hartree-Fock, as the correction tends towards the Δ_{scf} result. Koopmans' theory results, are typically accurate due to an error cancelation in Hartree-Fock between relaxation and correlation. Therefore correcting only the relaxation effects here reduces the accuracy of the result.

6.4.8   Use of the Correction as a Measure of Functional Performance

The exact DFT functional is known to have an exact relationship between the ionisation energy and the HOMO eigenvalue. Therefore, the exact functional has a

Table 6.7: The error calculating the core electron ionisation energies for LDA, and HF with various levels of correction applied. experimental results from Ref. [1]. All energies in eV.

MOL	EXP	LDA			HF	
		LDA	ZO	ZO+FO	HF	FO
HF	694	-38.93	26	-18.01	21.32	-11.9
HCN(1)	406.15	-27.99	21.71	-11.91	18.51	-6.33
HCN(2)	295.89	-27.88	14.22	-11.05	11.58	-6.31
CO(1)	542.51	-33.08	24.23	-15.5	19.85	-10.31
CO(2)	296.2	-26.45	15.66	-7.90	13.18	-2.74
N_2	409.9	-29.64	-1.42	-17.24	17.16	6.03
C_2H_2	291.14	-24.47	-0.3	-15.01	14.89	4.73
NH_3	405.6	-29.25	20.45	-13.14	17.16	-7.16
H_2O	539.7	-33.66	23.64	-15.68	19.7	-9.57
$H_2CO(1)$	539.42	-32.42	24.88	-16.27	20.47	-10.52
$H_2CO(2)$	294.47	-25.54	16.57	-8.93	14.2	-3.43
CH_4	290.83	-25.24	16.86	-10.01	14.12	-4.57
C_2H_4	290.7	-24.42	-0.51	-15.52	14.91	4.49
	AE	-29.15	15.54	-13.55	16.7	-4.43
	AAE	29.15	15.88	13.55	16.7	6.78

Table 6.8: The percentage error of the predicted ionisation energy for every orbital calculated via LDA and Hartree-Fock with various levels of the correction applied. Calculated with an pVTZ basis set. Experimental results from Ref [2]. All energies in eV.

MOL	Expt	LDA	ZO	ZO+FO	HF	FO
			LDA		HF	
N$_2$	15.58	-34.0%	10.9%	-6.8%	4.7%	-7.3%
	16.93	-31.7%	11.9%	-5.9%	1.3%	-9.1%
	18.75	-27.5%	8.6%	-4.8%	14.5%	7.5%
	37.3	-25.7%	2.2%	-12.6%	5.6%	-4.2%
	409.98	-7.3%	-0.4%	-4.2%	4.1%	1.4%
	409.98	-7.3%	-0.4%	-4.2%	4.2%	1.5%
CO	14.01	-35%	15.9%	-5.6%	8.0%	-4.0%
	16.91	-29.8%	18.8%	-7.1%	1.3%	-15.3%
	19.72	-28.3%	17.5%	-7.2%	10.7%	-7.1%
	38.3	-24.5%	3.4%	-13.8%	7.0%	-4.2%
	296.21	-8.9%	5.3%	-2.7%	4.4%	-0.9%
	542.55	-6.1%	4.5%	-2.9%	3.7%	-1.9%
HF	16.19	-42.4%	26.4%	-14.2%	8.0%	-18.3%
	19.9	-34.2%	17.1%	-8.4%	3.2%	-12.1%
	39.6	-25.9%	3.0%	-14.1%	9.2%	-1.7%
	694.23	-5.6%	3.7%	-2.6%	3.0%	-1.7%
H$_2$O	12.62	-44.8%	29.4%	-14.9%	8.8%	-19.6%
	14.74	-38.7%	23.6%	-11.6%	6.6%	-14.5%
	18.55	-30.7%	14.8%	-6.0%	3.2%	-9.8%
	32.2	-23.1%	7.5%	-10.8%	13.3%	2.2%
	539.9	-6.3%	4.3%	-2.9%	3.6%	-1.8%
AE(%)		-24.6%	10.8%	-7.8%	6.1%	-5.8%
AAE(%)		24.6%	10.9%	7.8%	6.1%	7.0%

total ionisation energy correction of zero. How close the functional is to the exact DFT functional can be judged by the scale of the correction. The results for the Hartree-Fock method, which has no zero order correction, demonstrate that in functionals where exchange is treated exactly the correction is reduced to first order and beyond, resulting in a smaller correction overall.

It is known that self-interaction effects are a major cause of the disagreement between the Δ_{scf} method and the orbital eigenvalues. The constrained DFA method from Chapter 4 uses a constrained KS potential to correct for self interaction effects and compared to the 4 eV error of the LDA HOMO energy, constrained LDA (CLDA) has an error of ~ 2 eV. Applying the Zero-order correction in this method, as can be seen from Table 6.9, the average size of the zero-order correction is reduced from 7.84 eV to 3.66 eV. This demonstrates that accounting for self-interaction effects reduces the size of the zero order term. It should be noted that when corrected to zero-order the results for both LDA and CLDA are the same to within 0.1 eV. This similarity is expected as the CLDA total energies are nearly identical to those from LDA. Therefore the ionisation energy calculated from a Δ_{scf} calculation are expected be the same for both LDA and CLDA as the corrections are correcting towards the same Δ_{scf} ionisation energy.

6.4.9 Series Approximation

When applying the correction, despite a significant improvement compared to experiment, the corrected results still do not approximate well the Δ_{scf} result. Higher order terms are available by continuing the expansion of the total energy with respect to the Kohn-Sham potential of the N electron system, giving a second order term as

$$I_{\mathrm{m,corr}}^{(2)} = \int d\mathbf{r} d\mathbf{r}' \frac{\delta^2 E[\rho - \rho_m]}{\delta V_{\mathrm{KS}}(\mathbf{r}) \delta V_{\mathrm{KS}}(\mathbf{r}')} v'(\mathbf{r}) v'(\mathbf{r}'). \tag{6.4.58}$$

These higher order terms would provide a more accurate correction, but are increasingly more difficult to calculate. An approximation to the full infinite series can be made by following the observation that the zero and first order corrections are both relatively large in magnitude with opposite signs. This results in these two

Table 6.9: The size of the zero order correction for LDA and the self-interaction corrected constrained LDA (CLDA), along with the average size of the correction for LDA and CLDA. Experimental results from Ref [1]. All energies in eV.

MOL	EXP	LDA	CLDA	ZO-LDA	ZO-CLDA
H_2	15.42	10.3	15.52	7.83	2.60
He	24.6	15.47	23.13	12.05	4.38
Be	9.32	5.6	8.53	4.19	1.25
Ne	21.6	13.17	18.89	13.12	7.40
H_2O	12.8	6.96	11.3	9.37	5.03
NH_3	10.8	5.99	9.82	7.92	4.09
CH_4	14.4	9.46	12.8	6.63	3.32
C_2H_2	11.5	7.28	10.53	6.06	2.80
CO	14.1	9.1	12.74	7.13	3.49
C_2H_4	10.7	6.9	9.83	5.72	2.78
NaCl	8.93	5.3	8.42	6.26	3.14
			Av. corr.	7.84	3.66

terms mostly canceling out leading to a small overall correction. One expectation of the higher order corrections is that they continue to alternate in sign with decreasing magnitude, mirroring the observed behaviour of the zero- and first-order corrections. This would imply a slow convergence of the correction as the results oscillate around the Δ_{scf} value. A way to obtain an estimate to the full correcting value is to approximate the higher order terms in the sequence as a geometric series with a constant ratio between consecutive terms

$$R = \frac{I_{\text{corr}}^{(n)}}{I_{\text{corr}}^{(n+1)}} \tag{6.4.59}$$

where $|R| < 1$ in order to achieve convergence in the infinite sum, and for an oscillating sequence $R < 0$. Under this approximation the infinite sum of correcting terms can be evaluated as

$$I_{\text{corr}} = \frac{I_{\text{corr}}^{(0)}}{1 + |R|}. \tag{6.4.60}$$

This allows a rough approximation to be made to the full correction using only the zero and first order terms to determine the ratio R. Table 6.10 compares the difference from the Δ_{scf} and experimental results for the ZO, FO and series correction. The series correction can be seen to improve the results in all cases across a range of considered orbitals. There is a clear improvement performing this additional approximation that gives results which are close to those from a Δ_{scf} calculation. This correction however is not based in an analytic property of the series expansion, but is merely an estimation of the higher order behaviour of the system. Therefore, care should be taken when applying this method and careful comparison with the zero- and first-order corrections should be made. The success of this series approximation for the LDA method suggest that this oscillatory behaviour would be observed for the higher order terms in the correction for the LDA functional. This approximation is also not immediately available for all methods as it relies on the zero-order term being larger than the first order term. In the CLDA method the zero order term is smaller than the first order term, and in Hartree-Fock there is no zero-order correction. A series approximation may exists for these methods but would require the second order term in the correction to be calculated.

Table 6.10: The difference of Δ_{scf} or experimental results with the LDA method with various levels of correction applied for HOMO, LUMO orbitals and all occupied orbitals and core orbitals for the same set of molecules analysed in table 6.7. All energies in eV.

Difference from Δ_{scf}(eV)					
HOMO	N	LDA	+ZO	+ZO+FO	+Series corr
AE	36	-4.40	1.93	-1.39	-0.22
AAE	36	4.40	1.93	1.39	0.24
LUMO	N	LDA	+ZO	+ZO+FO	+Series corr
AE	11	2.90	-1.42	0.80	0.03
AAE	11	2.90	1.42	0.80	0.18
Difference from experiment(eV)					
All orbs	N	LDA	+ZO	+ZO+FO	+Series corr
AE	21	-13.85	5.88	-6.02	-1.50
AAE	21	13.85	6.17	6.02	1.76
Core orbs	N	LDA	+ZO	+ZO+FO	+Series corr
AE	14	-29.79	14.25	-14.97	-3.27
AAE	14	29.79	14.93	14.97	4.10

6.5 Conclusions

This correction offers a simple, post-scf, method to correct ionisation energies predicted from the HOMO energy towards the ionisation energy. We have also seen that it provides a way to approximate ionisation energies for all electron orbitals from a single calculation to a level of accuracy approaching that of the Δ_{scf} method. The accuracy of this method can be improved either by finding the higher order corrections to the ionisation energy, or in an approximate manner making use of the series approximation to estimate the total value of the correction.

This method can also be used as a test for the closeness of a functional to the exact DFT functional, as in the exact DFT description the ionisation energy is given exactly by the negative of the HOMO energy and it follows that for the exact functional the correction is zero. A smaller correction would indicate a better functional, and in the case of Hartree-Fock the zero order correction is zero. The results of these calculations depend on the accuracy of the total energy calculations and the accuracy of the orbital energies to ionisation energies. The results shown here are all obtained for the LDA functional and using a more accurate energy functional will provide further improvements due to the increased accuracy of the Δ_{scf} method.

6.6 Summary

In thischapter a correction for the Kohn-Sham eigenvalues has been derived to first order and shown to offer significant improvements for DFT functionals when calculating the ionisation energy of all electron orbitals in a system. This correction is applied post-scf and allows a method to approximate ionisation energies through a single DFT calculation as opposed to two separate calculations for a Δ_{scf} calculation. These results are as yet unpublished and will be submitted for publication soon.

Chapter 7

Spin-DFT and the Implicit-DFA Method

7.1 Introduction

In thischapter it is demonstrated that SDFT can result in insulating ground state behaviour for unit cells containing an odd number of electrons, contrary to what is predicted from conventional band theory. An original restricted DFT method is also demonstrated that uses the OEP method and SDFT energy functionals to perform calculations on spin polarised systems with a common Kohn-Sham potential for both spin channels. This restricted case is also shown to produce insulating ground states for systems with an odd number of electrons per unit cell.

7.2 Unit Cells Containing an Odd Number of Electrons

DFT methods are known to well represent a wide variety of behaviours in solids. However, one situation where their typical application fails is the prediction of insulating behaviour in systems where there is an odd number of electrons in the primitive unit cell. Conventional band theory suggests [164] that in its ground state, a periodic system has doubly degenerate bands, and every band is equally

occupied in both the spin-up and spin-down channels. This assumption of a doubly degenerate ground state is often wrongly assumed to also hold for systems modelled using SDFT. In such a system as every band is equally occupied by spin-up and spin-down electrons, the system will have zero spin polarisation. In a spin unpolarised system with an odd number of electrons per unit cell, the highest occupied band will necessarily be fractionally occupied in both spin channels. This fractional occupation describes a system that is metallic and implies that any system with an odd number of electrons in its primitive unit cell will be metallic. While this conducting behaviour can be widely demonstrated, it does not hold for all systems. A well known contradiction can be found in the expected behaviour of a system in which interatomic bonds are stretched until the constituent atoms disassociate. The behaviour of such a stretched system would tend to that of isolated atoms, and electrons would localise on each atom. This localisation is indicative of an insulating system. This insulating behaviour is obtainable not only in the limit of disassociation, but can also occur at equilibrium as is the case for Mott insulators [165, 166]. These are materials predicted to be metallic by conventional band theory but are found to be insulating.

It is possible to describe the insulating behaviour in general by doubling the unit cell, e.g. treating the system as having an "electronic unit cell" that is a supercell of two primitive unit cells. In this case the electronic unit cell contains an even number of electrons and insulating behaviour is allowed by conventional band theory. This kind of insulating behaviour (by doubling the unit cell) is typically introduced through an antiferromagnetic ground state, or by a Peierls distortion of a 1-D lattice [167]. However, it would be expected, particularly in the case of a crystal disassociating into its component atoms, that insulating behaviour should be a property obtainable for a single unit cell containing an odd number of electrons. It will be shown that such insulating behaviour can be obtained, for both SDFT and a novel restricted Kohn-Sham method. This is achieved by considering magnetic states as opposed to only doubly degenerate bands. Magnetic states can be found by increasing the occupancy of one spin channel and reducing the occupancy of the opposite spin.

If, by such manipulation, bands in both spin channels are either completely empty, or filled, then insulating behaviour would be obtained. It will be shown that such states exist and can be found as ground states for systems with an odd number of electrons per unit cell. This allows the expected insulating behaviour of these systems to be observed.

7.3 Results

Solids are expected to become insulating as their interatomic bonds are stretched and the crystal disassociates into individual atoms. At short interatomic distances individual electrons will delocalise resulting in the metallic behaviour predicted by conventional band theory. As interatomic bonds are stretched a system will undergo a transition from metallic to insulating. As has been discussed, such a transition cannot occur in a spin-unpolarised system due to the presence of partially filled bands, so spin polarised systems must be considered. SDFT calculations can be performed for a fixed spin-state and finding the lowest energy spin-state for a particular system will allow the ground state to be determined. The magnetic state corresponding to the ground state is expected to change as the system transitions from metallic to insulating, and this allows for a change in behaviour. Once this ground state has been found, an analysis of the band structures of the ground state will determine whether a metal-insulator transition occurs and the behaviour of the system at this transition.

These magnetic states will be defined by their net spin per unit cell, $N_s = N^\uparrow - N^\downarrow$, which is proportional to the magnetisation of the system along the z-axis. $N_{\uparrow,\downarrow}$ may adopt any number from 0 to N, the number of electrons per unit cell. A net spin of $N_s = 0$ implies $N_\uparrow = N_\downarrow = \frac{1}{2}N$ and is the non-magnetic state which is predicted by conventional band theory. A net spin of $N_s = \pm N$ is a ferromagnetic state where all electrons are either entirely spin-up, or spin-down. As N_s is symmetric about 0 only spin states in the range $0 \leq N_s \leq N$ will be considered in the investigations undertaken in thischapter.

7.3.1 Hydrogen

The simplest system with an odd number of electrons per unit cell is a hydrogen crystal with a single hydrogen atom and one electron per primitive unit cell. This hydrogen crystal can be constructed as a 1-D chain, and 2-D plane or a 3-D primitive cubic crystal. It is expected that all these systems are metallic at short interatomic distances and will experience a metal-insulator transition as interatomic distances increase [166]. Conventional band theory predicts that such systems remain metallic for all interatomic separations. In order to find such behaviour using SDFT several magnetic states of these hydrogen systems will be investigated. For this investigation into hydrogen atoms, calculations were performed using the CASTEP solid state code with a 1500 eV cutoff energy, and 15 k-points were used to sample the Brillouin zone in each dimension. Fig. 7.1 shows the energetic behaviour of these different magnetic states for the 1-D hydrogen chain. For the 1-D chain the ground state of the system changes suddenly from $N_s = 0$ to $N_s = 1$ with no intermediate magnetic state with a lower energy. The equivalent results for the 2-D and 3-D case are shown in Fig. 7.2 and Fig. 7.3. In these cases the change in ground state from $N_s = 0$ to $N_s = 1$ is not as sudden as for the 1-D case and involves a transition through intermediate spin states. One might expect that during this transition the ground state N_s will vary smoothly over the range $0 \leq N_s \leq 1$. However, closer inspection of the 3-D transition point to $N_s = 1$ in Fig. 7.3 (inset) shows that the system transitions gradually to $N_s \sim 0.8$ then discontinuously to $N_s = 1$ without taking any intermediate state, and a similar transition is observed for the 2-D case 7.2 (inset) reaching $N_s \sim 0.6$ before transitioning to the $N_s = 1$ state.

All these hydrogen systems therefore exhibit a discontinuous jump to the $N_s = 1$ ground state, whether from $N_s = 0$ for 1-D hydrogen or an intermediate value of N_s for 2 and 3-D systems. Once the magnetic behaviour of the ground state is known the insulating behaviour can be determined by analysing these states. Any spin state which is not $N_s = \pm 1$ must have a metallic band structure due to the presence of partially filled bands. In the $N_s = \pm 1$ state, however, it is possible to fully occupy a single band in one spin channel and obtain an insulating system. As seen in Fig. 7.4, at short interatomic separations the $N_s = 1$ state does not fully occupy a single

Figure 7.1: The total energies of various spin states of the 1-D hydrogen chain with a single atom per unit cell as the interatomic separation is increased. Inset shows a zoomed image around the transition point.

H-2D
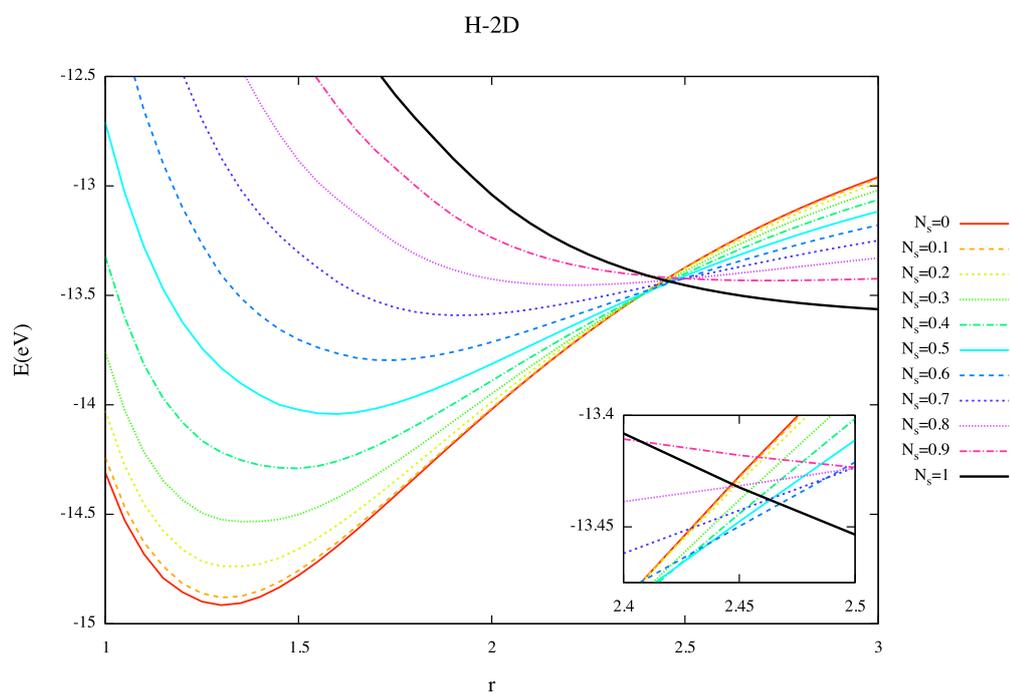
Figure 7.2: The total energies of various spin states of the 2-D hydrogen plane with a single atom per unit cell as the interatomic separation is increased. Inset shows a zoomed image around the transition point.
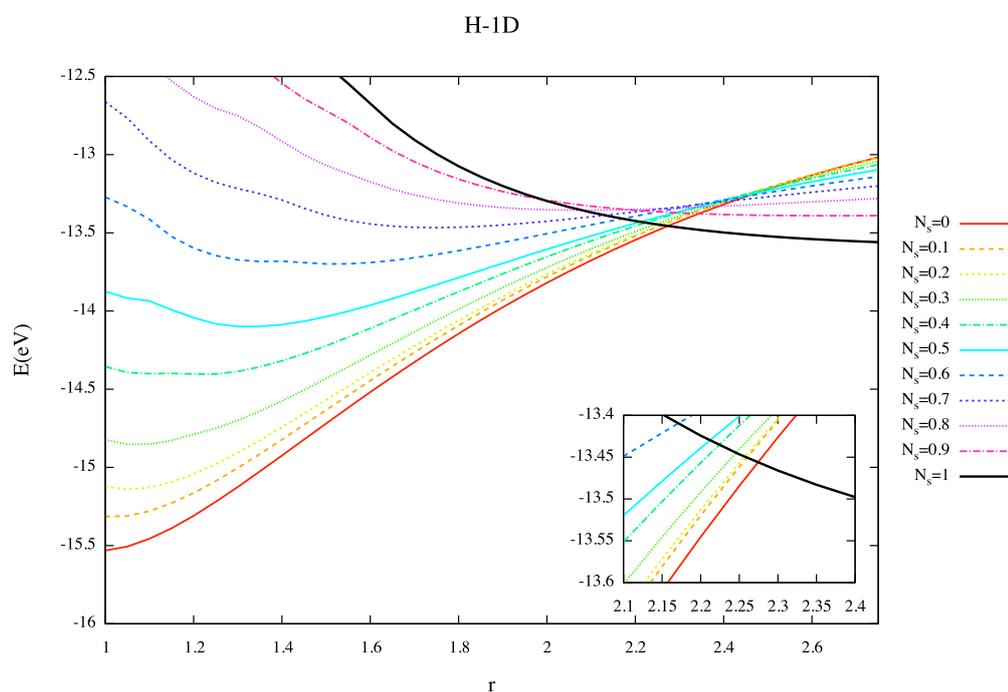
Figure 7.3: The total energies of various spin states of the 3-D simple cubic hydrogen lattice with a single atom per unit cell as the interatomic separation is increased. Inset shows a zoomed image around the transition point.

band and instead partially occupies the two lowest energy bands indicating metallic behaviour. For larger interatomic separation as seen in Fig. 7.5 a band gap opens between the lowest bands and only a single band is completely filled, resulting in an insulating state.
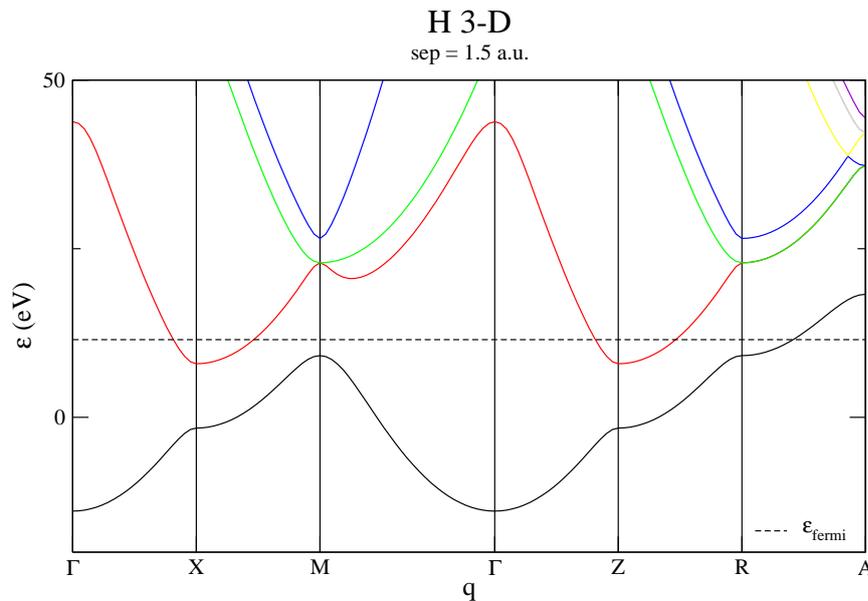
Figure 7.4: The metallic band structure of the ferromagnetic state of the one atom hydrogen unit cell in a 3D simple cubic lattice at a separation of 1.5 a.u..

The results shown in Figs. 7.4, 7.5 show that a metal-insulator transition occurs for the 3-D hydrogen system in the $N_s = 1$ state. Fig. 7.6 demonstrates that this transition occurs well before the ferromagnetic configuration becomes the lowest energy state. For 1-D and 2-D hydrogen a similar transition in the $N_s = 1$ is observed. This transition occurs well before the ferromagnetic state of the system becomes the ground state. Therefore, all these hydrogen systems experience a discontinuous transition from metallic to insulating when the $N_s = 1$ ferromagnetic state becomes energetically favourable. This result demonstrates that insulating behaviour is an allowed property of odd electron unit cells and does not require doubling of the unit cell and the effects of antiferromagnetism or Peierls distortions.

May, 2021
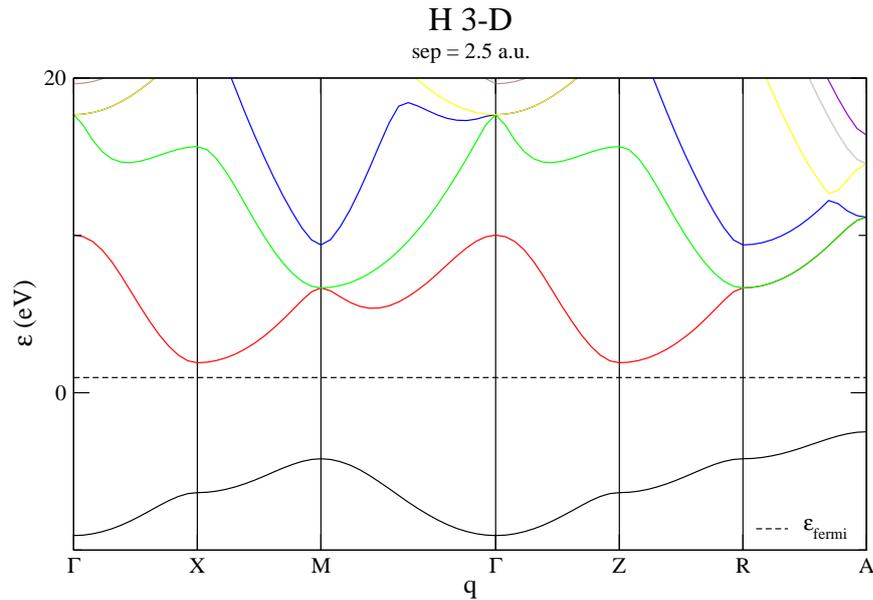
Figure 7.5: The insulating band structure of the ferromagnetic state of the one atom hydrogen unit cell in a 3D simple cubic lattice at a separation of 2.5 a.u..

7.3.2   Effective One-Electron Unit Cells

The pseudopotential treatment of core electrons in plane wave codes allows all group one elements to be treated as one-electron systems with a modified atomic potential that includes the effects of the core electrons. Therefore these effective one-electron systems will show similar behaviour to hydrogen when treated using a pseudopotential. For the investigation into periodic sodium systems, a cutoff energy of 1200 eV was used with the Brillouin zone sampled at 12 k-points in each dimension. As can be seen from Fig. 7.7 the general behaviour of sodium is the same as hydrogen with a transition from a spin-unpolarised ground state to a ferromagnetic ground state as the atomic separation is increased. Here the behaviour of the 3D system remains a sudden jump from $N_s = 0$ to $N_s = 1$ as is the case for the 1D hydrogen system. This indicates that the ferromagnetic $N_s = 1$ state is more favourable in sodium. The discontinuous change in spin state alone does not indicate a change in conducting behaviour. The analysis of the band structure of the system, as for hydrogen,
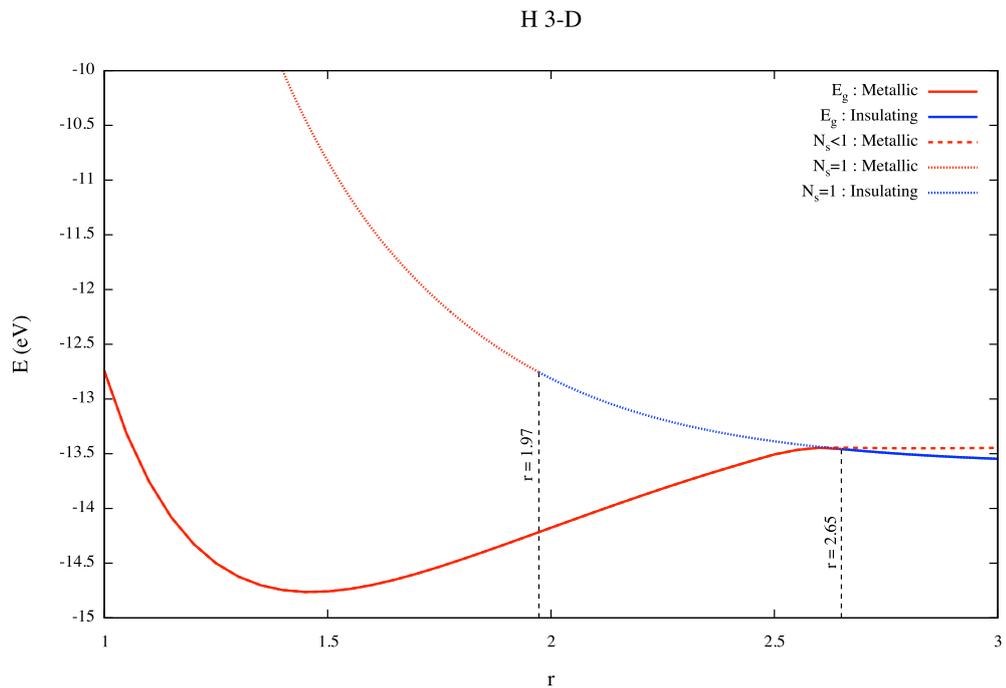
Figure 7.6: For the 3D simple cubic hydrogen crystal the total energy of: the ferromagnetic $N_s = 1$ state, the minimum energy state for $N_s < 1$ from Fig 7.3, and the lowest energy state E_g, plotted against interatomic separation r, showing the conducting vs insulating behaviour of these states.
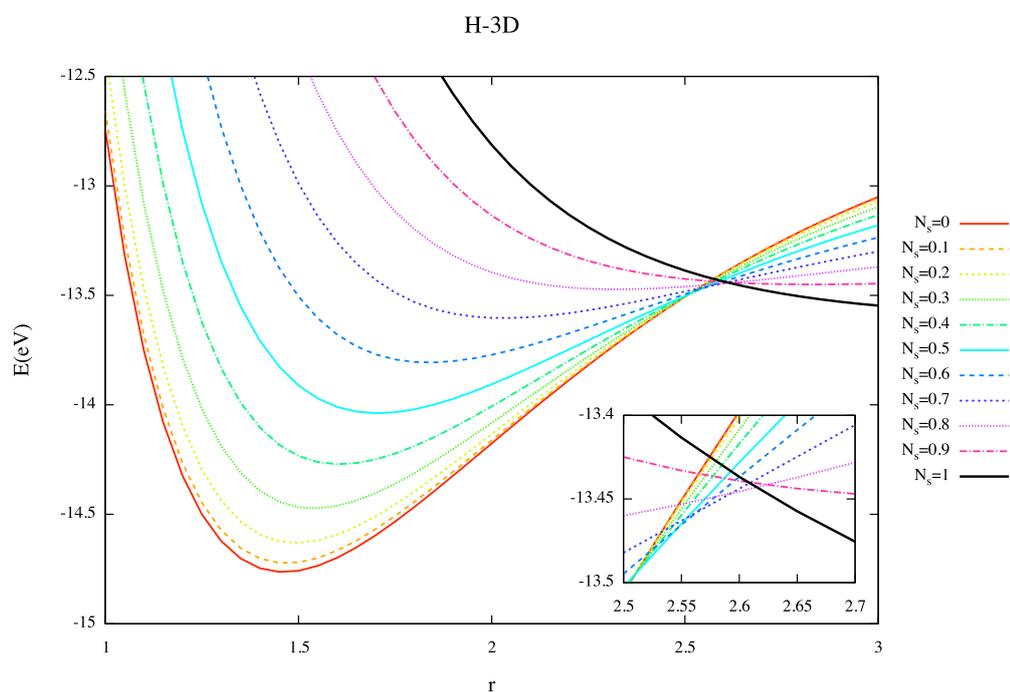
Figure 7.7: The total energies of various spin states of a 3-D simple cubic sodium crystal with a single atom per unit cell as the interatomic separation is increased. Inset shows a zoomed image around the transition point.

shows that the ferromagnetic state undergoes a metal insulator transition before this ferromagnetic state becomes energetically favourable. Therefore, the transition from metal to insulator can be shown for sodium through the use of SDFT, and this transition from metallic to insulating is a first order phase transition.

7.3.3 Single Atoms

While insulating behaviour has been shown in one-electron systems when including magnetic states, it is expected that the same mechanism will allow insulating states in multi-electron systems. Fig. 7.8 shows the behaviour of aluminium under the increasing interatomic separation. When using a pseudopotential representation aluminium has 3 electrons that are treated using SDFT. While the system has 3 electrons, Fig. 7.8 the most energetically favourable states are found for $0 \leq N_s \leq 1$ as the interatomic distance is increased. This is to be expected as the aluminium s-orbital will have a lowest energy configuration when doubly occupied, so the magnetic behaviour is effectively determined by a single unpaired electron. At short interatomic distances it is energetically favourable to delocalise this unpaired electron, and as such the $N_s = 0$ state is favourable which changes to the $N_s = 1$ state at larger interatomic separations. Unlike hydrogen and sodium, this transition is a continuous change in magnetic state with the ground state of aluminium smoothly changing from $N_s = 0$ to $N_s = 1$. This result demonstrates that this method can also be applied to multi-electron systems and that the predicted transition from metal to insulator can occur smoothly as interatomic separation is increased.

7.3.4 Comparison With Doubling the Unit Cell

Typically in order to obtain a metal-insulator transition using SDFT the unit cell would be doubled. This results in an even number of electrons in the unit cell and allows an insulator to be obtained under conventional band theory. Insulating states can be found for these doubled unit cells as the system transitions from a non-magnetic state at short separation to an antiferromagnetic state, where in both states $N_s = 0$. A comparison between the single and double unit cells energies can be
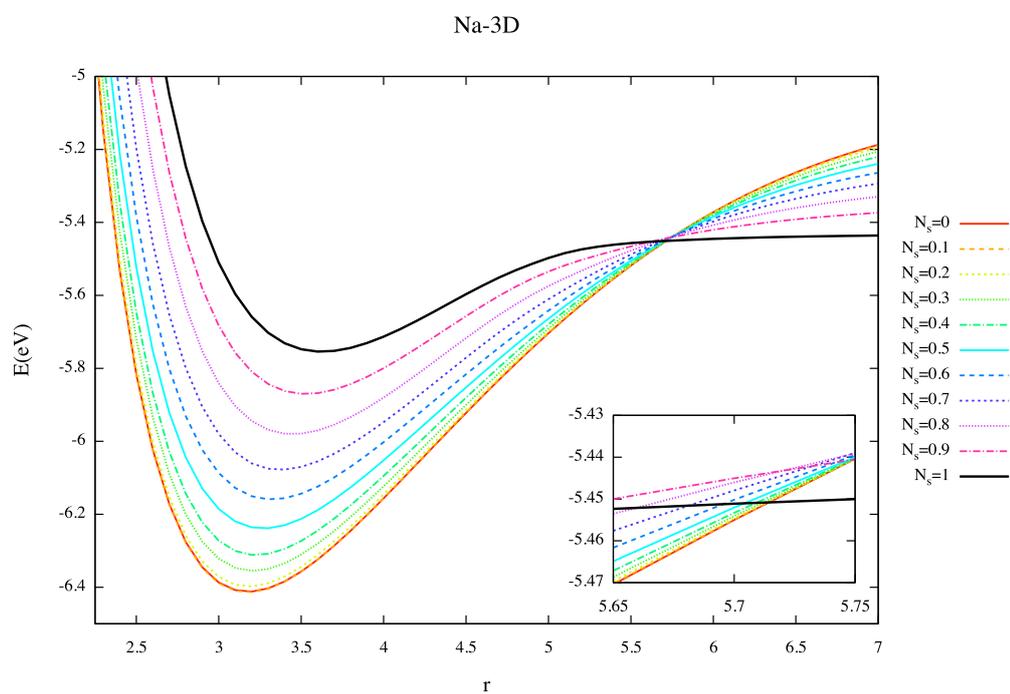
Al-3D
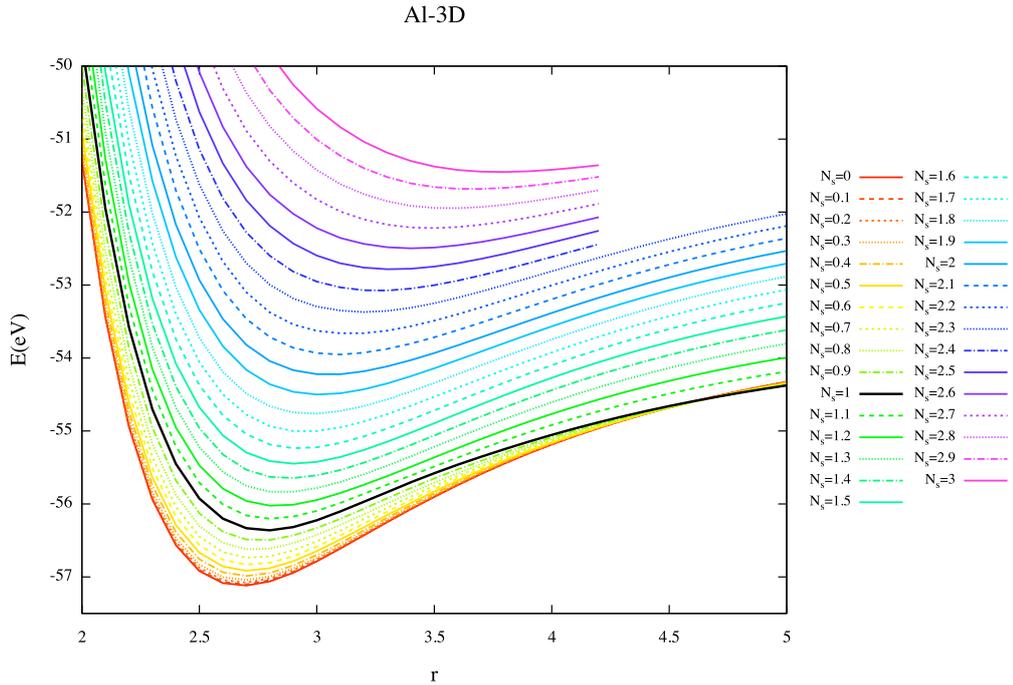
Figure 7.8: The total energies of various spin states of a 3-D BCC aluminium with a single atom per unit cell as the interatomic separation is increased.

seen in Fig. 7.9. At short interatomic separation the doubled unit cell result agrees with the single unit cell with $N_s = 0$ as the electrons are delocalised throughout the system and therefore there is no spin polarisation. At larger interatomic separation the antiferromagnetic state is lower in energy than the ferromagnetic result as seen in Fig. 7.9. However, as interatomic distances increase the strength of any interaction between adjacent atoms will decrease and the ferromagnetic energy will tend toward that of the antiferromagnetic state. At intermediate separations there is a deviation of the doubled unit cell energies from those of the single unit cell. This difference is due to an increase in degrees of freedom for the doubled unit cell, and the doubled unit cell is able to adopt lower energy configurations as electrons begin to localise on each hydrogen atom.

7.3.5 Conclusions

It has been demonstrated that insulating states for systems in unit cells with an odd number of electrons can be obtained by allowing magnetic states. These results have
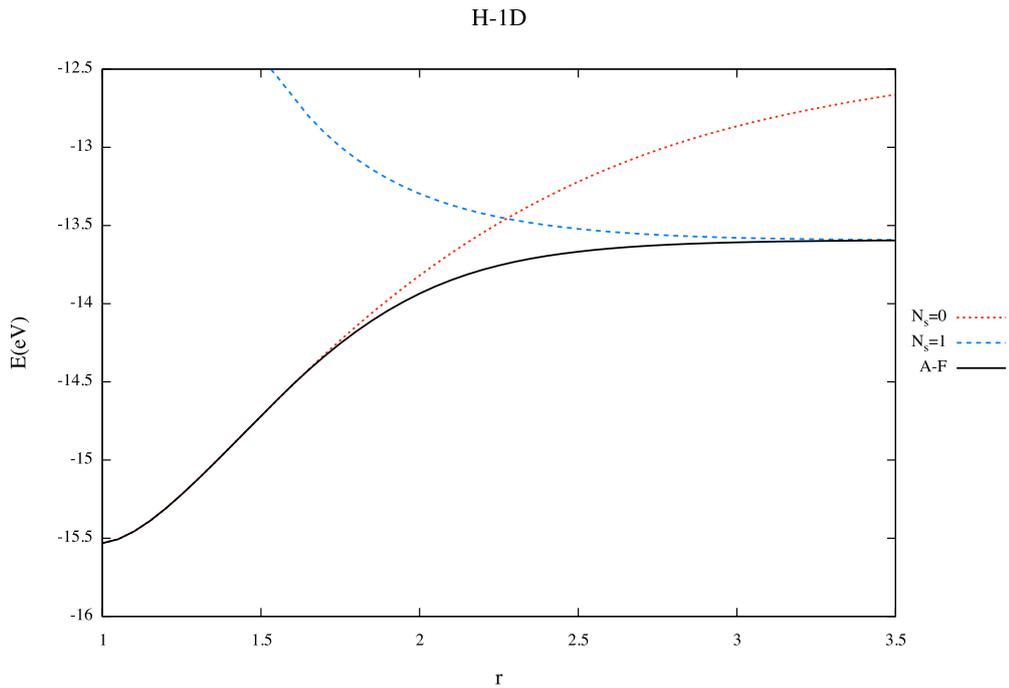
Figure 7.9: Total energy per atom for the $N_s = 1$ and $N_s = 0$ states for the one atom unit cell and the antiferromagnetic (A-F) $N_s = 0$ two atom unit cell result.

been demonstrated for several atomic systems where such a transition occurs with increasing interatomic separation. At short interatomic separation the energetically favourable state is the same $N_s = 0$ state as predicted by conventional band theory and SDFT calculations for a doubled unit cell. For larger interatomic separation a metal-insulator transition is found when a ferromagnetic state becomes the minimum energy configuration. This transition from non-magnetic to ferromagnetic is responsible for a transition in the conducting state of the system from metallic to insulating. This transition is found to be discontinuous in some systems (H,Na) and continuous in others (Al). This demonstrates that the metal-insulator transition is allowed in unit cells containing an odd number of electrons and does not necessarily require a doubling of the unit cell to obtain.

7.4   The Implicit-DFA Method

Despite the simplicity of SDFT, for systems without an external magnetic field it should be possible, in principle, to do perform DFT calculations with a single common Kohn-Sham potential. The lack of a single common potential in SDFT introduces a non-orthogonality between the electron orbitals of opposing spin. This results in spin contamination [168], where the ground state is not an eigenstate of the total angular momentum operator $\langle \hat{S}^2 \rangle$. A symptom of this spin contamination is that the total angular momentum of the system is not equal to $S(S + 1)$ the expected quantum mechanical result. For SDFT methods the spin contamination is typically a relatively small effect [169–171]. Nevertheless, spin contamination in SDFT methods is generally seen as a source of error and a large deviation of the total angular momentum from $S(S + 1)$ can indicate an erroneous result. Using a single common potential in each spin channel would automatically result in all electron orbitals being orthogonal, preventing spin contamination in most cases.

Non-spin polarised DFT methods use a common potential for all electron orbitals, but in general are not applied to spin-dependent system. This is due to the difficulty of developing accurate energy functionals that correctly reflect the magnetic behaviour of the system. SDFT methods use energy functionals which are dependent on the spin densities ρ^σ where each spin density is treated as an independent function. This gives a greater freedom when constructing energy functionals allowing accurate approximations to be easily developed. In these approximations the total energy must be minimised for each spin density separately resulting in separate Kohn-Sham potentials. In the absence of an external magnetic field the spin densities may be regarded as being dependent on the total electron density, i.e. implicit functionals of ρ. In this way the exchange energy from SDFT that is dependent on the spin densities $\rho^\uparrow$, $\rho^\downarrow$ becomes an implicit functional of the density and the whole scheme becomes a DFT method, as opposed to SDFT. In order to combine spin-dependent energy functionals with a common Kohn-Sham potential the OEP method is used. This allows a minimisation with respect to the implicit dependence of the exchange-correlation energy functionals on the total density. The application

of the OEP method to a SDFT energy functional will henceforth be referred to as the implicit-DFA method.

7.4.1 Derivation

The implicit-DFA method uses a spin-dependent energy functional taken from SDFT methods

$$E[\rho] = T_{\mathrm{s}}[\rho] + E_{\mathrm{en}}[\rho] + E_{\mathrm{H}}[\rho] + E_{\mathrm{XC}}\left[\rho^\uparrow[\rho], \rho^\downarrow[\rho]\right] \tag{7.4.1}$$

where $E_{\mathrm{XC}}\left[\rho^\uparrow[\rho], \rho^\downarrow[\rho]\right]$ is a functional of the spin density through $\rho^\uparrow[\rho]$, $\rho^\downarrow[\rho]$. This total energy is minimised with respect to an effective potential $V_{\mathrm{eff}}(\mathbf{r})$ that is common in both spin channels. As such, the electron orbitals for both spin-up and down are determined from the spin-independent Kohn-Sham equations

$$\left[-\frac{\nabla^2}{2} + V_{\mathrm{en}}(\mathbf{r}) + V_{\mathrm{eff}}(\mathbf{r})\right]\phi_i(\mathbf{r}) = \epsilon_i\phi_i(\mathbf{r}). \tag{7.4.2}$$

In this formulation each orbital $\phi_i(\mathbf{r})$ is occupied by up to two electrons with opposite spins. The resulting spin-densities are given by

$$\rho^\sigma(\mathbf{r}) = \sum_i^{N^\sigma} f_i^\sigma \left|\phi_i(\mathbf{r})\right|^2 \tag{7.4.3}$$

where $0 \leq f_i^\sigma \leq 1$ determines the occupancy of the ith electron state for a particular spin, with the restriction $\sum_i f_i^\sigma = N^\sigma$.

The derivative of the total energy with respect to this potential is

$$\frac{\delta E[\rho]}{\delta V_{\mathrm{eff}}(\mathbf{r})} = \frac{\delta T_{\mathrm{s}}[\rho]}{\delta V_{\mathrm{eff}}(\mathbf{r})} + \frac{\delta E_{\mathrm{en}}[\rho]}{\delta V_{\mathrm{eff}}(\mathbf{r})} + \frac{\delta E_{\mathrm{H}}[\rho]}{\delta V_{\mathrm{eff}}(\mathbf{r})} + \frac{\delta E_{\mathrm{XC}}\left[\rho^\uparrow[\rho], \rho^\downarrow[\rho]\right]}{\delta V_{\mathrm{eff}}(\mathbf{r})} \tag{7.4.4}$$

which is equal to zero when the total energy is minimised. These derivatives can be evaluated using the chain rule as

$$\frac{\delta T_{\mathrm{s}}[\rho]}{\delta V_{\mathrm{eff}}(\mathbf{r})} = \int d\mathbf{r}' \frac{\delta T_{\mathrm{s}}[\rho]}{\delta \rho(\mathbf{r}')} \frac{\delta \rho(\mathbf{r}')}{\delta V_{\mathrm{eff}}(\mathbf{r})} \tag{7.4.5}$$

$$\frac{\delta E_{\mathrm{en}}[\rho]}{\delta V_{\mathrm{eff}}(\mathbf{r})} = \int d\mathbf{r}' \frac{\delta E_{\mathrm{en}}[\rho]}{\delta \rho(\mathbf{r}')} \frac{\delta \rho(\mathbf{r}')}{\delta V_{\mathrm{eff}}(\mathbf{r})} \tag{7.4.6}$$

$$\frac{\delta E_{\mathrm{H}}[\rho]}{\delta V_{\mathrm{eff}}(\mathbf{r})} = \int d\mathbf{r}' \frac{\delta E_{\mathrm{H}}[\rho]}{\delta \rho(\mathbf{r}')} \frac{\delta \rho(\mathbf{r}')}{\delta V_{\mathrm{eff}}(\mathbf{r})} \tag{7.4.7}$$

$$\frac{\delta E_{\mathrm{XC}}[\rho^\uparrow, \rho^\downarrow]}{\delta V_{\mathrm{eff}}(\mathbf{r})} = \sum_\sigma \int d\mathbf{r}' \frac{\delta E_{\mathrm{XC}}[\rho^\uparrow, \rho^\downarrow]}{\delta \rho^\sigma(\mathbf{r}')} \frac{\delta \rho^\sigma(\mathbf{r}')}{\delta V_{\mathrm{eff}}(\mathbf{r})}. \tag{7.4.8}$$

The derivative of the density with respect to the potential is the density-density response function given by

$$\frac{\delta \rho(\mathbf{r}')}{\delta V_{\mathrm{eff}}(\mathbf{r})} = \sum_\sigma^{\uparrow\downarrow} \sum_i^{N^\sigma} \sum_{a=N^\sigma+1}^{\infty} f_i^\sigma \frac{[\phi_i^\sigma(\mathbf{r})]^* \phi_a^\sigma(\mathbf{r}) \phi_i^\sigma(\mathbf{r}') [\phi_a^\sigma(\mathbf{r}')]^*}{\epsilon_i - \epsilon_a} + \mathbf{c.c.} = \chi(\mathbf{r}, \mathbf{r}'). \tag{7.4.9}$$

Similarly the derivative of the spin density ρ^σ is given as

$$\frac{\delta \rho^\sigma(\mathbf{r}')}{\delta V_{\mathrm{eff}}(\mathbf{r})} = \sum_i^{N^\sigma} \sum_{a=N^\sigma+1}^{\infty} f_i^\sigma \frac{[\phi_i^\sigma(\mathbf{r})]^* \phi_a^\sigma(\mathbf{r}) \phi_i^\sigma(\mathbf{r}') [\phi_a^\sigma(\mathbf{r}')]^*}{\epsilon_i - \epsilon_a} + \mathbf{c.c.} = \chi^\sigma(\mathbf{r}, \mathbf{r}') \tag{7.4.10}$$

with

$$\chi(\mathbf{r}, \mathbf{r}') = \chi^\uparrow(\mathbf{r}, \mathbf{r}') + \chi^\downarrow(\mathbf{r}, \mathbf{r}'), \tag{7.4.11}$$

where $\chi(\mathbf{r}, \mathbf{r}')$ is the density-density response function. This allows the derivative in Eq. 7.4.4 to be written as

$$\frac{\delta E[\rho]}{\delta V_{\mathrm{eff}}(\mathbf{r})} = \int d\mathbf{r}' \left[V_{\mathrm{H}}(\mathbf{r}') - V_{\mathrm{eff}}(\mathbf{r}') \right] \chi(\mathbf{r}, \mathbf{r}') + \sum_\sigma^{\uparrow\downarrow} \int d\mathbf{r}' V_{\mathrm{XC}}^\sigma(\mathbf{r}') \chi^\sigma(\mathbf{r}, \mathbf{r}') \tag{7.4.12}$$

which is equal to zero when the total energy is minimised.

While so far the potential for both the up and down spins have been taken to be "common", a constraint where $N^\uparrow \neq N^\downarrow$ is inconsistent with a common Fermi energy for the two spin channels. If the band energies are equal for both spin-up and down

then the system will fill both spin-up and spin-down bands evenly up to the electron Fermi energy resulting in a spin unpolarised system. In order to perform spin polarised calculations the Fermi energies of the two spin channels must be different. The bands can then be filled unevenly for each spin, allowing $N^\uparrow \neq N^\downarrow$ and spin polarisation to occur. This difference in the Fermi energies with a common potential is equivalent to a common Fermi energy with a constant difference between the spin potentials $V^\uparrow = V^\downarrow + C$. This can be seen as a homogeneous magnetic field $B = \frac{C}{2\mu_0}$ aligned along the z-axis [50]. This constant difference will not change the electron wave functions but will shift the band energies ϵ_i^σ in one spin channel relative to the other.

This formulation allows a common Kohn-Sham potential to be determined that minimises the energy of a SDFT energy functional. In the case of a spin unpolarised system i.e. $N^\uparrow = N^\downarrow$, the implicit-DFA method reproduces the DFT result as one would expect from a system with no spin polarisation. For the fully spin polarised system $N^\uparrow = 0$ or $N^\downarrow = 0$, the implicit-DFA result is trivially the SDFT result, because for such a system only a single spin channel is utilised and all the electrons share a single Kohn-Sham potential. The implicit-DFA method is a restricted form of the SDFT method. While the results are the same for the cases of no spin and full ferromagnetism, the intermediate spin states of the implicit-DFA will be higher in energy due to the additional constraint that the spin potentials are common. Overall the implicit-DFA method is a simple way of performing spin polarised calculations with reduced spin contamination, along with providing a simple, restricted picture for DFT calculations.

7.5   Results

The implicit-DFA method is expected to find a solution as close to the SDFT results as possible while having a common spin potential. In general this result will be higher in energy than the SDFT method except in the case of spin unpolarised systems or fully spin polarised ferromagnetic systems. Despite these restrictions

that this method can still reproduce the metallic-insulating transition already found using SDFT.

7.5.1 Hydrogen

Repeating the calculations for hydrogen with the implicit-DFA method allows a comparison with the SDFT results. These calculations are again carried out with a cutoff energy of 1500 eV and 15 k-points in each dimension. For hydrogen the $N_s = 0$ and $N_s = 1$ SDFT results are trivially the same as the implicit-DFA results in these cases as there is either no spin-polarisation, or the system is fully polarised and only a single spin channel is active. States with intermediate N_s will have different behaviour to the SDFT results and are a restricted set of calculations which will, in general, have a higher energy. For hydrogen the behaviour at short and long interatomic separation are the $N_s = 0$ and $N_s = 1$ states. Therefore this general behaviour will be exactly reproduced when using the implicit-DFA method. As can be seen in Fig. 7.10 the short and long range behaviour is identical to the SDFT method, while intermediate states are higher in energy, as expected from a more restricted method.

While the implicit-DFA total energies are very similar to the hydrogen results for a single one-electron unit cell in SDFT, the implicit-DFA method does not reproduce the SDFT results in a double unit cell. Instead, the results for a double cell are identical to those for a single unit cell. This is due to the method not currently being able to treat systems with an antiferromagnetic electron configuration. As the Kohn-Sham potential is common for both spin channels then only the Fermi energy can differ for each spin component in order to allow magnetic states. In the case of a system with $N_s = 0$ then the Fermi energies are equal in order to equally occupy both spin channels; forcing the system to adopt a non-magnetic state. Therefore, the implicit-DFA method cannot predict an antiferromagnetic system when $N_s = 0$ and the spin densities for spin-up and spin-down are different throughout the system.
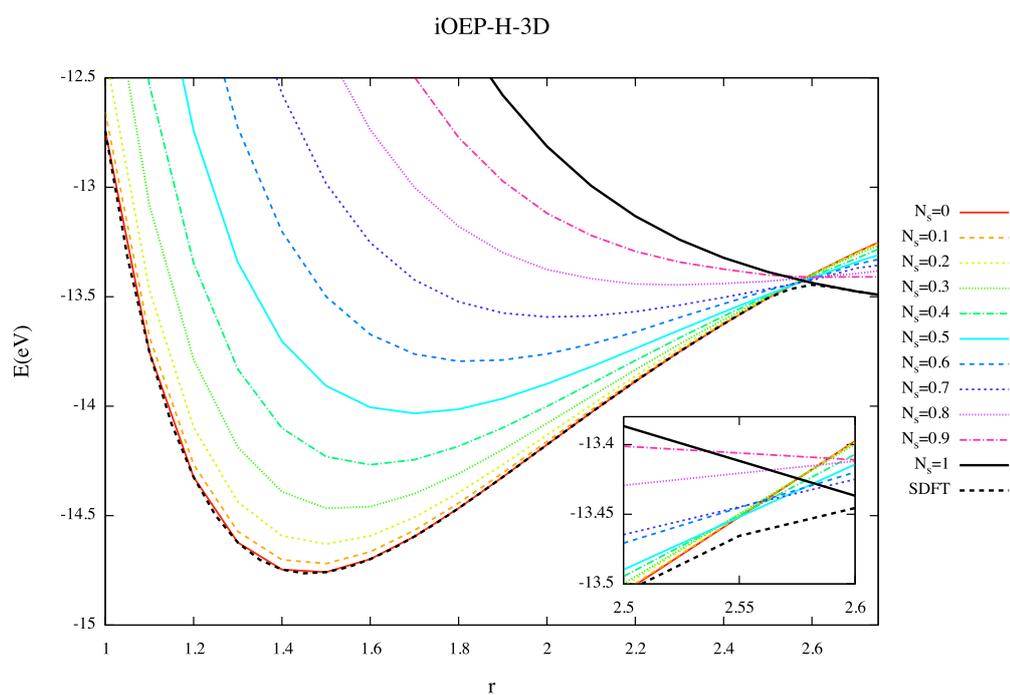
Figure 7.10: The total energies of the implicit-DFA method for various spin states of the 3-D hydrogen crystal with a single atom per unit cell as the interatomic separation is increased. Inset shows a zoomed image around the transition point. The dashed line shows the minimum energy state of the SDFT method from Fig. 7.3

7.5.2 Larger Atoms

In the hydrogen case the result for $N_s = 0$ and $N_s = 1$ are trivially the same as for the SDFT method. For aluminium this is the case for the $N_s = 0$ and $N_s = 3$ spin states, however the ground state at large interatomic separation for SDFT was seen to occur for $N_s = 1$, not trivially equal to the implicit-DFA result. However the comparison of the total energies of the results for SDFT and implicit-DFA show almost identical behaviour with a maximum difference of 7 meV observed between the SDFT and implicit-DFA total energies. This indicates that the implicit-DFA method is similar to the SDFT method when describing multi-electron atoms. Further investigation into the quality of the implicit-DFA results for more complicated multi-electron system will be required to perform a full investigation into the performance of the implicit-DFA method.

7.5.3 Conclusions

The implicit-DFA method for solids has been introduced as a constrained version of SDFT methods that treat spin in a system in a restricted manner with a common Kohn-Sham spin potential. This method reproduces the same metal insulator transition as observed in SDFT despite the restricted nature of the Kohn-Sham potential, appears to produce total energies that are close to those predicted by SDFT. This method offers a simple way to remove spin-contamination and also fine control over the spin state of the system. However, this method cannot reproduce antiferromagnetic behaviour, and additions to the method to describe such behaviour could be an avenue for future research.

7.6 Summary

Contrary to the prediction of simple band theory, it has been shown that insulating states can be obtained for an odd number of electrons in a unit cell, by allowing magnetic ground states. While this method has not been extended to account for the antiferromagnetic ground state that can be found in SDFT by doubling the unit cell, it otherwise manages to produce a qualitatively similar energy curves. The implicit-

DFA method was introduced as a method for performing DFT calculations for spin dependent systems with a common Kohn-Sham potential for both the spin-up and spin-down electrons. Using this newly introduced method it was demonstrated that the metal-insulator transition demonstrated for SDFT can also be found using the implicit-DFA method, despite the additional restriction of a common Kohn-Sham potential that has been imposed. These results are as yet unpublished and will be submitted for publication soon.

Chapter 8

Conclusions and Future Work

8.1 Conclusions

In Chapter 4 of this thesis the constrained method of self-interaction correction for DFT functionals has been developed and applied to show that constraining the effective potential significantly improves ionisation predictions from the highest Kohn-Sham eigenvalue for several commonly used DFT functionals. Extensions were then shown for this constrained method, allowing the method to be more generally applicable. These extensions addressed errors introduced through finite-basis effects, and redefined the auxiliary density in order to automatically satisfy the positivity requirement without the need for an explicit constraint.

In Chapter 5, a simple self-interaction free hybrid function was developed utilising the constrained method. This method demonstrated large improvements when calculating ionisation energies from the Kohn-Sham eigenvalues. These improvements were not just present in the ionisation of the highest energy electron, but for all electron orbitals and electron affinities.

Chapter 6 introduces a post-scf method that corrected the ionisation energy predicted by the Kohn-Sham eigenvalues towards the results obtained when performing a Δ_{scf} calculation. The zero, and first order terms of this correction were applied to the LDA functional demonstrating a large reduction in the error of the ionisation en-

ergies. This correction was also calculated and applied for all occupied Kohn-Sham orbitals, showing a relationship between the Δ_{scf} ionisation energies and the Kohn-Sham eigenvalues. This brings into question the assertion that only the highest occupied Kohn-Sham eigenvalue has a physically meaningful relation to ionisation energies. The magnitude of this correction to the ionisation energy of the highest occupied electron also allows an assessment of the quality of a DFT functional. because for the exact DFT functional this correction is zero.

In Chapter 7, the final work of this thesis focused on SDFT in solids, and new methods of implementing a spin-dependent functional using the OEP method. It was shown that when SDFT is applied to periodic unit cells with odd electron numbers of electrons, it can correctly predict insulating states. A fact that is not expected under conventional band theory. A metal-insulator transition appears in the 1, 2, and 3-D hydrogen crystal as interatomic distances are increased. This method can also be applied to multi electron systems, and demonstrates the same expected metal-insulator transition with increasing interatomic distances. A method of performing DFT with a common Kohn-Sham effective potential for spin-polarised systems was also demonstrated. Here the OEP method was used to minimise the total energy of a SDFT energy functional with respect to a spin independent Kohn-Sham potential. The metal-insulator transition found using SDFT was also found for this new, restricted method.

8.2 Future Work

8.2.1 Constrained Method in Solids

The constrained self-interaction correction method currently is limited to molecular systems due to the vanishing difference between N and $N-1$ as the number of electrons in a system increases. For molecular systems the asymptotic behaviour of the Kohn-Sham is known however in a periodic system such asymptotic behaviour is not well defined. In molecular systems the effect of a self-interaction correction is less crucial as accurate ionisation energies are accessible through a Δ_{scf} calcula-

tion. However, in periodic systems ionisation energies cannot be calculated with a Δ_{scf} calculation. Thus self-interaction corrections for periodic systems are an important method that will allow for improvements to band structure calculations in solids. Future work would be to apply the current implementation of the constrained method to periodic systems. This implementation requires the constraints on the self-interaction free auxiliary density to be investigated in periodic systems. For isolated systems the constraint on the auxiliary density is that it integrates to $N-1$ so as to reproduce the expected asymptotic behaviour. Applying this constraint that is dependent on the number of electrons per unit cell in a periodic system would result in an auxiliary density that would be different when considering a single unit cell compared to a supercell. This non-size-extensive behaviour can be seen by comparing the constraint on a single unit cell of $N-1$ with a supercell of m single unit cells, that would have a constraint of $mN-1$. Using a supercell with a large enough number of unit cells the constraint would tend towards mN, essentially removing the constraint. In order to apply this method in periodic systems, a size extensive constraint on the self-interaction free system must be determined. The behaviour of this constraint in a self-interaction free method can be investigated for the OEP method applied to the exact exchange method. Applying Poisson's law to the exact-exchange OEP potential would result in an effective density which can be used to identify a set of size extensive constraints on the auxiliary density of the self-interaction free periodic Kohn-Sham potential. Limits of this constraint can be predicted, and for a periodic system of sufficiently well separated atoms or molecules the constraint will be identical to the $N-1$ constraint used already. For metals, where electrons are fully delocalised and are well described by the homogeneous electron gas, self-interaction effects are expected to disappear, and in this case the constraint on the auxiliary density will tend towards N. In intermediate systems where electrons are partially delocalised the expected behaviour of this constraint is unknown and further investigation will aim to provide a general constraint for periodic systems.

8.2.2 Ionisation Corrected Functionals

In Chapter 6 a series of correcting terms for the Kohn-Sham eigenvalues were derived that correct the eigenvalues such that they correspond to the ionisation energy calculated through the Δ_{scf}method. This correction was applied post-SCF and is different for every orbital. The zero-order correction is given by

$$I_{\text{m,corr}}^{(0)} = \langle \phi_m^{(N)} | V_{\text{KS}}^{(N)} | \phi_m^{(N)} \rangle + E_{\text{HXC}}[\rho^{(N)}(\mathbf{r}) - \rho_m(\mathbf{r})] - E_{\text{HXC}}[\rho^{(N)}(\mathbf{r})] \qquad (8.2.1)$$

for each orbital m, and the correction for the electron affinity is

$$A^{(0)} = \langle \phi_{N+1}^{(N)} | V_{\text{KS}}^{(N)} | \phi_{N+1}^{(N)} \rangle + E_{\text{HXC}}[\rho^{(N)}] - E_{\text{HXC}}[\rho^{(N)} + \rho_{N+1}]. \qquad (8.2.2)$$

These expressions are simple to calculate as they only involve the orbitals of the N electron system. When this correction is added post-scf to a DFT method the ionisation energies predicted from the orbital eigenvalues are brought in line with those from Hartree-Fock; a significant improvement over uncorrected DFT. For the exact functional it is known from the DFT Koopmans' theorem that this correction goes to zero for the ionisation energy of the highest occupied orbital. The condition on the first order correction for the exact system is

$$I_{\text{N,corr}}^{(0)} = 0 \qquad (8.2.3)$$

and this can be imposed as a constraint on a DFT method. We propose constructing an objective functional as

$$G[V_{\text{KS}}] = E_{\text{tot}}[V_{\text{KS}}] - \lambda_N I_{\text{N,corr}}^{(0)}[V_{\text{KS}}] \qquad (8.2.4)$$

where the wave function dependent constraint can be written as implicit functionals of the Kohn-Sham potential. This expression has a trivial solution of $V_{\text{KS}} = V_{\text{DFA}} + C$ where C is a constant, and the potential must also satisfy $\lim^{r \to \infty} V_{\text{KS}}(\mathbf{r}) = 0$. This objective functional can then be minimised with respect to the Kohn-Sham potential through the OEP method in order to obtain a ground state solution where the Kohn-Sham potential satisfies the constraint.

The minimum of the objective functional is found when

$$\frac{\delta G[V_{\mathrm{KS}}]}{\delta V_{\mathrm{KS}}(\mathbf{r})} = \frac{\delta E_{\mathrm{tot}}[V_{\mathrm{KS}}]}{\delta V_{\mathrm{KS}}(\mathbf{r})} - \lambda_N \frac{\delta I_{\mathrm{N,corr}}^{(0)}[V_{\mathrm{KS}}]}{\delta V_{\mathrm{KS}}(\mathbf{r})} = 0. \tag{8.2.5}$$

The derivative $\frac{\delta E_{\mathrm{tot}}[V_{\mathrm{KS}}]}{\delta V_{\mathrm{KS}}(\mathbf{r})}$ is known from standard application of the OEP method to be

$$\frac{\delta E_{\mathrm{tot}}[V_{\mathrm{KS}}]}{\delta V_{\mathrm{KS}}(\mathbf{r})} = \int d\mathbf{r}' \left[V_{\mathrm{HXC}}(\mathbf{r}') - V_{\mathrm{KS}}(\mathbf{r}') \right] \chi(\mathbf{r}, \mathbf{r}') \tag{8.2.6}$$

where $\chi(\mathbf{r}, \mathbf{r}')$ is the usual density-density response functional. The derivative of the constraint on the ionisation energy is

$$\frac{\delta I_{\mathrm{N,corr}}^{(0)}[V_{\mathrm{KS}}]}{\delta V_{\mathrm{KS}}(\mathbf{r})} = \rho_N + \int d\mathbf{r}' V_{\mathrm{KS}}(\mathbf{r}') \chi_N(\mathbf{r}, \mathbf{r}') - \int d\mathbf{r}' V_{\mathrm{HXC}}[\rho](\mathbf{r}') \chi(\mathbf{r}, \mathbf{r}')$$
$$+ \int d\mathbf{r}' V_{\mathrm{HXC}}[\rho - \rho_N](\mathbf{r}') \left[\chi(\mathbf{r}, \mathbf{r}') - \chi_N(\mathbf{r}, \mathbf{r}') \right] \tag{8.2.7}$$

where χ_N is the response function of the single orbital density ρ_N given by

$$\chi_N(\mathbf{r}, \mathbf{r}') = \sum_{j \neq N}^{\infty} \frac{\phi_j(\mathbf{r}) \phi_N(\mathbf{r}) \phi_j(\mathbf{r}') \phi_N(\mathbf{r}')}{\epsilon_N - \epsilon_j}. \tag{8.2.8}$$

These equations can be used to evaluate the derivative in Eq. (8.2.6) giving

$$\frac{\delta G[V_{\mathrm{KS}}]}{\delta V_{\mathrm{KS}}(\mathbf{r})} = \int d\mathbf{r}' \left[V_{\mathrm{HXC}}(\mathbf{r}') - V_{\mathrm{KS}}(\mathbf{r}') \right] \chi(\mathbf{r}, \mathbf{r}') - \lambda_N \left[\rho_N + \int d\mathbf{r}' V_{\mathrm{KS}}(\mathbf{r}') \chi_N(\mathbf{r}, \mathbf{r}') \right.$$
$$\left. - \int d\mathbf{r}' V_{\mathrm{HXC}}[\rho](\mathbf{r}') \chi(\mathbf{r}, \mathbf{r}') + \int d\mathbf{r}' V_{\mathrm{HXC}}[\rho - \rho_N](\mathbf{r}') \left[\chi(\mathbf{r}, \mathbf{r}') - \chi_N(\mathbf{r}, \mathbf{r}') \right] \right] \tag{8.2.9}$$

which equals zero at the minimum. Defining

$$\Delta E_N = E_{\mathrm{HXC}}[\rho^{(N)}(\mathbf{r}) - \rho_m(\mathbf{r})] - E_{\mathrm{HXC}}[\rho^{(N)}(\mathbf{r})] \tag{8.2.10}$$

$$\Delta V_N(\mathbf{r}) = \int d\mathbf{r}' V_{\mathrm{KS}}(\mathbf{r}') \chi_N(\mathbf{r}, \mathbf{r}') - \int d\mathbf{r}' V_{\mathrm{HXC}}[\rho](\mathbf{r}') \chi(\mathbf{r}, \mathbf{r}')$$
$$+ \int d\mathbf{r}' V_{\mathrm{HXC}}[\rho - \rho_N](\mathbf{r}') \left[\chi(\mathbf{r}, \mathbf{r}') - \chi_N(\mathbf{r}, \mathbf{r}') \right] \tag{8.2.11}$$

allows the Lagrange multiplier to be determined as

$$\lambda_N = \frac{\int d\mathbf{r} d\mathbf{r}' \left[V_{\text{HXC}}(\mathbf{r}') - V_{\text{KS}}(\mathbf{r}') \right] \chi(\mathbf{r}, \mathbf{r}') V_{\text{KS}}(\mathbf{r})}{\Delta E_N + \int d\mathbf{r} V_{\text{KS}}(\mathbf{r}) \Delta V_N(\mathbf{r})}. \tag{8.2.12}$$

A functional that satisfies this expression should reduce the error in the ionisation energy of the highest occupied electron, improving these results when calculated with this method. It is known that for the exact functional the ionisation correction is zero. Therefore, this will correct a DFT method towards the exact functional. However, a more stringent correction can be applied to not only the Nth ionisation energy but to all energy levels. This is done by constraining all ionisation energy corrections to equal zero. Constraining all orbitals to obey Koopmans' theorem may lead to improved ionisation energies for every orbital, but it is unknown if this constraint would be satisfied exactly by the exact DFT functional. However, this condition is at least approximately satisfied [154–157]. Further work would investigate how this method would be affected by the choice of constrained orbitals and the effect on total energies and ionisation energies calculated using these constraints.

8.3   Final Remarks

The demonstration that by including magnetic ground states we can predict behaviours that are not expected in conventional band theory highlights the importance of the magnetic properties of a system's ground state. This may lead to demonstration of further properties which do not require the doubling of the unit cell to demonstrate. The introduction of a new implicit-DFA method with which to perform DFT calculations on spin polarised systems, in the absence of an external magnetic field, with a common potential could allow for the development of other DFT methods for spin-polarised systems. Further application of this method may allow more control over magnetic properties of a system through additional constraints on the potential.

The methods in Chapters 4,5,6 aim to reduce the effect of self-interaction errors on the effective potential in DFT calculations. Understanding and correcting for self-interaction errors is important in solids and molecules where they can introduce large

errors especially in the calculation of ionisation energies. The methods introduced in this thesis can be used to correct for these errors and their simplicity and inexpensive computation could be important in developing future self-interaction free methods for widespread use.

Bibliography

[1] R. D. Johnson III. NIST computational chemistry comparison and benchmark database, NIST standard reference database number 101, release 15b. 2011. *cccbdb. nist. gov.*, 2005.

[2] D. S. Ranasinghe, J. T. Margraf, A. Perera, and R. J. Bartlett. Vertical valence ionization potential benchmarks from equation-of-motion coupled cluster theory and qtp functionals. *J. Chem. Phys.*, 150(7):074108, 2019.

[3] M. Born and R. Oppenheimer. Zur quantentheorie der molekeln. *Annalen der physik*, 389(20):457–484, 1927.

[4] D. R. Hartree and W. Hartree. Self-consistent field, with exchange, for beryllium. *Proc. R. Soc. Lond.*, 150(869):9–33, 1935.

[5] J. C. Slater. The theory of complex spectra. *Phys. Rev.*, 34(10):1293, 1929.

[6] E. Condon. The theory of complex spectra. *Phys. Rev.*, 36(7):1121, 1930.

[7] C. Møller and M. S. Plesset. Note on an approximation treatment for many-electron systems. *Phys. Rev.*, 46(7):618, 1934.

[8] G. Das. Multiconfiguration self-consistent field (mcscf) theory for excited states. *J. Chem. Phys.*, 58(11):5104–5110, 1973.

[9] F. Coester. Bound states of a many-particle system. *Nucl. Phys.*, 7:421–424, 1958.

[10] F. Coester and H. Kümmel. Short-range correlations in nuclear wave functions. *Nucl. Phys.*, 17:477–485, 1960.

[11] J. Čížek. On the correlation problem in atomic and molecular systems. calculation of wavefunction components in ursell-type expansion using quantum-field theoretical methods. *J. Chem. Phys.*, 45(11):4256–4266, 1966.

[12] T. Koopmans. Über die zuordnung von wellenfunktionen und eigenwerten zu den einzelnen elektronen eines atoms. *Physica*, 1(1-6):104–113, 1934.

[13] P. Politzer and F. Abu-Awwad. A comparative analysis of hartree-fock and kohn-sham orbital energies. *Theor. Chem. Acc.*, 99(2):83–87, 1998.

[14] L. H. Thomas. The calculation of atomic fields. In *Math. Proc. Camb. Philos. Soc.*, volume 23, pages 542–548. Cambridge University Press, 1927.

[15] E. Fermi. Un metodo statistico per la determinazione di alcune priorieta dell'atome. *Rend. Accad. Naz. Lincei*, 6(602-607):32, 1927.

[16] P. Hohenberg and W. Kohn. Inhomogeneous electron gas. *Phys. Rev.*, 136(3B):B864, 1964.

[17] M. Levy. Universal variational functionals of electron densities, first-order density matrices, and natural spin-orbitals and solution of the v-representability problem. *Proc. Natl. Acad. Sci. U.S.A.*, 76(12):6062–6065, 1979.

[18] E. H. Lieb. Density functionals for coulomb systems. In *Inequalities*, pages 269–303. Springer, 2002.

[19] M. Levy. Constrained-search formulation and recent coordinate scaling in density-functional theory. In *Advances in quantum chemistry*, volume 21, pages 69–95. Elsevier, 1990.

[20] T. L. Gilbert. Hohenberg-kohn theorem for nonlocal external potentials. *Phys. Rev. B*, 12(6):2111, 1975.

[21] N. L. Balàzs. Formation of stable molecules within the statistical theory of atoms. *Phys. Rev.*, 156(1):42, 1967.

[22] P. Hertel, H. Narnhofer, and W. Thirring. Thermodynamic functions for fermions with gravostatic and electrostatic interactions. *Commun. math. Phys.*, 28(2):159–176, 1972.

[23] J. Sheldon. Use of the statistical field approximation in molecular physics. *Phys. Rev.*, 99(4):1291, 1955.

[24] E. Teller. On the stability of molecules in the thomas-fermi theory. *Rev. Mod. Phys.*, 34(4):627, 1962.

[25] W. Kohn and L. J. Sham. Self-consistent equations including exchange and correlation effects. *Phys. Rev.*, 140(4A):A1133, 1965.

[26] J. P. Perdew, A. Ruzsinszky, J. Tao, V. N. Staroverov, G. E. Scuseria, and G. I. Csonka. Prescription for the design and selection of density functional approximations: More constraint satisfaction with fewer fits. *J. Chem. Phys.*, 123(6):062201, 2005.

[27] F. Furche. Molecular tests of the random phase approximation to the exchange-correlation energy functional. *Phys. Rev. B*, 64(19):195120, 2001.

[28] Z. Yan, J. P. Perdew, and S. Kurth. Density functional for short-range correlation: Accuracy of the random-phase approximation for isoelectronic energy changes. *Phys. Rev. B*, 61(24):16430, 2000.

[29] P. A. Dirac. Note on exchange phenomena in the thomas atom. In *Math. Proc. Camb. Philos. Soc.*, volume 26, pages 376–385. Cambridge University Press, 1930.

[30] J. C. Slater. A simplification of the hartree-fock method. *Phys. Rev.*, 81(3):385, 1951.

[31] S. H. Vosko, L. Wilk, and M. Nusair. Accurate spin-dependent electron liquid correlation energies for local spin density calculations: a critical analysis. *Can. J. Phys.*, 58(8):1200–1211, 1980.

[32] J. P. Perdew and Y. Wang. Accurate and simple analytic representation of the electron-gas correlation energy. *Phys. Rev. B*, 45(23):13244, 1992.

[33] J. P. Perdew and A. Zunger. Self-interaction correction to density-functional approximations for many-electron systems. *Phys. Rev. B*, 23(10):5048, 1981.

[34] F. W. Kutzler and G. Painter. Energies of atoms with nonspherical charge densities calculated with nonlocal density-functional theory. *Phys. Rev. Lett.*, 59(12):1285, 1987.

[35] E. Clementi and S. J. Chakravorty. A comparative study of density functional models to estimate molecular atomization energies. *J. Chem. Phys.*, 93(4):2591–2602, 1990.

[36] J. P. Perdew, J. A. Chevary, S. H. Vosko, K. A. Jackson, M. R. Pederson, D. J. Singh, and C. Fiolhais. Atoms, molecules, solids, and surfaces: Applications of the generalized gradient approximation for exchange and correlation. *Phys. Rev. B*, 46(11):6671, 1992.

[37] D. C. Langreth and J. P. Perdew. Theory of nonuniform electronic systems. i. analysis of the gradient approximation and a generalization that works. *Phys. Rev. B*, 21(12):5469, 1980.

[38] D. C. Langreth and M. Mehl. Beyond the local-density approximation in calculations of ground-state electronic properties. *Phys. Rev. B*, 28(4):1809, 1983.

[39] J. P. Perdew, K. Burke, and M. Ernzerhof. Generalized gradient approximation made simple. *Phys. Rev. Lett.*, 77(18):3865, 1996.

[40] C. Lee, W. Yang, and R. G. Parr. Development of the colle-salvetti correlation-energy formula into a functional of the electron density. *Phys. Rev. B*, 37(2):785, 1988.

[41] A. D. Becke. Density-functional exchange-energy approximation with correct asymptotic behavior. *Phys. Rev. A*, 38(6):3098, 1988.

[42] J. P. Perdew. Accurate density functional for the energy: Real-space cutoff of the gradient expansion for the exchange hole. *Phys. Rev. Lett.*, 55(16):1665, 1985.

[43] J. Paier, M. Marsman, and G. Kresse. Why does the b3lyp hybrid functional fail for metals? *J. Chem. Phys.*, 127(2):024103, 2007.

[44] S. K. Ghosh and R. G. Parr. Phase-space approach to the exchange-energy functional of density-functional theory. *Phys. Rev. A*, 34(2):785, 1986.

[45] A. Becke and M. R. Roussel. Exchange holes in inhomogeneous systems: A coordinate-space model. *Phys. Rev. A*, 39(8):3761, 1989.

[46] N. Mardirossian and M. Head-Gordon. Thirty years of density functional theory in computational chemistry: an overview and extensive assessment of 200 density functionals. *Mol. Phys.*, 115(19):2315–2372, 2017.

[47] Y. Zhao, N. E. Schultz, and D. G. Truhlar. Exchange-correlation functional with broad accuracy for metallic and nonmetallic compounds, kinetics, and noncovalent interactions, 2005.

[48] S. Y. Haoyu, X. He, S. L. Li, and D. G. Truhlar. Mn15: A kohn–sham global-hybrid exchange–correlation density functional with broad accuracy for multi-reference and single-reference systems and noncovalent interactions. *Chem. Sci.*, 7(8):5032–5051, 2016.

[49] M. G. Medvedev, I. S. Bushmarinov, J. Sun, J. P. Perdew, and K. A. Lyssenko. Density functional theory is straying from the path toward the exact functional. *Science*, 355(6320):49–52, 2017.

[50] N. I. Gidopoulos. Potential in spin-density-functional theory of noncollinear magnetism determined by the many-electron ground state. *Phys. Rev. B*, 75(13):134408, 2007.

[51] J. Kubler, K.-H. Hock, J. Sticht, and A. Williams. Density functional theory of non-collinear magnetism. *J. Phys. F Met. Phys.*, 18(3):469, 1988.

[52] L. Sandratskii. Noncollinear magnetism in itinerant-electron systems: theory and applications. *Adv. Phys.*, 47(1):91–160, 1998.

[53] A. D. Becke. A new mixing of hartree–fock and local density-functional theories. *J. Chem. Phys.*, 98(2):1372–1377, 1993.

[54] A. D. Becke. Density-functional thermochemistry. iii. the role of exact exchange. *J. Chem. Phys.*, 98(7):5648–5652, apr 1993.

[55] A. D. Becke. Correlation energy of an inhomogeneous electron gas: A coordinate-space model. *J. Chem. Phys.*, 88(2):1053–1062, 1988.

[56] A. Görling and M. Levy. Hybrid schemes combining the hartree–fock method and density-functional theory: Underlying formalism and properties of correlation functionals. *J. Chem. Phys.*, 106(7):2675–2680, 1997.

[57] A. Seidl, A. Görling, P. Vogl, J. A. Majewski, and M. Levy. Generalized kohn-sham schemes and the band-gap problem. *Phys. Rev. B*, 53(7):3764, 1996.

[58] V. Barone, L. Orlandini, and C. Adamo. Density functional study of diborane, dialane, and digallane. *J. Phys. Chem. A*, 98(50):13185–13188, 1994.

[59] F. Wang, C. Di Valentin, and G. Pacchioni. Electronic and structural properties of wo3: a systematic hybrid dft study. *J. Phys. Chem. A C*, 115(16):8345–8353, 2011.

[60] C. Tuma, A. D. Boese, and N. C. Handy. Predicting the binding energies of h-bonded complexes: A comparative dft study. *Phys. Chem. Chem. Phys.*, 1(17):3939–3947, 1999.

[61] J. P. Perdew, M. Ernzerhof, and K. Burke. Rationale for mixing exact exchange with density functional approximations. *J. Chem. Phys.*, 105(22):9982–9985, 1996.

[62] P. J. Stephens, F. J. Devlin, C. F. Chabalowski, and M. J. Frisch. Ab initio calculation of vibrational absorption and circular dichroism spectra using density functional force fields. *J. Phys. Chem. A*, 98(45):11623–11627, 1994.

[63] K. Burke, M. Ernzerhof, and J. P. Perdew. The adiabatic connection method: a non-empirical hybrid. *Chem. Phys. Lett.*, 265(1-2):115–120, 1997.

[64] R. Sharp and G. Horton. A variational approach to the unipotential many-electron problem. *Phys. Rev.*, 90(2):317, 1953.

[65] J. D. Talman and W. F. Shadwick. Optimized effective atomic central potential. *Phys. Rev. A*, 14(1):36, 1976.

[66] V. Sahni, J. Gruenebaum, and J. Perdew. Study of the density-gradient expansion for the exchange energy. *Phys. Rev. B*, 26(8):4371, 1982.

[67] S. Hirata, S. Ivanov, I. Grabowski, R. J. Bartlett, K. Burke, and J. D. Talman. Can optimized effective potentials be determined uniquely? *J. Chem. Phys.*, 115(4):1635–1649, 2001.

[68] N. I. Gidopoulos and N. N. Lathiotakis. Nonanalyticity of the optimized effective potential with finite basis sets. *Phys. Rev. A*, 85(5):052508, 2012.

[69] V. N. Staroverov, G. E. Scuseria, and E. R. Davidson. Optimized effective potentials yielding hartree–fock energies and densities, 2006.

[70] N. I. Gidopoulos and N. N. Lathiotakis. Constraining density functional approximations to yield self-interaction free potentials. *J. Chem. Phys.*, 136(22):224109, 2012.

[71] J. Krieger, Y. Li, and G. Iafrate. Systematic approximations to the optimized effective potential: Application to orbital-density-functional theory. *Phys. Rev. A*, 46(9):5453, 1992.

[72] O. Gritsenko and E. Baerends. Orbital structure of the kohn-sham exchange potential and exchange kernel and the field-counteracting potential for molecules in an electric field. *Phys. Rev. A*, 64(4):042506, 2001.

[73] E. A. Hylleraas. Über den grundterm der zweielektronenprobleme von H⁻, He, Li⁺, H⁺⁺ usw. *Z. Phys.*, 65(3-4):209–225, 1930.

[74] T. W. Hollins, S. J. Clark, K. Refson, and N. I. Gidopoulos. Optimized effective potential using the hylleraas variational method. *Phys. Rev. B*, 85(23):235126, 2012.

[75] T. L. Beck. Real-space mesh techniques in density-functional theory. *Rev. Mod. Phys.*, 72(4):1041, 2000.

[76] J. Bernholc, M. Hodak, and W. Lu. Recent developments and applications of the real-space multigrid method. *J. Phys. Condens. Matter*, 20(29):294205, 2008.

[77] E. Briggs, D. Sullivan, and J. Bernholc. Real-space multigrid-based approach to large-scale electronic structure calculations. *Phys. Rev. B*, 54(20):14362, 1996.

[78] T. Torsti, V. Lindberg, I. Makkonen, E. Ogando, E. Rasanen, H. Saarikoski, M. Puska, and R. Nieminen. Real-space electronic-property calculations for nanoscale structures. *Handb. Theor. Comput. Nanotechnology*, 8:771–795, 2006.

[79] J. C. Slater. Atomic shielding constants. *Phys. Rev.*, 36(1):57, 1930.

[80] J. Foster and S. Boys. A quantum variational calculation for hcho. *Rev. Mod. Phys.*, 32(2):303, 1960.

[81] W. J. Hehre, R. F. Stewart, and J. A. Pople. self-consistent molecular-orbital methods. i. use of gaussian expansions of slater-type atomic orbitals. *J. Chem. Phys.*, 51(6):2657–2664, 1969.

[82] C. Reeves and R. Fletcher. Use of gaussian functions in the calculation of wavefunctions for small molecules. iii. the orbital basis and its effect on valence. *J. Chem. Phys.*, 42(12):4073–4081, 1965.

[83] J. L. Whitten. Gaussian expansion of hydrogen-atom wavefunctions. *J. Chem. Phys.*, 39(2):349–352, 1963.

[84] R. Ditchfield, W. J. Hehre, and J. A. Pople. Self-consistent molecular-orbital methods. ix. an extended gaussian-type basis for molecular-orbital studies of organic molecules. *J. Chem. Phys.*, 54(2):724–728, 1971.

[85] A. McLean and G. Chandler. Contracted gaussian basis sets for molecular calculations. i. second row atoms, z= 11–18. *J. Chem. Phys.*, 72(10):5639–5648, 1980.

[86] F. Jensen. Atomic orbital basis sets. *Wiley Interdiscip. Rev. Comput. Mol. Sci.*, 3(3):273–295, 2013.

[87] T. H. Dunning Jr. Gaussian basis sets for use in correlated molecular calculations. i. the atoms boron through neon and hydrogen. *J. Chem. Phys.*, 90(2):1007–1023, 1989.

[88] D. E. Woon and T. H. Dunning Jr. Gaussian basis sets for use in correlated molecular calculations. iii. the atoms aluminum through argon. *J. Chem. Phys.*, 98(2):1358–1371, 1993.

[89] D. E. Woon and T. H. Dunning Jr. Gaussian basis sets for use in correlated molecular calculations. iv. calculation of static electrical response properties. *J. Chem. Phys.*, 100(4):2975–2988, 1994.

[90] H. J. Monkhorst and J. D. Pack. Special points for brillouin-zone integrations. *Phys. Rev. B*, 13(12):5188, 1976.

[91] J. D. Pack and H. J. Monkhorst. "special points for brillouin-zone integrations" a reply. *Phys. Rev. B*, 16(4):1748, 1977.

[92] J. C. Phillips. Energy-band interpolation scheme based on a pseudopotential. *Phys. Rev.*, 112(3):685, 1958.

[93] J. C. Phillips and L. Kleinman. New method for calculating wave functions in crystals and molecules. *Phys. Rev.*, 116(2):287, 1959.

[94] B. J. Austin, V. Heine, and L. Sham. General theory of pseudopotentials. *Phys. Rev.*, 127(1):276, 1962.

[95] P. Pulay. Convergence acceleration of iterative sequences. the case of scf iteration. *Chem. Phys. Lett.*, 73(2):393–398, 1980.

[96] P. Pulay. Improved scf convergence acceleration. *J. Comput. Chem.*, 3(4):556–560, 1982.

[97] R. Shepard and M. Minkoff. Some comments on the diis method. *Mol. Phys.*, 105(19-22):2839–2848, 2007.

[98] N. Lathiotakis and M. A. Marques. Benchmark calculations for reduced density-matrix functional theory. *J. Chem. Phys.*, 128(18):184103, 2008.

[99] M. A. Marques, M. J. Oliveira, and T. Burnus. Libxc: A library of exchange and correlation functionals for density functional theory. *Comput. Phys. Commun.*, 183(10):2272–2281, 2012.

[100] M. W. Schmidt, K. K. Baldridge, J. A. Boatz, S. T. Elbert, M. S. Gordon, J. a. H. Jensen, S. Koseki, N. Matsunaga, K. A. Nguyen, S. Su, T. L. Windus, M. Dupuis, and J. A. M̃ontgomery Jr. General atomic and molecular electronic structure system. *J. Comput. Chem.*, 14(11):1347–1363, 1993.

[101] M. S. Gordon and M. W. Schmidt. Chapter 41 - advances in electronic structure theory: Gamess a decade later. In C. E. Dykstra, G. Frenking, K. S. Kim, and G. E. Scuseria, editors, *Theory and Applications of Computational Chemistry*, pages 1167 – 1189. Elsevier, Amsterdam, 2005.

[102] B. P. Pritchard, D. Altarawy, B. Didier, T. D. Gibson, and T. L. Windus. New basis set exchange: An open, up-to-date resource for the molecular sciences community. *J. Chem. Inf. Model.*, 59(11):4814–4820, 2019. PMID: 31600445.

[103] M. Segall, P. J. Lindan, M. a. Probert, C. J. Pickard, P. J. Hasnip, S. Clark, and M. Payne. First-principles simulation: ideas, illustrations and the castep code. *J. Phys. Condens. Matter*, 14(11):2717, 2002.

[104] S. J. Clark, M. D. Segall, C. J. Pickard, P. J. Hasnip, M. I. Probert, K. Refson, and M. C. Payne. First principles methods using castep. *Z. Kristallogr. Cryst. Mater.*, 220(5-6):567–570, 2005.

[105] J. P. Perdew, R. G. Parr, M. Levy, and J. L. Balduz Jr. Density-functional theory for fractional particle number: derivative discontinuities of the energy. *Phys. Rev. Lett.*, 49(23):1691, 1982.

[106] J. P. Perdew and M. Levy. Comment on "significance of the highest occupied kohn-sham eigenvalue". *Phys. Rev. B*, 56(24):16021, 1997.

[107] M. Levy, J. P. Perdew, and V. Sahni. Exact differential equation for the density and ionization energy of a many-particle system. *Phys. Rev. A*, 30(5):2745, 1984.

[108] C.-O. Almbladh and U. von Barth. Exact results for the charge and spin densities, exchange-correlation potentials, and density-functional eigenvalues. *Phys. Rev. B*, 31(6):3231, 1985.

[109] M. I. Aroyo, D. Orobengoa, G. de la Flor, E. S. Tasci, J. M. Perez-Mato, and H. Wondratschek. Brillouin-zone database on the bilbao crystallographic server. *Acta Crystallogr. A*, 70(2):126–137, 2014.

[110] I. Remediakis and E. Kaxiras. Band-structure calculations for semiconductors within generalized-density-functional theory. *Phys. Rev. B*, 59(8):5536, 1999.

[111] N. D. Mermin. Thermal properties of the inhomogeneous electron gas. *Phys. Rev.*, 137(5A):A1441, 1965.

[112] N. Marzari, D. Vanderbilt, and M. C. Payne. Ensemble density-functional theory for ab initio molecular dynamics of metals and finite-temperature insulators. *Phys. Rev. Lett.*, 79(7):1337, 1997.

[113] A. De Vita. *The energetics of defects and impurities in metals and ionic materials from first principles.* PhD thesis, University of Keele, 1992.

[114] M. Lundberg and P. E. Siegbahn. Quantifying the effects of the self-interaction error in dft: When do the delocalized states appear? *J. Chem. Phys.*, 122(22):224103, 2005.

[115] T. Bally and G. N. Sastry. Incorrect dissociation behavior of radical ions in density functional calculations. *J. Phys. Chem. A*, 101(43):7923–7925, 1997.

[116] J. Gräfenstein, E. Kraka, and D. Cremer. The impact of the self-interaction error on the density functional theory description of dissociating radical cations: Ionic and covalent dissociation limits. *J. Chem. Phys.*, 120(2):524–539, 2004.

[117] Y. Zhang and W. Yang. A challenge for density functionals: Self-interaction error increases for systems with a noninteger number of electrons. *J. Chem. Phys.*, 109(7):2604–2608, 1998.

[118] N. Rösch and S. Trickey. Comment on "concerning the applicability of density functional methods to atomic and molecular negative ions". *J. Chem. Phys.*, 106(21):8940–8941, 1997.

[119] C. Toher, A. Filippetti, S. Sanvito, and K. Burke. Self-interaction errors in density-functional calculations of electronic transport. *Phys. Rev. Lett.*, 95(14):146402, 2005.

[120] S. Goedecker and C. Umrigar. Critical assessment of the self-interaction-corrected–local-density-functional method and its algorithmic implementation. *Phys. Rev. A*, 55(3):1765, 1997.

[121] J. P. Perdew and M. Levy. Physical content of the exact kohn-sham orbital energies: band gaps and derivative discontinuities. *Phys. Rev. Lett.*, 51(20):1884, 1983.

[122] A. Ruzsinszky, J. P. Perdew, G. I. Csonka, O. A. Vydrov, and G. E. Scuseria. Density functionals that are one-and two-are not always many-electron self-interaction-free, as shown for H_2^+, He_2^+, LiH^+, and Ne_2^+. *J. Chem. Phys.*, 126(10):104102, 2007.

[123] P. Mori-Sánchez, A. J. Cohen, and W. Yang. Many-electron self-interaction error in approximate density functionals. *J. Chem. Phys.*, 125(20):201102, 2006.

[124] T. Schmidt and S. Kümmel. One-and many-electron self-interaction error in local and global hybrid functionals. *Phys. Rev. B*, 93(16):165120, 2016.

[125] E. Engel, J. Chevary, L. Macdonald, and S. Vosko. Asymptotic properties of the exchange energy density and the exchange potential of finite systems: relevance for generalized gradient approximations. *Z. Phys. D: At., Mol. Clusters*, 23(1):7–14, 1992.

[126] R. Van Leeuwen and E. Baerends. Exchange-correlation potential with correct asymptotic behavior. *Phys. Rev. A*, 49(4):2421, 1994.

[127] A. J. Cohen, P. Mori-Sánchez, and W. Yang. Insights into current limitations of density functional theory. *Science*, 321(5890):792–794, 2008.

[128] A. Ruzsinszky, J. P. Perdew, G. I. Csonka, O. A. Vydrov, and G. E. Scuseria. Spurious fractional charge on dissociated atoms: Pervasive and resilient self-interaction error of common density functionals. *J. Chem. Phys.*, 125(19):194112, 2006.

[129] J. P. Perdew and A. Zunger. Self-interaction correction to density-functional approximations for many-electron systems. *Phys. Rev. B*, 23:5048–5079, 1981.

[130] R. van Leeuwen and E. J. Baerends. Exchange-correlation potential with correct asymptotic behavior. *Phys. Rev. A*, 49:2421–2431, 1994.

[131] C. Legrand, E. Suraud, and P.-G. Reinhard. Comparison of self-interaction-corrections for metal clusters. *J Phys. B-At. Mol. Opt.*, 35(4):1115, 2002.

[132] T. Tsuneda and K. Hirao. Self-interaction corrections in density functional theory. *J. Chem. Phys.*, 140(18):18A513, 2014.

[133] M. R. Pederson, A. Ruzsinszky, and J. P. Perdew. Communication: Self-interaction correction with unitary invariance in density functional theory. *J. Chem. Phys.*, 140(12):121103, 2014.

[134] N. Gidopoulos and N. N. Lathiotakis. Constrained local potentials for self-interaction correction. *Adv. At. Mol. Opt. Phys.*, 64:129 – 142, 2015.

[135] S. J. Clark, T. W. Hollins, K. Refson, and N. I. Gidopoulos. Self-interaction free local exchange potentials applied to metallic systems. *J. Phys.: Condens. Matter*, 00:8pp, 2017.

[136] É. Brémond, Á. J. Pérez-Jiménez, J. C. Sancho-García, and C. Adamo. Range-separated hybrid density functionals made simple. *J. Chem. Phys.*, 150(20):201102, 2019.

[137] J. Toulouse, F. Colonna, and A. Savin. Long-range–short-range separation of the electron-electron interaction in density-functional theory. *Phys. Rev. A*, 70(6):062505, 2004.

[138] O. A. Vydrov and G. E. Scuseria. Assessment of a long-range corrected hybrid functional. *J. Chem. Phys.*, 125(23):234109, 2006.

[139] N. Gidopoulos and N. N. Lathiotakis. Constrained local potentials for self-interaction correction. *Adv. At. Mol. Opt. Phys.*, 64:129 – 142, 2015.

[140] T. Pitts, N. I. Gidopoulos, and N. N. Lathiotakis. Performance of the constrained minimization of the total energy in density functional approximations: the electron repulsion density and potential. *Eur. Phys. J. B*, 91(6):130, 2018.

[141] N. I. Gidopoulos and N. N. Lathiotakis. Nonanalyticity of the optimized effective potential with finite basis sets. *Phys. Rev. A*, 85:052508, 2012.

[142] G. Zhang and C. B. Musgrave. Comparison of dft methods for molecular orbital eigenvalue calculations. *J. Phys. Chem. A*, 111(8):1554–1561, 2007.

[143] O. Gritsenko, Ł. Mentel, and E. Baerends. On the errors of local density (lda) and generalized gradient (gga) approximations to the kohn-sham potential and orbital energies. *J. Chem. Phys.*, 144(20):204114, 2016.

[144] O. Gritsenko, R. van Leeuwen, E. van Lenthe, and E. J. Baerends. Self-consistent approximation to the kohn-sham exchange potential. *Phys. Rev. A*, 51(3):1944, 1995.

[145] P. R. Schipper, O. V. Gritsenko, S. J. van Gisbergen, and E. J. Baerends. Molecular calculations of excitation energies and (hyper) polarizabilities with a statistical average of orbital model exchange-correlation potentials. *J. Chem. Phys.*, 112(3):1344–1352, 2000.

[146] A. Unsöld. Quantentheorie des wasserstoffmolekülions und der born-landéschen abstoßungskräfte. *Z. Phys.*, 43(8):563–574, 1927.

[147] T. J. Callow, B. J. Pearce, T. Pitts, N. N. Lathiotakis, M. J. Hodgson, and N. I. Gidopoulos. Improving the exchange and correlation potential in density-functional approximations through constraints. *Faraday Discuss.*, 224:126–144, 2020.

[148] N. A. Group. *NAG Fortran Library Manual, Mark 16: F03-F06*. NAG Fortran Library Manual, Mark 16. NAG, 1993.

[149] C. Adamo and V. Barone. Toward reliable density functional methods without adjustable parameters: The pbe0 model. *J. Chem. Phys.*, 110(13):6158–6170, 1999.

[150] R. Van Meer, O. Gritsenko, and E. Baerends. Physical meaning of virtual kohn–sham orbitals and orbital energies: an ideal basis for the description of molecular excitations. *J. Chem. Theory Comput.*, 10(10):4432–4441, 2014.

[151] D. P. Chong, O. V. Gritsenko, and E. J. Baerends. Interpretation of the kohn–sham orbital energies as approximate vertical ionization potentials. *J. Chem. Phys.*, 116(5):1760–1772, 2002.

[152] S. Hamel, P. Duffy, M. E. Casida, and D. R. Salahub. Kohn–sham orbitals and orbital energies: fictitious constructs but good approximations all the same. *J Electron Spectros Relat Phenomena*, 123(2-3):345–363, 2002.

[153] M. Grüning, O. Gritsenko, S. Van Gisbergen, and E. Baerends. The failure of generalized gradient approximations (ggas) and meta-ggas for the two-center three-electron bonds in He^{2+}, $(H_2O)^{2+}$, and $(NH_3)^{2+}$. *J. Phys. Chem. A*, 105(40):9211–9218, 2001.

[154] R. J. Bartlett, V. F. Lotrich, and I. V. Schweigert. Ab initio density functional theory: The best of both worlds? *J. Chem. Phys.*, 123(6):062205, 2005.

[155] D. S. Ranasinghe, J. T. Margraf, Y. Jin, and R. J. Bartlett. Does the ionization potential condition employed in qtp functionals mitigate the self-interaction error? *J. Chem. Phys.*, 146(3):034102, 2017.

[156] R. J. Bartlett. Towards an exact correlated orbital theory for electrons. *Chem. Phys. Lett.*, 484(1-3):1–9, 2009.

[157] R. J. Bartlett and D. S. Ranasinghe. The power of exact conditions in electronic structure theory. *Chem. Phys. Lett.*, 669:54–70, 2017.

[158] R. O. Jones and O. Gunnarsson. The density functional formalism, its applications and prospects. *Rev. Mod. Phys.*, 61(3):689, 1989.

[159] A. Hellman, B. Razaznejad, and B. I. Lundqvist. Potential-energy surfaces for excited states in extended systems. *J. Chem. Phys.*, 120(10):4593–4602, 2004.

[160] J. Gavnholt, T. Olsen, M. Engelund, and J. Schiøtz. δ self-consistent field method to obtain potential energy surfaces of excited molecules on surfaces. *Phys. Rev. B*, 78(7):075441, 2008.

[161] S. Kirklin, J. E. Saal, B. Meredig, A. Thompson, J. W. Doak, M. Aykol, S. Rühl, and C. Wolverton. The open quantum materials database (oqmd): assessing the accuracy of dft formation energies. *Npj Comput. Mater.*, 1(1):1–15, 2015.

[162] A. Görling. Density-functional theory beyond the hohenberg-kohn theorem. *Phys. Rev. A*, 59(5):3359, 1999.

[163] P. Verma and R. J. Bartlett. Increasing the applicability of density functional theory. iv. consequences of ionization-potential improved exchange-correlation potentials. *J. Chem. Phys.*, 140(18):18A534, 2014.

[164] N. W. Ashcroft and N. D. Mermin. *Solid State Physics*. Holt-Saunders, 1976.

[165] N. F. Mott. The basis of the electron theory of metals, with special reference to the transition metals. *Proc. Phys. Soc. Sec. A*, 62(7):416, 1949.

[166] N. F. Mott. Metal-insulator transitions. *Contemporary Physics*, 14(5):401–413, 1973.

[167] R. Peierls. *Quantum Theory of Solids*. International Series of Monographs on Physics. Clarendon Press, 1996.

[168] J. P. Perdew, A. Ruzsinszky, L. A. Constantin, J. Sun, and G. I. Csonka. Some fundamental issues in ground-state density functional theory: A guide for the perplexed. *J. Chem. Theory Comput.*, 5(4):902–908, 2009.

[169] J. Baker, A. Scheiner, and J. Andzelm. Spin contamination in density functional theory. *Chem. Phys. Lett.*, 216(3-6):380–388, 1993.

[170] J. A. Pople, P. M. Gill, and N. C. Handy. Spin-unrestricted character of kohn-sham orbitals for open-shell systems. *Int. J. Quantum Chem.*, 56(4):303–305, 1995.

[171] J. Wang, A. D. Becke, and V. H. Smith Jr. Evaluation of¡ s 2¿ in restricted, unrestricted hartree–fock, and density functional based theories. *J. Chem. Phys.*, 102(8):3477–3480, 1995.

Appendix A

Perturbation Theory

A.1   First order Perturbation theory

As shown by the Hohenberg-Kohn theorem in 2.3.2 all quantities are dependent on the electron density, or Kohn-Sham potential, and varying either the electron density or potential will result in a change in all these quantities. In the DFT methods, especially those involving the OEP method, it is often necessary to know the response of the Kohn-Sham orbitals to a perturbation in the Kohn-Sham potential, this can be accomplished using first order perturbation theory. The Kohn-Sham orbitals are defined by the hamiltonian equation

$$\hat{H}\phi_i(\mathbf{r}) = \epsilon_i\phi_i(\mathbf{r}) \tag{A.1.1}$$

where the Hamiltonian $\hat{H}$ is a combination of the kinetic energy operator, external potential, and the Kohn-Sham potential. considering a perturbation in the Kohn-Sham potential pf V' there will be a corresponding perturbation in the Kohn-Sham orbitals

$$\left(\hat{H} + V'\right)|\phi_i + \phi_i' + \ldots\rangle = (\epsilon_i + \epsilon_i' + \ldots)|\phi_i + \phi_i' + \ldots\rangle \tag{A.1.2}$$

which, to first order gives

$$\left(\hat{H} - \epsilon_i\right)|\phi_i'\rangle = (\epsilon_i' - V')|\phi_i\rangle. \tag{A.1.3}$$

The perturbed orbitals are still normalised to 1 which requires the perturbation in the first order orbital to satisfy

$$\langle\phi_i|\phi_i'\rangle + \langle\phi_i'|\phi_i\rangle = 0 \tag{A.1.4}$$

which can be satisfied by projecting the orbital onto the unperturbed orbitals by

$$\phi_i'(\mathbf{r}) = \sum_{j\neq i} c_{ij}\phi_j(\mathbf{r}) \tag{A.1.5}$$

where the orthonormality of the Kohn-Sham orbitals give the required normalisation condition.

Substituting this expression into the first order Kohn-Sham equation multiplying by an orbital ϕ_k where $k \neq i$ and integrating gives

$$\sum_{j\neq i} c_{ij}\langle\phi_k|\left(\hat{H} - \epsilon_i\right)|\phi_j\rangle = \langle\phi_k|(\epsilon_i' - V')|\phi_i\rangle \tag{A.1.6}$$

where due to the orthonormality of the electron orbitals

$$c_{ik}\langle\phi_k|\left(\hat{H} - \epsilon_i\right)|\phi_k\rangle = -\langle\phi_k|V'|\phi_i\rangle \tag{A.1.7}$$

evaluating $\langle\phi_k|\hat{H}|\phi_k\rangle = \epsilon_k$ and rearranging for c_{ik} gives

$$c_{ik} = -\frac{\langle\phi_k|V'|\phi_i\rangle}{\epsilon_k - \epsilon_i}. \tag{A.1.8}$$

Evaluating the perturbed orbital gives

$$\phi_i'(\mathbf{r}) = \sum_{j\neq i} c_{ij}\phi_j(\mathbf{r}) = -\sum_{j\neq i} \frac{\langle\phi_j|V'|\phi_i\rangle}{\epsilon_j - \epsilon_i}\phi_j(\mathbf{r}) \tag{A.1.9}$$

where this can be represent the perturbed induced in the orbital by changing the Kohn-Sham potential.

A.2 Degenerate perturbation theory

When considering a Kohn-Sham system under the removal or addition of an electron it is common for there to be a degeneracy between the occupied and unoccupied

electron orbitals. This degeneracy introduces a difficulty in evaluating the density-density response function, which has the denominator $\epsilon_i - \epsilon_a$, which upon electron removal or addition can result in occupied orbitals which are degenerate with unoccupied orbitals. This introduces terms for which the denominator $\epsilon_i - \epsilon_a = 0$ and these orbitals must be treated under degenerate perturbation theory in order to provide a finite perturbation. When dealing with degenerate orbitals the perturbed orbital $|\phi_i'\rangle$ is considered to be composed of a linear combination of degenerate orbitals $|m_j\rangle$ in the degenerate subspace $j \in \mathcal{D}$ such that

$$|\phi_i'\rangle = \sum_{j \in \mathcal{D}} c_{ij} |m_j\rangle \tag{A.2.10}$$

the equations for the perturbed degenerate orbitals becomes

$$\left[\hat{H}_0 + \hat{V}\right] |\phi_i'\rangle = \left[\hat{H}_0 + \hat{V}\right] \sum_{j \in \mathcal{D}} c_{ij} |m_j\rangle = \epsilon_j' |\phi_i\rangle \tag{A.2.11}$$

where ϵ_j' is the perturbed orbital energy. For all the degenerate states

$$\hat{H}_0 |m_k\rangle = \epsilon_D |m_k\rangle \tag{A.2.12}$$

where ϵ_D is the energy of the degenerate state. Therefore, multiplying Eq. A.2.11 on the left by a degenerate state $\langle m_k|$, and utilising the orthogonality of the orbitals states gives

$$\sum_{j \in \mathcal{D}} c_{ij} \left[\langle m_k| \hat{V} |m_j\rangle - \delta_{kj}\Delta_i\right] = 0 \tag{A.2.13}$$

where $\Delta_i = \epsilon_i' - \epsilon_D$. This eigenvalue equation must be solved in order to determine the coefficient c_{ij}, this is typically a simple procedure as the degenerate space only consists of a small set of orbitals. The perturbed degenerate orbitals can then be found from

$$|\phi_i'\rangle = \sum_{j \in \mathcal{D}} c_{ij} |m_j\rangle = |m_i\rangle + \sum_{j \in \mathcal{D}} [c_{ij} - \delta_{ij}] |m_j\rangle \tag{A.2.14}$$

allowing subsequent calculation of a perturbed densies and other quantities to be constructed similarly to non-degenerate perturbation theory. For orbitals which

are not part of a degenerate space the perturbation can be determined from non-degenerate perturbation theory.